Universidad Autónoma de Madrid

Alternative p38 mitogen-activated protein kinases p38γ and p38δ: important players in skin inflammation and skin tumorigenesis

PhD thesis

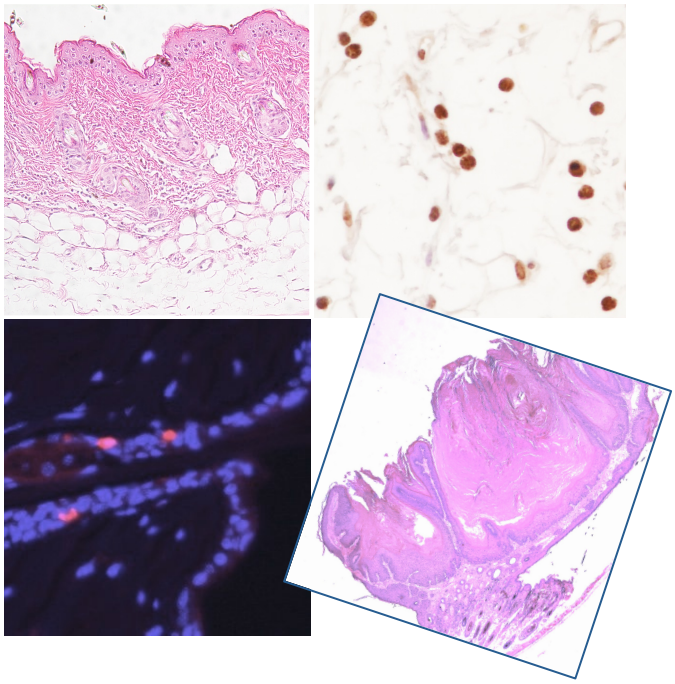

Rafał Żur

Madrid 2014

DEPARTAMENTO DE BIOLOGÍA MOLECULAR
FACULTAD DE CIENCIAS
UNIVERSIDAD AUTÓNOMA DE MADRID

PhD thesis

Alternative p38 mitogen-activated protein kinases p38γ and p38δ: important players in skin inflammation and skin tumorigenesis

Rafał Żur, M.Sc.

Thesis Director:
Dr. Ana Cuenda

Departamento de Inmunología y Oncología, Centro Nacional de Biotecnología (CNB), Consejo Superior de Investigaciones Científicas (CSIC)

Madrid 2014

This thesis is dedicated to the memory of my grandmother, who died of cancer.
Niniejszą pracę dedykuję pamięci mojej babci zmarłej na raka.

Władysława Szczukowska Hein
(1929-2000)

I would also like to express my sincere gratitude
to all the people who have been supporting me
professionally and personally during these years.
I will never forget. Thank you.

La Caixa International PhD Fellowship (2010-2014)
has supported the realisation of the presented work.

Scientific work must not be considered from the point of view of the direct usefulness of it. It must be done for itself, for the beauty of science, and then there is always the chance that a scientific discovery may become, like the radium, a benefit.

Praca naukowa nie może być mierzona bezpośrednią użytecznością.
Musi być uprawiana dla samej siebie,
dla swojego piękna, a wówczas zawsze jest sposobność, by odkrycia naukowe
stały się tym co rad, dobrodziejstwem.

Marie Skłodowska-Curie (1867-1934)

LIST OF ABBREVIATIONS

AP-1	Activator protein-1
BrdU	5-bromo-2´-deoxyuridine
BSA	Bovine serum albumin
BCC	Basal cell carcinoma
cDNA	Complementary deoxyribonucleic acid
CD	Cluster of differentiation
DETC	Dendritic epidermal T cell
DMBA	7,12-dimethylbenz[α]anthracene
DMEM	Dulbecco's Modified Eagle Medium
DMSO	Dimethylsulfoxide
EDTA	Ethylenediaminetetraacetic acid
EGF	Epidermal growth factor
EGFR	Epidermal growth factor receptor
EMT	Epithelial-to-mesenchymal transition
ERK	Extracellular signal-regulated kinase
GDP	Guanosine diphosphate
GSK3	Glycogen synthase kinase 3
GTP	Guanosine triphosphate
HE	Haematoxylin-eosin
HEK293T	Human Embryonic Kidney 293T
HNSCC	Head and neck squamous cell carcinoma
IL	Interleukin
KC	keratinocyte-derived chemokine (CXCL1)
JNK	c-Jun N-terminal kinase
kDa	Kilo Dalton
LPS	lipopolysaccharide
MAPK	Mitogen-activated protein kinase
MEF	Mouse embryonic fibroblast
MIP-2	macrophage inflammatory protein-2 (CXCL2)
MKK	Mitogen-activated protein kinase kinase (MAP2K)
MKKK	Mitogen-activated protein kinase kinase kinase (MAP3K)
mRNA	Messenger ribonucleic acid
MPO	Myeloperoxidase
NF-κB	Nuclear factor-κB
NMSC	Non-melanoma skin cancer

OSCC	Oral squamous cell carcinoma
PBS	Phosphate buffered saline
PCR	Polymerase chain reaction
Pdcd	Programmed cell death protein
PI3K	Phosphoinositide-3-kinase
PKB	Protein kinase B
PKC	Protein kinase C
PLCγ	Phospholipase C γ
qPCR	Quantitative polymerase chain reaction
SAP97/hDlg	Synapse-associated protein 97/ human discs large homolog 1
SAPK	Stress-activated protein kinase
SCC	Squamous cell carcinoma
SDS	Sodium dodecyl sulfate
SEM	Standard error of the mean
shRNA	Short hairpin ribonucleic acid
STAT3	Signal transducer and activator of transcription 3
TCR	T cell receptor
TdT	Deoxynucleotidyltransferase
TGF	Transforming growth factor
TNF	Tumour necrosis factor
TPA	12-O-tetradecanoylphorbol-13-acetate
TUNEL	Deoxynucleotidyltransferase-mediated dUTP nick-end label
WT	Wild type

LIST OF FIGURES

LIST OF TABLES

PRESENTACIÓN

La señalización dependiente de las proteínas quinasa activadas por mitógeno p38 (p38 MAPK) tiene un papel importante en el control de los procesos celulares tales como la proliferación, crecimiento celular y diferenciación. Hay cuatro miembros de la familia de las quinasas p38: p38α, p38β, p38γ y p38δ. Hasta ahora no existe mucha información sobre las funciones de las p38γ y p38δ. Utilizando modelos de ratón, nuestro grupo ha demostrado, en los últimos años, la importancia de las dos isoformas p38γ y p38δ en la inflamación y en la producción de citoquinas en condiciones de choque séptico, artritis reumatoide y cáncer de colon asociado a colitis (Risco et al., 2012; Criado et al., 2014, del Reino et al., 2014). Sin embargo, el involucramiento de las p38γ y p38δ en la tumorigénesis de piel asociada a inflamación hasta ahora no estaba bien descrita. Esta tesis representa un trabajo que se llevo a cabo para describir, por primera vez en este grupo, estas dos quinasas en la piel de ratón.

Está ampliamente reconocido que las neoplasias, incluido el cáncer de piel, están provocadas, al menos parcialmente, por la inflamación crónica (Balkwill et al., 2005). La carcinogénesis de piel químicamente inducida es uno de los mejores modelos *in vivo* para investigar los distintos estadios del desarrollo tumoral. Representa un modelo clásico del tumor asociado a inflamación que consiste en la exposición a un carcinógeno (7,12-dimetilbenzo(a)antraceno o DMBA) y, después, durante una fase de promoción, al compuesto 12-O-tetradecanoilforbol-13-acetato (TPA), que es un potente inductor de la inflamación en la piel (DiGiovanni, 1992). Los tumores de piel (también designados como papilomas de piel) desarrollados en este modelo representan un estadio intermedio entre la piel sana y un estadio maligno de carcinoma de piel, parecido al cáncer escamoso en los humanos.

Aquí mostramos resultados sobre la implicación de p38γ y p38δ en la inflamación de piel de ratón y la promoción tumoral de la piel a través del protocolo del DMBA/TPA, así como usando sólo el tratamiento con el TPA. Las dos quinasas p38 se fosforilan en respuesta al TPA, indicando su implicación en la regulación de la inflamación y la tumorigénesis en la piel. También mostramos que la ausencia de ambas proteínas quinasas suprime significativamente la tumorigénesis de la piel. Por otro lado, con el tratamiento tópico con TPA, hemos demostrado la importancia de p38γ y p38δ en la producción de citoquinas, reclutamiento de neutrófilos y en el control de la proliferación epidermal.

INTRODUCTION

1. Skin carcinogenesis.

1.1. Skin structure and functions.

The skin is the largest organ of the human body and a primary barrier against physical insults and microbial pathogens. It represents a complex environment in which skin cells maintain the tissue homeostasis and, under pathological conditions, are capable of provoking protective reactions. This protection is possible thanks to the unique anatomy and cellular composition of the skin, particularly the vast network of skin-associated immune cells (Tay et al., 2013).

1.1.1. Skin anatomy.

The skin is composed of epidermis, dermis and subcutaneous layer, which contain an array of cell types and skin structures (Fig. I-1).

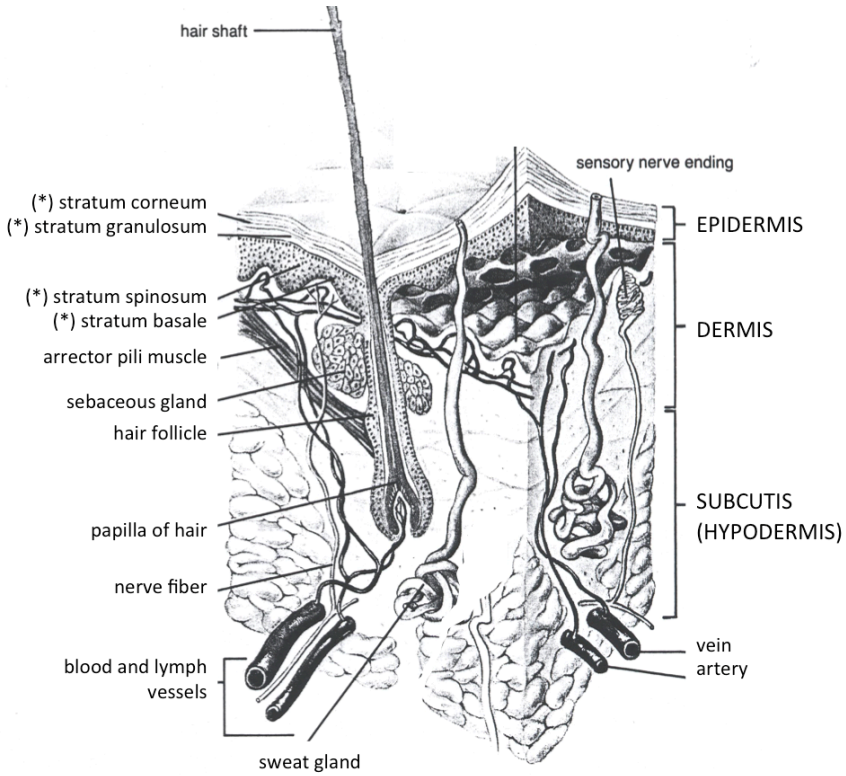

Figure I-1. Cross-section of the human skin with its characteristic elements. (*) The names of four layers of the epidermis (adapted from http://www.coenzyme-a.com/skinmatrix_article.html).

The epidermis is the top layer of the skin. Apart from predominant keratinocytes, which produce keratin, the epidermis is also comprised of melanocytes and Langerhans cells. Melanocytes produce a brown pigment, melanin, which gives dark colour to the skin and protects stem cells and proliferating keratinocytes in the deeper layers from the harmful effects of ultraviolet (UV) radiation in the sunlight (Teichert and Bikle, 2011). Langerhans cells that are a specialised

subpopulation of antigen-presenting immune cells, called dendritic cells, are the frontline defense of the immune system in the skin. The epidermis is divided into four layers based on different levels of cell differentiation. Starting with the deepest one, situated just above the basement membrane, which is composed of the basal lamina and the reticular lamina, they are: basal layer (*stratum basale*), spinous layer (*stratum spinosum*), granular layer (*stratum granulosum*) and the outermost - cornified layer (*stratum corneum*). The latter is made up of dead keratinocytes called corneocytes. Together with *stratum granulosum,* rich in tight junctions, corneocytes ensure an effective physical barrier between deeper layers and the environment.

As for the dermis, its major cell type is fibroblasts, including the specialized group of fibroblasts in dermal papilla at the base of the hair follicle. Similarly to the epidermis, this skin fraction is highly complex and contains a range of structures, such as hair follicles, sweat glands (absent in mice), sebaceous glands, nerve endings, capillary blood vessels and lymphatic vessels, sustained in skin structure by collagen, a protein giving the skin its elasticity and strength.

The deepest part of the skin, the subcutaneous layer or subcutis forms with the lowest parts of the dermis a network of collagen and adipocytes (fat cells) (www.cancer.org).

1.1.2. Skin immune cells.

The group of skin-resident immune cells is composed of myeloid cells (macrophages, dendritic cells, mast cells) and lymphocytes: γδ T cells, αβ T cells (CD4+ and CD8+) and innate lymphoid cells (natural killer cells) as shown in Figure I-2 and reviewed by Tay et al. (2013).

Macrophages within the skin exhibit a diverse distribution, they are either associated with blood vessels (perivascular macrophages), lymphatic vessels or they reside in the intervascular space. The perivascular macrophages regulate leukocyte extravasation thanks to their proximity to blood vessels, while those associated with lymphatic vessels are important during lymphangiogenesis (Weber-Matthiesen and Sterry, 1990).

Dendritic cells are constituted by the mentioned Langerhans cells in the basal and suprabasal epidermis and by dermal dendritic cells. They are responsible for immune response initiation thanks to high efficiency at capturing dead cells and presenting antigens, such as viruses other intracellular pathogens or skin-associated self antigens, to immune effectors, T cells, present in skin-draining lymph nodes (Bedoui et al., 2009).

Most of the T cells found in the healthy skin are tissue-resident memory T (T_{RM}) cells. This type of cells belongs to a group of memory T cells together with two subsets of circulating T cells: effector memory T (T_{EM}) and central memory T (T_{CM}) cells (Shin and Iwasaki, 2013). The T_{RM} in the epidermis are CD8+ T cells. They are long-term resident subset disconnected from the circulation, which get cytotoxic and kill target cells upon activation. CD4+ T cells, found in the dermis, are either T_{RM} or helper T cells with modulatory functions. As for the remaining dermis-residing T lymphocytes, most of them express Vγ5/Vδ1 T cell receptor (TCR) and are named dermal γδ T cells. They have been reported to enhance CD4+ T cell immunity to some infections, which appears to be facilitated by the production of interleukin (IL)-17 by dermal γδ T cells, leading to neutrophil recruitment (Heath and Carbone, 2013).

Epidermal fraction of γδ T cells is constituted by so-called dendritic epidermal T lymphocytes or DETCs (Sumaria et el., 2011). They are called so for their unique dendritic morphology. DETCs sense skin injury through recognition of an unknown ligand expressed by stressed or damaged keratinocytes. Similarly to dermal γδ T cells, the γδ TCR activation in a subset of DETCs is followed by IL-17 production, which induces expression of multiple host-defense molecules in epidermal keratinocytes (MacLeod et al., 2013).

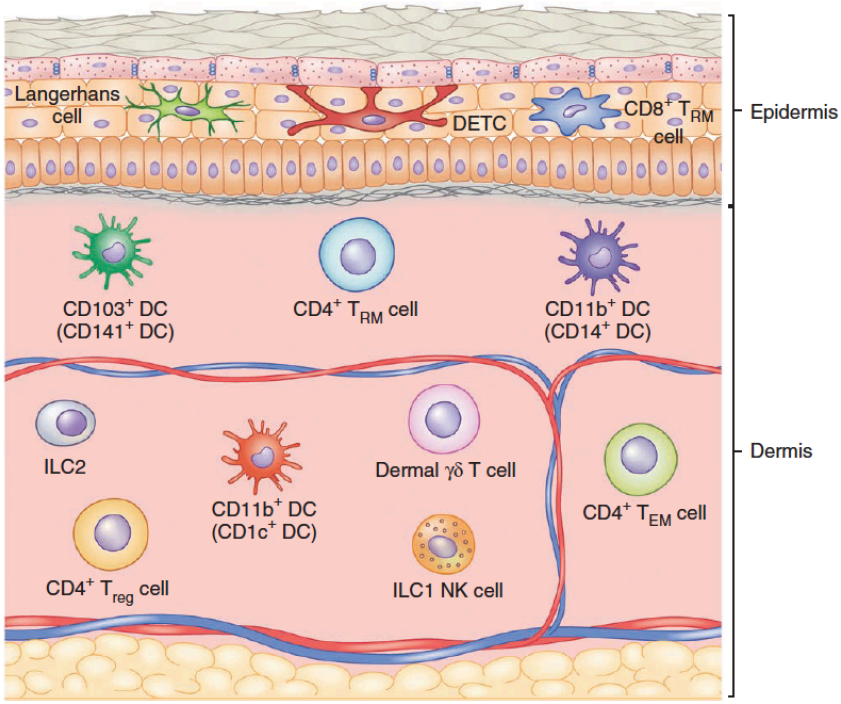

Figure I-2. Schematic representation of skin resident immune cells. DETC: dendritic epidermal T cell. T_{RM} cell: tissue-residing memory T cell. T_{EM} cell: effector memory T cell. T_{reg} cell: regulatory T cell. DC: dendritic cell. ILC: innate lymphoid cell. NK: natural killer. Note that macrophages and mast cells are not shown (Heath and Carbone, 2013).

1.2. Squamous cell carcinoma.

Skin cancers are commonly divided into two groups: melanomas and non-melanoma skin cancers (NMSC). NMSC are the most common form of malignancy in humans. In the USA there are more than 2 million cases of NMSC each year. They represent almost 95% of all cutaneous neoplasms (Dubas and Ingraffea, 2013, Kim and Armstrong, 2012). NMSC comprise two main groups: basal cell carcinoma (BCC) and squamous cell carcinoma (SCC), also called epidermoid carcinoma. BCC and SCC are named after the type of skin cells from which the tumours originate: basal cells of the basal layer and flat squamous cells of the spinous layer, respectively (www.cancer-researchuk.org). Besides, there are other less common NMSC types: keratoacanthoma, Merkel cell carcinoma, Kaposi sarcoma, cutaneous (skin) lymphoma and skin adnexal tumours (starting in hair follicles and skin glands).

Although SCC is less frequent in comparison with BCC (20% and 80%, respectively), it belongs to the most common invasive cancers in the world, with an annual incidence of 250,000 in the USA (Fig. I-3) (Chen at al., 2001). The elevated risk of metastasis of SCC is accompanied by many characteristics of lethal solid tumours of the internal organs, absent in BCC. In many countries the incidence of SCC is rising and its occurrence is usually associated with chronic UV exposure and, therefore, is especially common in people with sun-damaged skin, fair skin and albinism. Another factors that contribute to SCC development are ionising radiation, chemical agents (e.g. polycyclic aromatic hydrocarbons), human papilloma virus infections and the genetic predispositions (e.g. hereditary defects in DNA repair genes in xeroderma pigmentosum patients).

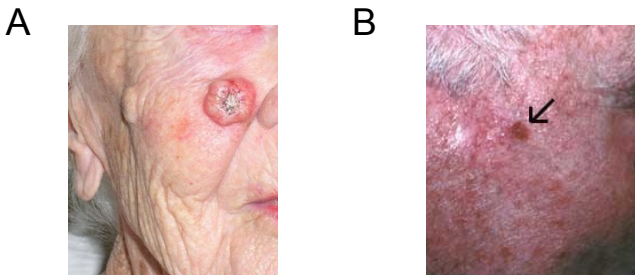

Figure I-3. Clinical demonstration of the squamous cell carcinoma on the face skin of two elderly patients. Sources: (A) American Osteopathic College of Dermatology website. (B) American Academy of Dermatology website.

Moreover, SCCs are more likely to arise in injured and chronically diseased skin (Mueller, 2006). Patients with impaired immune functions, for example those receiving immunosuppressive drugs following allogenic organ transplantation or as a therapy of inflammatory disease (e.g. in Crohn

disease) and those with lymphoma or leukaemia are also at higher risk of this tumour (Zitelli et al., 2013, Motley et al., 2002). Head and neck squamous cell carcinoma (HNSCC) is a clinical subtype of SCC and the sixth most common cancer in the world (American Cancer Society: Cancer Facts and Figures 2008). It is a result of an aberrant proliferation of the squamous epithelium lining the mucosal surfaces of the head and neck. The primary epithelial tumours of this type can develop in any mucosa-lined regions, such as the tympanic cavity, paranasal sinuses, nasal cavity, pharynx, oral cavity and larynx, whereas the metastases can occur in the neck lymph nodes, lungs and liver (reviewed by Lin and Rocco, 2011).

1.3. Genetic background of skin SCCs.

Genetic analyses of the squamous tumours revealed common mutations such as inactivation of p53, inactivation of cell cycle inhibitors, upregulation of cell cycle enhancers, mutational up-regulation of epidermal growth factor receptor (EGFR), reduction in transforming growth factor (TGF)-β signalling and activating mutations of Ras proteins (Cataisson and Yuspa, 2011). Aberrant signalling of Ras-dependent pathways has been linked to a range of human neoplasms, including skin. Activating mutations of *RAS* are found in approximately 15% of human cancers (Bos, 1989). The clinical observations and experimental data reveal that mutations of the proto-oncogene *Harvey RAS* (*H-RAS*) belong to the most frequent genetic alterations found in human skin tumours (Ananthaswamy and Pierceall, 1992). For instance, in the case of SCCs the majority of the tumours display elevated levels of guanosine triphosphate (GTP)-bound active RAS (Ridky and Khavari, 2004). Also, animal model studies show that heterozygous activation of Ras in keratinocytes is sufficient to induce benign squamous lesions. Among *Ras* gene alterations observed in murine skin carcinogenesis, *H-Ras* mutations are predominant as well (Balmain and Brown, 1988).

A number of carcinogens can provoke *Ras* mutations in the skin. The most commonly used in murine skin carcinogenesis studies is 7,12-dimethylbenz[α]anthracene (DMBA) (Hennings and Boutwell, 1970). The majority of DMBA-induced skin cancers contain mutational activation of H-Ras, which results from adenine transversion to thymidine (A>T) at the second base in codon 61 (Balmain et al., 1984). The mechanism underlying this mutation depends on T>A substitution during the first round of replication provoked by carcinogen-diol-epoxide binding to DNA, followed by a fixed transversion A:T>T:A after the second round of replication. This results in the replacement of glutamine by leucine in the protein, which, in turn, impairs the intrinsic GTPase activity. As a result mutant Ras is accumulated in its GTP-bound active form and, thereby, causes the cancerous skin phenotype.

In order to identify exact mechanisms by which the gene mutations lead to cancer, including skin cancer, molecular information obtained from human tumour studies is linked with biological processes also observed in animal experimentation. This is achieved by using an appropriate animal model that at least partially mimics the phenotypic changes along with genetic and epigenetic events (Cataisson and Yuspa, 2011).

Since H-Ras is a common signal transducer in epithelial cells, multiple changes in signalling pathways controlled by H-Ras (described in section 2.1.1) are observed in skin papillomas developed in the most studied mouse skin carcinogenesis model – the chemically induced two-stage DMBA/TPA model.

1.4. Mouse model of chemically induced two-stage skin tumorigenesis.

Cancer development, including skin cancer, is a multiple step process during which originally normal cells undergo a number of progressive changes, leading to increased proliferation phenotype. Varied physicochemical and biological factors are commonly recognised to be capable of initiation of tumorigenesis in skin (Evan and Vousden, 2001). For example, UV radiation is a skin tumour-initiating factor present in the sunlight. Another initiating agent in skin tumorigenesis is the mentioned carcinogen DMBA. However, single administration of DMBA onto shaved murine skin is not sufficient to induce skin tumorigenesis. A standard procedure established in the 1940s (Boutwell, 1964), namely the two-stage skin carcinogenesis, consists of the DMBA initiation followed by repeated applications of promoting agent, typically phorbol ester, 12-O-tetradecanoylphorbol-13-acetate (TPA), usually for 20 weeks (Fig. I-4).

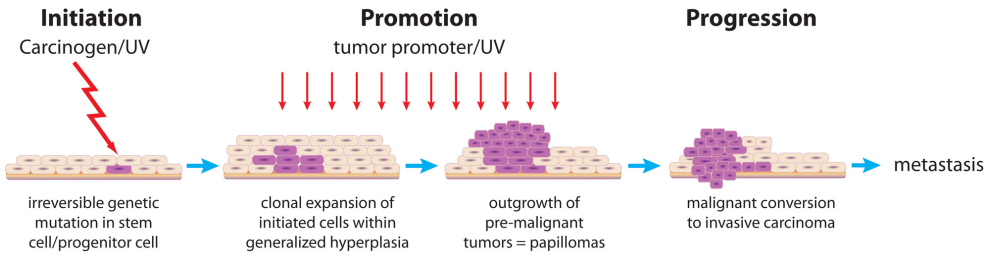

Figure I-4. Multistage mouse skin carcinogenesis model (Rundhaug and Fischer, 2010).

At the molecular level, the initiation involves DNA damage that causes mutations in specific cells of the skin, which then are exposed to regular promotion. Specifically, over 90% of tumours initiated with DMBA have a point mutation in the *H-Ras* gene (see section 1.3) (Quintanilla et al., 1986). During the promotion, enhanced proliferation and altered cell activity take place. As for

specific target cells in skin during these events, it is believed that stem cells in the interfollicular epidermis acquire *H-Ras* mutations and give rise to mutated progenitors (Schwarz et al., 2013). These, in turn, need tumour promoter (TPA), which stimulates cell divisions and leads to skin thickening, increasing the probability of survival and clonal expansion of initiated, *H-Ras* mutated cells, as illustrated in Figure I-5.

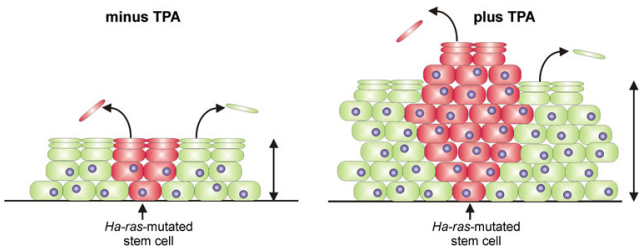

Figure I-5. Clonal outgrowth/cell death balance of progeny cells of epithelial stem cells with DMBA-induced mutations in the absence and presence of TPA treatment (Schwarz et al., 2013).

Skin papillomas, developed in the DMBA/TPA protocol, arise from hyperproliferating epidermal cells as protuberances on the skin. They form keratinized lesions due to changes in epithelial cell physiology and morphology during the tumour growth (Fig. I-6). They are characterised by certain features absent in normal skin epithelium. Tumour stroma, consisting of connective tissue and filling this protuberance from within, is separated from tumour-forming epithelial cells by a basal membrane. The basal membrane is composed of a compact, normally intact layer of highly proliferating cells. In a standard haematoxylin-eosin staining the basal cells are darker and have a dark nucleus. The tumour part above the basal membrane is formed by epithelial cells derived from basal cells. They are predominantly oval and contain a prominent pale nucleus with a large nucleolus. During the growth of tumour the cells differentiate and get keratinized, losing their vital functions.

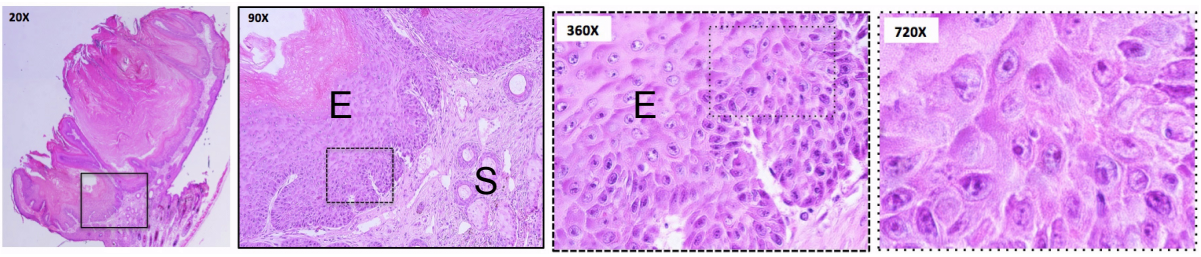

Figure I-6. Representative skin papilloma developed in the two-stage skin tumorigenesis protocol stained with haematoxylin and eosin. A whole tumour image with three rising magnifications from left to right are shown. Characteristic epithelial cells with a large pale nucleus and a prominent nucleolus can be observed. E – tumour epithelium. S – tumour stroma.

While skin papillomas are exophytic tumours that show no evidence of stromal invasion, squamous cell carcinomas have a more endophytic appearance, with stromal invasion evidenced by loss of basal membrane continuity and development of an inflammatory stromal response (Thomas-Ahner et al., 2007).

TPA is not the only chemical skin tumour promoter. The promotion stage in mouse skin can be accomplished by a wide variety of weak or noncarcinogenic agents, other than TPA, characterised by different potency (Table I-1). TPA, however, is most commonly used in the skin research.

Skin tumour promoter	Potency	Skin tumour promoter	Potency
Croton oil and its certain phorbol esters	strong	Phenolic compounds	weak
Some synthetic phorbol esters	strong	Extracts of unburn tobacco	moderate
Anthralin	moderate	Iodoacetic acid	weak
Certain long chain alkanes	weak	1-fluoro-2,4-dinitrobenzene	moderate

Table I-1. Skin tumour promoters and their potency (adapted from Slaga, 1983).

It has been demonstrated, that in the late stages of the tumour promotion a certain percentage of benign papillomas progress to carcinomas, giving rise to SCCs. This occurs spontaneously at a low frequency (Quintanilla et al., 1986). This conversion is strain-dependent and not all mouse strains are capable of developing malignant skin lesions (Woodworth et al., 2004). The mechanism underlying this process still needs a better understanding. An insight into a possible regulation of the progression was delivered by experiments with transgenic mice, selectively over-expressing the *H-ras* oncogene under different keratin promoters. It turned out that hair bulge stem cells-derived papillomas are more prone to malignant transformation, while the ones developed from interfollicular stem cell population progress into carcinomas less frequently (Brown et al., 1998).

While most human skin SCCs are associated with UV, rather than chemical carcinogenesis, 10% of the skin SCCs do have *RAS* gene mutations (Lopez-Pajares et al., 2013), and DMBA/TPA carcinogenesis has contributed substantially to the understanding of the steps of tumour development in the human skin (Hirst and Balmain, 2004).

2. Molecular mechanisms of skin tumour promotion.

Multiple molecular mechanisms are involved in the promotion stage in the two-stage skin tumorigenesis protocol. Keratinocytes with DMBA-induced mutations maintain an elevated level

of proliferation by a direct, TPA-induced activation of mitotic signalling pathways or, indirectly, as a response to inflammatory processes in skin, dependent on immunological tissue response. It has been observed that chronic wounding might also contribute to the skin tumour promotion (Rundhaug and Fischer, 2010). Moreover, since epithelial tumour development is associated with impairment in tissue structure organization, especially during progression into malignant skin carcinomas, cell adhesion-controlling molecular events may also be affected.

2.1. Signalling pathways in DMBA/TPA challenged skin and in epithelial tumours.

As mentioned above, the Ras pathway is affected due to the mutational activity of DMBA during the tumour initiation stage. Noteworthy, Ras is also one of the downstream elements of the EGFR-induced signalling pathway, activated in response to TPA challenge, occurring during skin tumour promotion (Laurent-Puig et al., 2009).

2.1.1. Ras signalling.

H-Ras forms with K- and N-Ras a family of small guanosine triphosphotases (GTPases) that transduce signal from bound receptors to downstream effector pathways (Cataisson and Yuspa, 2011).

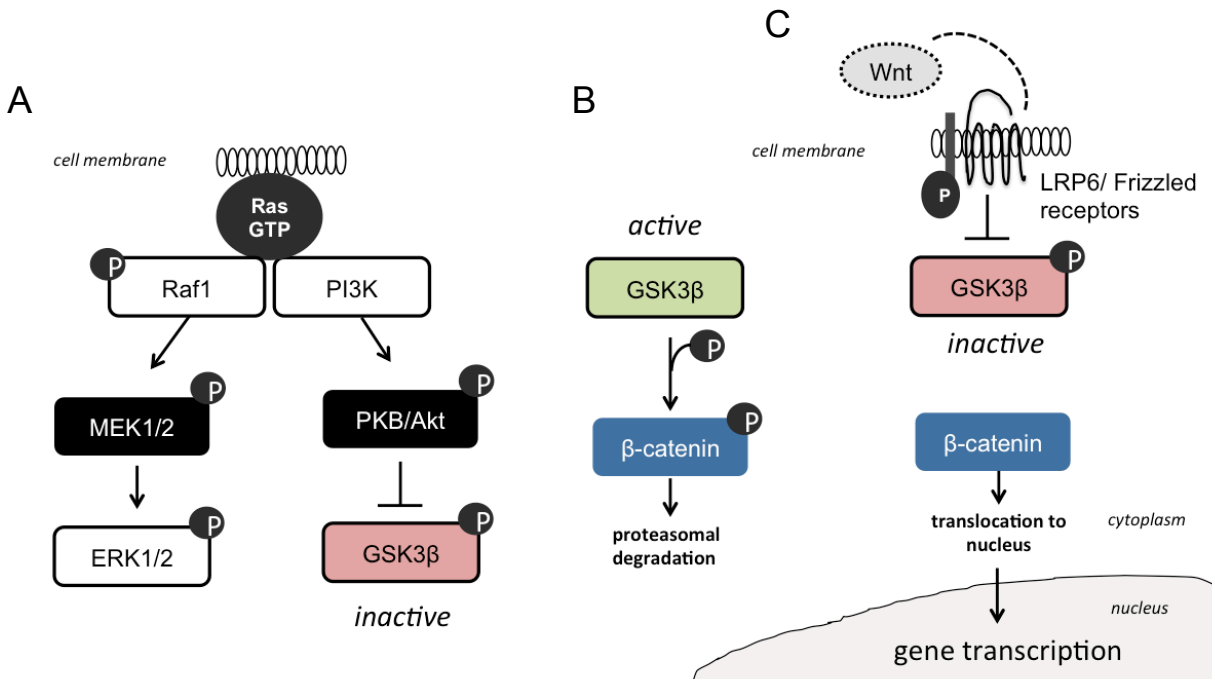

Figure I-7. (A) Ras-dependent signalling pathways. (B) Negative turnover of β-catenin by GSK3β degradation complex. Phosphorylation of β-catenin by GSK3β signals for ubiquitylation and proteasomal degradation (Aberle et al., 1997). (C) Wnt pathway. LRP – low-density lipoprotein receptor-related protein. Not all known elements are shown.

Ras cycles between inactive, guanosine diphosphate (GDP)-bound, and active, GTP-bound conformations. Ras proteins signal through extracellular signal-regulated kinase (ERK) 1/2 and phosphoinositide-3-kinase (PI3K), which are involved in the regulation of a variety of cellular responses including proliferation, survival, apoptosis and cell cycle (Schwarz et al., 2013). ERK1/2 are activated by MEK (or MKK) 1/2, whose phosphorylation depends on the upstream regulator, called Raf-1 (Fig. I-7A). The Raf-1 family, which is composed of serine/threonine kinases A-raf, B-raf and C-raf, directly interacts with the membrane anchored GTP-complexed Ras (Ehrenreiter et al., 2009).

The other target of Ras, PI3K, acts through serine/threonine protein kinase B (PKB/Akt) (Rodriguez-Viciana et al., 1994). Akt inhibits glycogen synthase kinase (GSK) 3β, which is involved in the turnover of a transcriptional factor, β-catenin (Fig. I-7B) (The GSK3β inactivation results in the accumulation of the unphosphorylated functional β-catenin (Manoukian and Woodgett, 2002).

Apart from the direct Ras-dependent pathways, there is a crosstalk between Ras signalling and protein kinase C (PKC) pathway activated by TPA. Specifically, activated PKC phosphorylates Raf kinase inhibitory protein, leading to its inactivation, thus inducing the signalling of the Ras/Raf-1/ERK1/2 (Nishizuka, 1988).

2.1.2. β-catenin signalling.

Wnt proteins are secreted factors interacting with transmembrane receptors of the Frizzled family and are expressed in adult mouse epidermis (Fig. I-7C), where they control mesenchymal-epithelial communication (Saitoh et al., 1998). β-catenin is a cytoplasmic transcription factor involved in Wnt-mediated regulation of cell adhesion, which is important in the maintenance of epithelial structures, including skin (Liu and Millar, 2010). Normal epithelium is characterised by membranous and cytoplasmic localization of β-catenin. The translocation of E-cadherin, interacting with β-catenin (Adams et al., 1996), was observed in mouse epidermis treated with TPA, which negatively influenced gap junctional cell communication by decreasing the membrane localization of E-cadherin (Jansen et al., 1996).

The nuclear localisation of β-catenin is the hallmark of constitutive signal activation and its elevated expression has been observed in epithelial tumours in mice and humans. It has been also correlated with the tumour size and its clinical stage (Lee at al., 2012). The upregulation of β-catenin pathway has also been observed in many SCCs and associated with their malignant

transformation (Malanchi et al., 2008). One of the targets of a β-catenin-mediated cascade encodes the oncogene c-Myc, whose constitutive activation often leads to carcinogenesis, especially in colon (Giles et al., 2003).

Apart from clinical observations, the importance of β-catenin signalling in epithelial tumorigenesis has been demonstrated by *in vivo* experiments in animal models. Transgenic mice expressing an activated form of β-catenin were more prone to skin tumours development (Chan et al., 1999). Moreover, it was reported that downregulation of β-catenin in human SCC13 cells by short hairpin RNA strongly decreased tumour growth of xenografts in nude mice. Moreover, the β-catenin gene ablation in the chemically induced DMBA/TPA skin tumorigenesis led to a complete regression, whereas the growth of control skin tumours was unaffected (Malanchi et al., 2008).

2.1.3. EGFR signalling.

Epidermal growth factor (EGF) is a potent mitogen for keratinocytes and is essential for normal skin epithelium. Since tumour promotion relies on cell proliferation, EGFR signalling plays an important role in skin carcinogenesis; it is one of the most frequently altered proteins in cancer. Alterations in its activity have been demonstrated in many human tumours (Harari, 2004). In particular, EGFR overexpression, the main mechanism causing the EGFR upregulation, has been observed in colon, lung, breast, cervical, prostate and HNSCC. In the case of the head and neck tumours 90% showed elevated EGFR expression (Grandis and Tweardy, 1993).

The EGFR activation is initiated upon binding to such ligands as EGF, TGF-α, heparin-binding EGF-like growth factor, amphiregulin and betacellulin (Harris et al., 2003). EGFR receptors can also be activated through ligand-independent mechanisms, including reactive oxygen species induced by UV, G protein-coupled receptors, tyrosine kinase receptors and cell adhesion molecules (Repertinger et al., 2011). Upon activation the EGFR subunits are subject to conformational changes enabling homo- and heterodimerization. This activation leads to the transcriptional activation of specific genes encoding proteins which control cell proliferation, survival, adhesion, migration and differentiation and this occurs through signalling pathways such as Ras/ERK1/2, PI3K/Akt, phospholipase C γ (PLCγ), PKC and STAT, summarised in Figure I-8 (Markovic and Chung, 2012).

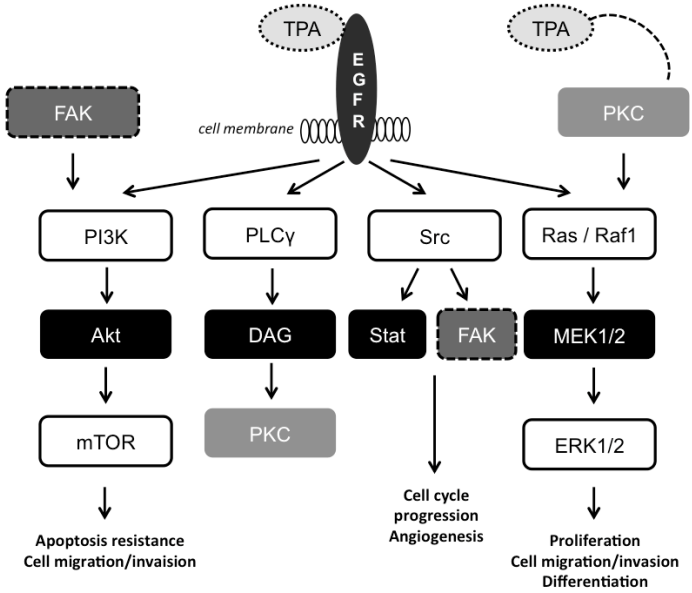

Figure I-8. EGFR downstream signalling cascades. mTOR: mammalian target of rapamycin. DAG: diacyloglycerol. FAK: focal adhesion kinase. TPA mimics the stimulatory action of the secondary messenger DAG on PKC enzymes. PKC positively induces Raf1/MEK/ERK1/2 pathway through inactivating phosphorylation of Raf kinase inhibitory protein. Not all known elements of the pathways are shown.

The expression of the EGFR ligands is increased in neoplastic keratinocytes (Dlugosz et al., 1995). TPA can also activate downstream EGFR cascades in murine skin that is accompanied by the receptor phosphorylation, indicating a direct interaction between TPA and EGFR signalling (Cichocki et al., 2012). Moreover, the chemical inhibition of EGFR effectively reduces TPA-stimulated EGFR tyrosine phosphorylation in a dose-dependent manner (Lu et al., 2007).

The implication of EGFR signalling in skin tumour promotion has been highlighted by *in vivo* experiments. For instance, transgenic mice overexpressing the ligand TGF-α in the skin developed skin papillomas in response to TPA promotion without carcinogen initiation (in the absence of *Ras* mutations), which indicates that abundance of TGF-α can act as an initiating agent and enhance tumour promotion (Wang et al., 1994).

Also, studies on the impairment of downstream elements of EGFR signalling have established its critical contribution during initiation and promotion during skin carcinogenesis. It has been demonstrated that the epidermis of mice lacking signal transducer and activator of transcription (STAT) 3, which is the Src-mediated EGFR effector, were characterised by reduced proliferative response after treatment with TPA, due to a defect in G1/S cell cycle progression (Chan et al., 2004).

2.1.4. TGF-β signalling.

Members of the transforming growth factor-β family (TGF-β1, TGF-β2, and TGF-β3) form a group of highly conserved cytokines (Roberts and Sporn, 1993). TGF-β, in the classical pathway, exerts its functions through binding to the type II receptor TβR-II, which then recruits the type I receptor, TβR-I. The latter one phosphorylates Smad2 and Smad3 proteins. Phosphorylated Smad2/3 are then able to form a complex with Smad4, which then translocate to the nucleus to modulate gene expressions as transcriptional factors (Konig et al., 2005).

Cell responses provoked by TGF-β are highly contextual throughout development, across different tissues, and also in cancer (Massague, 2008). In the skin TGF-β is required for epidermal dendritic cells (Langerhans cells) development (Kaplan et al., 2007). In skin keratinocytes, TGF-β plays a dual role. On one hand, in the physiological state, TGF-β controls skin homeostasis, on the other hand, it responds to tissue injury and inflammatory conditions, by local induction of epithelial-to-mesenchymal transition (EMT) (Roberts et al., 2001). Constitutively induced activation of TGF-β in chronically inflamed epithelium brings about permanent conversion of keratinocytes to myofibroblasts followed by complete loss of epithelial phenotype and tissue fibrosis (Border and Noble, 1994). This is in line with the observation that persistent induction of EMT via TGF-β signalling is associated with metastatic character of many cancers, including skin cancers. Moreover, mutational inactivation of the receptor TβR-II has been reported in colon, gastric, pulmonary and HNSC carcinomas (Levy and Hill, 2006).

2.2. Cytokines.

Another event in the skin during TPA-induced skin tumour promotion is the recruitment of inflammatory cells into the dermis. It is caused by secretion of proinflammatory molecules in epidermal keratinocytes. The activated macrophages, lymphocytes and leukocytes infiltrating the skin produce growth factors, cytokines and chemokines that promote cell proliferation, tissue matrix remodelling, impairment of adaptive immunity and angiogenesis (Yoshimura, 2006). When it comes to the cytokines, they are small proteins, important in inflammation signalling, such as: tumour necrosis factors, interleukins, chemokines, colony forming factors, growth factors and interferons. They also perform pivotal roles during malignant progression and, on the one hand, they induce malignant transformation, tumour growth, invasion and metastasis. However, they are also capable of activation of mechanisms leading to the tumour-limiting immune reactions. Host cells (stroma and immune cells) can produce cytokines as a response to other transforming factors or as an integral part of inflammation accompanying the tumour growth. Cytokines can

also be secreted by malignant cells due to acquired genetic alterations in cytokine expression pathways or in response to host-derived cytokines (Apte and Voronov, 2002).

2.2.1. TNF-α.

Tumour necrosis factor-α (TNF-α) plays an important role in host defence and is a critical cytokine during inflammation, including inflammation of the skin induced by tumour promoters. It is synthesised as a transmembrane pro-peptide and, following proteolytic conversion, is released in a soluble homotrimer (Balkwill, 2006). Two TNF-α receptors, TNFR1 and TNFR2, have specific expression patterns and are activated differently. TNFR1 is expressed constitutively in most cells and binds soluble TNF-α, whereas TNFR2 is specific mostly for hematopoietic and immune cells, and binds membrane-bound TNF-α. Activated TNFRs signal through multiple signalling pathways, e.g. IκB kinase (IKK)/nuclear factor (NF)-κB and MAPKs/activator protein (AP)-1 (Wajant et al., 2003). The activation of the transcription factors leads to upregulation of genes involved in the differentiation and apoptosis (anti-apoptotic factors in the case of NF-κB or pro- and anti-apoptotic in the case of AP-1).

The data from murine cancer models suggest that the mechanism by which TNF-α promotes the early stages of cancer involves both the initiated cancerous cells and inflammatory cells in the surrounding stroma. Indeed, TNF-α produced chronically in the tumour microenvironment may contribute to malignant promotion and progression via the induction of expression of chemokines and their receptors (e.g. CXCR4, CXCL12, CCL8) and, therefore, has anti-apoptotic or mitogenic roles (Balkwill, 2006). When it comes to TNF-α in skin tumorigenesis, its implication was highlighted by Moore et al. (1999) who demonstrated that mice deficient in TNF-α during the two-stage DMBA/TPA skin protocol developed 5-10% of the number of tumours in wild type mice. It has also been observed that TNFR1$^{-/-}$ mice were shown to confer a profound resistance in this protocol too (Arnott et al., 2004), and the tumour promoting activity of TNF-α in the skin was linked with the regulation of B cells (Schioppa et al., 2011).

2.2.2. Interleukins.

Although the interleukin (IL) family is large and its members have pleiotropic effects in inflammation and immune responses, only some of them play roles in the skin and are undoubtedly linked with skin tumour promotion and skin cancer (Rundhaug and Fisher, 2010). The predominant interleukins in skin are IL-1, IL-6 and IL-17.

IL-1α and IL-1β, constitutively expressed in cultured keratinocytes, are upregulated by exposure to TPA (Kupper et al., 1987; Oberyszyn et al., 1993). Another example is NF-κB-inducible cytokine, IL-6, which promotes STAT3 activation and promotes tumorigenic phenotype of HNSCC in humans (Lee et al., 2006). The transcription factor STAT3 is constitutively activated in many human malignancies and has been suggested to play an important role in carcinogenesis (Al Zaid and Turkson, 2008; Kim et al., 2007). Tumour promoters, including TPA, activate STAT3 in mouse epidermis and STAT3 is maintained in an activated state in DMBA/TPA-induced papillomas (Chan et al., 2004). In line with these observations are studies showing that increased levels of IL-6 are considered a bad prognostic factor in oral SCC (OSCC) (Culig, 2013). IL-6-dependent tumorigenic effects can be also mediated at the epigenetic level. Specifically, OSCC cells induced by IL-6 have been shown to promote gene expression alterations through DNA hypomethylation and abberant promoters hypermethylation (Gasche et al., 2011).

IL-17 is produced in skin by dermal and epidermal γδ T cells (the latter are called DETC) and T helper 17 (Th17) cells. γδ T cells are an innate source of IL-17, preceding the development of the adaptive Th17 cell response (Martin et al., 2009). IL-17 has been linked with pro-oncogenic roles in DMBA-induced skin carcinogenesis, through IL-6-mediated STAT3 signalling regulation (Wang et al., 2010). Also, the pathogenesis of psoriatic disease has been associated with IL-17 functions (Raychaudhuri, 2013).

2.3. Post-transcriptional regulation.

TPA-dependent signalling alterations in post-transcriptional regulation of protein expression have been linked with skin cancer development as well. One of the processes affected by TPA in epithelial cells is the proteasomal degradation of proteins.

The translation inhibitor, programmed cell death protein 4 (Pdcd4) is the first tumour suppressor found to regulate protein translation. The decrease in Pdcd4 levels, upon TPA treatment, was attributed to increased proteasomal degradation through ubiquitylation, catalysed by the E3-ubiquitin ligase β-TrCP1 (Schmid et al., 2008). The negative regulation of Pdcd4 in response to TPA has been reported in murine skin and in vitro in keratinocytes and the deregulated protein translation has been associated with carcinogenesis, including skin carcinogenesis. Also, Pdcd4-haploinsufficient and Pdcd4-deficient mice have increased papilloma incidence in a chemically induced DMBA/TPA skin carcinogenesis protocol, suggesting that Pdcd4 protects against skin tumour formation. Interestingly, the negative regulator of Pdcd4, β-TrCP1, has been biochemically and genetically shown to control the stability of β-catenin (Latres et al., 1999). On the other hand,

the data on the natural compound, erioflorin, have revealed its stabilizing effect on both Pdcd4 and β-catenin, thanks to the inhibition of TPA-induced β-TrCP1/target-protein interactions (Blees et al., 2012). Moreover, it has been reported that expression patterns of PDCD4 correlated with β-catenin protein levels in gastric cancers in humans (Kakimoto et al., 2011).

Taken together, the data on the TPA-induced proteasomal regulation indicate, that tumorigenesis, including skin tumorigenesis, can be controlled at the level of ubiquitylation and that tumour promoters might target tumour suppressors functioning at the post-transcriptional level.

3. p38γ and p38δ MAPKs.

3.1. MAPKs.

Mitogen-activated protein kinase (MAPK) signalling plays a pivotal role in eukaryotic cell physiology. Its deregulation may lead to diseases and cancer development. Through multiple co-ordinated pathways, MAPKs control a wide range of cell responses, such as growth, proliferation, differentiation, migration and apoptosis, depending on cell type and stimulus (Chen et al., 2001). The MAPK pathways are activated by a range of external stimuli resulting from physicochemical changes of the cell microenvironment. This activation requires ligand binding to different receptors such as tyrosine kinase receptors (hormones and growth factors), cytokine receptors or serine-threonine kinase receptors (TGF-β-related polypeptides). Besides, the exposure to environmental stresses (osmotic shock, ionizing radiation and ischemic injury) can also bring about MAPKs-dependent reactions in a cell (Kyriakis and Avruch, 2012).

There are four well-characterised conventional MAPK subfamilies: ERK1/2, ERK5, Jun N-terminal kinases (JNK) 1/2 and p38 kinases (designated as p38 MAPK). In the basal state they are catalytically inactive and require activating phosphorylation by upstream kinases, whose activity is also regulated by phosphorylation, so that signal transduction occurs by sequential phosphorylation of the following protein kinase families: MAPK kinase kinases (MKKKs or MAP3Ks), MAPK kinases (MKKs or MEKs or MAP2Ks) and MAPKs (Cuenda and Rousseau, 2007; Keshet and Seger, 2010) (Fig. I-9).

The activation of the MAPKs relies on dual phosphorylation of threonine (T) and tyrosine (Y) in a conserved T-X-Y motif (where X are different amino acids depending on the MAPK) in an activation loop of the subdomain VIII.

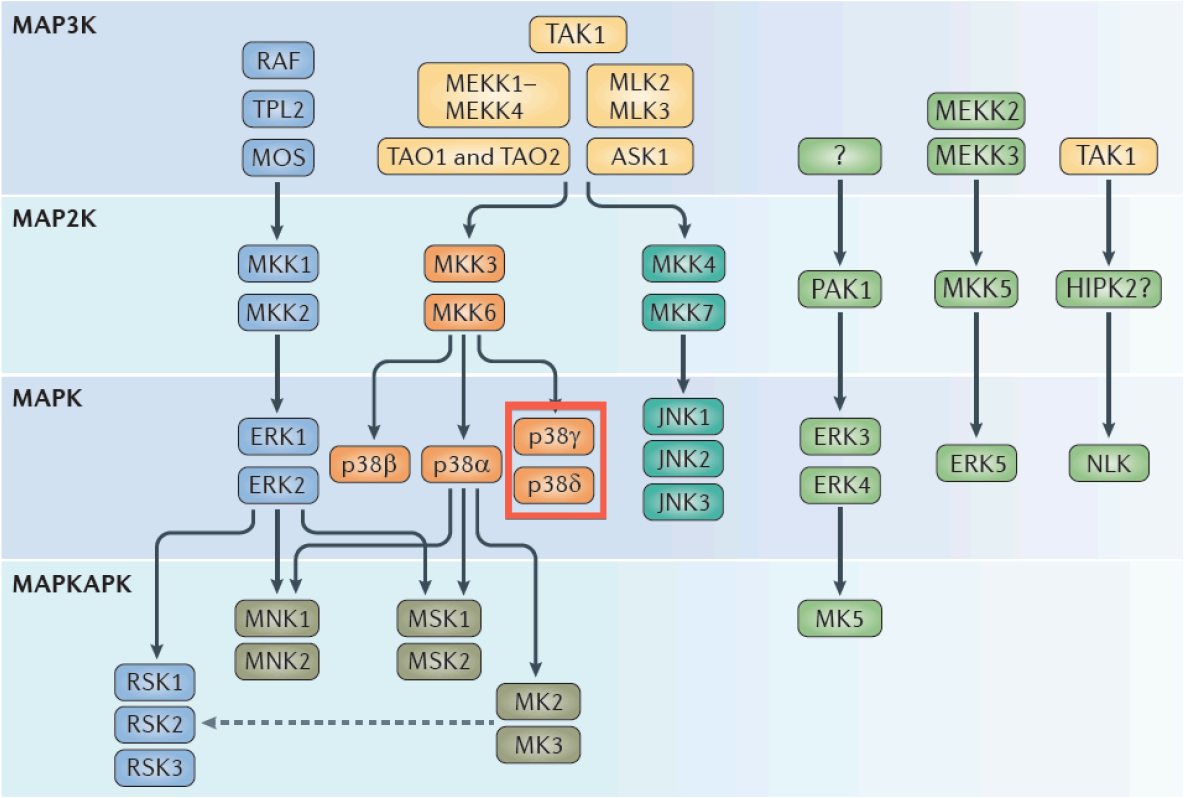

Figure I-9. Canonical mammalian MAPK signalling pathways (Arthur and Ley, 2013). p38γ and p38δ are highlighted in a red frame.

These phosphorylations lead to conformational reorganizations that stabilize the activation loop in an open and extended conformation, enabling substrate binding and its phosphorylation (Cuenda and Rousseau, 2007). MAPKs' targets (substrates) include another protein kinases (such as MAP kinase activated proteins kinase, MAPKAPK), transcription factors and other cytoplasmic targets (Risco and Cuenda, 2012).

3.2. p38 MAPKs.

The mammalian p38 subfamily of MAPK has four members (p38α, p38β, p38γ, p38δ) encoded by different genes, which share high homology reaching approximately 60% of the sequence. Among p38 MAPK isoforms, p38α, often referred to as stress-activated protein kinase (SAPK) 2a was identified at first by four independent groups (Han et al., 1994; Rouse et al., 1994; Freshney et al., 1994; Lee et al., 1994) and is the best-described isoform so far.

It has been widely described that p38α contributes to the regulation of pro-inflammatory and anti-inflammatory cytokines production during inflammation (Cuenda and Rousseau, 2007), both at transcriptional and post-transcriptional levels (Wagner and Nebreda, 2009). Of note, the production of inflammatory agents, such as TNF-α, IL-1β and IL-6 is a crucial factor involved in a

number of human pathologies (Crohn disease, rheumatoid arthritis, psoriasis) (Cuenda and Rousseau, 2007). Besides, p38α has been associated with proliferation (Halawani et al., 2004), survival (Aguirre-Ghiso, 2007), differentiation (Ventura et al., 2007; Cuadrado and Nebreda, 2010), cell migration and metastasis (Rousseau et al., 2006), all hallmarks of carcinogenesis (Hanahan and Weinberg, 2011). Moreover, p38α knock-out mice are embryonically lethal (Allen et al., 2000).

Since the identification of p38α, three additional isoforms have been identified: p38β (or SAPK2b) (Jiang et al., 1996), p38γ (or SAPK3) (Lechner et al., 1996; Li et al., 1996; Mertens et al., 1996) and p38δ (or SAPK4) (Goedert et al., 1997; Jiang et al., 1997). The four isoforms are characterised by different tissue expression patterns, with p38α being ubiquitously expressed at a high level in most cells and with the remaining three p38s distributed in a more tissue-specific manner. p38β is specific for brain tissue, p38γ is abundantly expressed in skeletal muscle and p38δ in endocrine glands and small intestine (Cuadrado and Nebreda, 2010; Risco and Cuenda, 2012). Contrary to p38α knock-out mice, p38β, p38γ and p38δ-deficient mice develop normally (Sabio et al., 2005; Beardmore et al., 2005).

Although all p38 isoforms share some substrate specificities, there is similarity between p38α and p38β kinases and between p38γ and p38δ, due to the existence of particular substrates being better phosphorylated by the former ones than the latter ones and the other way around (Cuenda and Rousseau, 2007; Risco and Cuenda, 2012). For example all p38α, p38β (p38α/β), p38γ and p38δ (p38γ/δ) phosphorylate the transcription factors ATF2, Elk-1 and SAP1 at similar rate but p38γ/δ are much less effective than p38α/β in activating MAPKAP kinase-2 and MAPKAP kinase-3 (Cuenda et al., 1997; Goedert et al., 1997). Another reason for the division of p38s into p38α/β and p38γ/δ is the amino acid sequence similarities: p38β is 75% identical to p38α, whereas p38γ and p38δ - only 62% and 61%, respectively. Of note, p38γ and p38δ are more identical to each other and share ~70% of the amino acid sequence. Moreover, they differ in response to chemical inhibition, namely to the compounds SB203580 and SB202190. It has been demonstrated that only p38α and p38β are inhibited by these compounds, whereas p38γ/δ were completely unaffected by the inhibitors.

The activation of distinct p38 MAPK isoforms is regulated by selective and synchronized action of the MKKs, in response to cell stress (Risco and Cuenda, 2012). p38α activation in response to TNF-α is severely impaired in cells lacking MKK3 and MKK6, suggesting that both kinases are

necessary for full p38α activity in response to this cytokine (Brancho et al., 2003). MKK3 and MKK6 are also essential for the activation of p38γ and p38β induced by environmental stress (Fig. I-10).

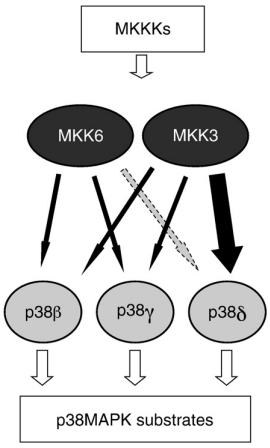

Fig. I-10. Activation of p38β, p38γ and p38δ by MKK3 and MKK6. MKK6 phosphorylates and activates p38β and p38γ, and also p38δ only in the absence of MKK3. MKK3 phosphorylates and activates p38β and p38γ, and is the principal p38δ activator. MKK3 and MKK6 are activated by different MKKK, and p38MAPK phosphorylates several substrates following activation (Remy et al., 2010).

MKK6 is besides the major activator of p38γ in response to TNF-α, whereas p38δ activation by ultraviolet radiation, hyperosmotic shock, anisomycin or TNF-α is mediated by MKK3. Moreover, in response to osmotic stress, MKK3 and MKK6 are crucial in regulating the phosphorylation of the p38γ substrate SAP97/hDlg and its activity as scaffold protein (Remy et al., 2010).

3.3. p38γ and p38δ.

A growing number of evidences reveal important roles of the alternative p38 MAPKs in pathological processes. Altered expression of p38γ/δ has been correlated with some pathophysiological conditions in animals and humans. For example, elevated level of p38γ protein has been reported in gliomas (Yang et al., 2013). An important step in understanding the functions of p38γ and p38δ was the generation of mice deficient in p38γ, p38δ and both p38γ/δ (Sabio et al., 2005), which delivered a potent tool in animal based-research. Indeed, a growing number of experiments with knock-out mice in the last 5 years demonstrate an increasing interest in p38γ and p38δ as shown in Table I-2.

Nonetheless and contrary to p38α, little is known about the exact mechanisms of p38γ/δ functions and the contribution of p38γ/δ to human pathologies remains largely unknown.

Model	Observations	Reference
Knock-out	p38γ/δ$^{-/-}$ mice have decreased tumour number comparing with WT in colitis-associated colon cancer model.	del Reino et al., 2014
Knock-out	p38γ$^{-/-}$ mice are resistant to cardiac hypertrophy.	Thomas et al., 2014
Knock-out	p38γ/δ deficiency reduces arthritis severity and inflammatory response in collagen-induced arthritis model.	Criado et al., 2014
Knock-out	p38γ/δ deficiency reduces cytokine production in response to lipopolysaccharide.	Risco et al., 2012
Knock-out	p38γ is activated in slow skeletal muscle and is involved in the normal growth and their development.	Foster et al., 2012
Conditional knock-out	Global and myeloid cell-targeted p38δ loss decreases alveolar neutrophil accumulation and attenuates ALI*.	Ittner et al., 2012
Xenograft	p38γ-deficiency in Ras-transformed fibroblasts increases tumorigenesis.	Cerezo-Guisado et al., 2011
Xenograft	p38γ knocking-down delays tumorigenesis in breast cancer cells and long-distance metastasis to the lungs.	Meng et al., 2011
Xenograft	p38γ and its specific phosphatase PTPH1 exert oncogenic activities in Ras-activated colon cancer cells.	Hou et al., 2010
Knock-out	p38δ$^{-/-}$ mice display improved glucose tolerance due to enhanced insulin secretion from pancreatic β cells.	Sumara et al., 2009
Knock-out	p38δ$^{-/-}$ mice exhibit marked resistance to chemically induced two-stage skin carcinogenesis.	Schindler et al., 2009

Table I-2. Selected data from mouse model research on the involvement of p38γ/δ in different pathologies. (*) inflammation induced acute lung injury.

They have been described to be involved in such processes as proliferation, apoptosis, cell cycle regulation, regulating tumorigenesis, as well as in metabolic disease and tissue regeneration (Risco and Cuenda, 2012; Cuadrado and Nebreda, 2010; Cuenda and Rousseau, 2007). Moreover, apoptosis in keratinocytes treated with okadaic acid has been linked with p38δ-dependent regulation (Kraft et al., 2007).

3.3.1. p38γ and p38δ in tumorigenesis and inflammation.

Evidences from cell base assays support p38γ and p38δ tumorigenic functions by modulating processes implicated in cellular malignant transformation (Risco and Cuenda 2012; Yang et al., 2013; Faraone et al., 2009).

It has been described that p38δ promotes the malignant phenotype of squamous cell carcinoma by regulating cell proliferation and invasion (Junttila et al., 2007). In rat intestinal epithelial cells (IEC) and in human breast cancer, p38γ RNA and protein expression increases during RAS-

induced transformation (Loesch and Chen, 2008; Tang et al., 2005). p38γ knock-down in IEC blocks the Ras transformation activity and results in the significant diminution of the oncogenic characteristics of breast cancer cells (Meng et al., 2011). Additionally, one recent study shows that p38γ mediates Ras-induced senescence at least partly by stimulating the transcriptional activity of p53 through direct phosphorylation; in contrast p38α appears to regulate senescence in a p53-independent manner (Kwong et al., 2009). These results indicate that increased p38γ gene expression is required for *Ras* oncogene activity but the mechanism by which p38γ may promote Ras transformation is not clear. Interestingly, p38δ was recently shown to mediate TPA-induced epidermal cell proliferation in mice, and mice lacking p38δ show reduced susceptibility to the development of TPA-induced skin carcinomas (Schindler et al., 2009). All these results indicate the oncogenic function of p38γ and p38δ.

Contrary, there is one study that shows pieces of evidence indicating that p38γ and p38δ have a role in the suppression of tumour development using mouse embryonic fibroblasts (MEFs) derived from mice lacking p38γ or p38δ (Cerezo-Guisado et al., 2011). Lack of either p38γ or p38δ increases cell migration and metalloproteinase-2 secretion, whereas only p38δ deficiency impairs cell contact inhibition. In addition, lack of p38γ in K-Ras-transformed fibroblasts leads to increased cell proliferation as well as tumorigenesis both *in vitro* and *in vivo* (Cerezo-Guisado et al., 2011). Moreover, it has been shown that p38δ regulates the expression of the zonula occludens (ZO)-1 protein, an integral component of functional tight junctions in differentiating human epidermal keratinocytes and in human SCC cell lines (Siljamäki et al., 2014). Considering the fact that ZO-1 is associated with the motility of malignant cells (Tuomi et al., 2009), this observation is in agreement with the increased cell migration of p38δ-deficient MEFs (Cerezo-Guisado et al., 2011). Nonetheless, the discrepancies between different studies could be due not only to the difference in the experimental model and approaches used, but also to the distinct nature of cells and processes that are involved in each study.

In addition to the potential role of p38γ and p38δ in tumorigenesis, they have a critical role in inflammation, which is an important process in tumour promotion (Hanahan and Weinberg, 2011). Recent studies in mice deficient in p38γ, p38δ, or both showed that they are essential for the innate immune response (Arthur and Ley, 2013; Risco et al., 2012; Criado et al., 2014). Combined deletion of p38γ and p38δ impairs proinflammatory cytokine production in macrophages and dendritic cells in response to the bacterial lipopolysaccharide (LPS) (Risco et al., 2012). p38γ/δ deficient mice are less sensitive than controls to LPS-induced septic shock and, in a mouse collagen-induced arthritis model, p38γ/δ deficiency greatly reduced symptom severity and

joint damage compared to WT mice (Criado et al., 2014). In both experimental models, p38γ/δ deficient mice produced lower levels of cytokines such as IL-1β, TNF-α, INF-γ and IL-17 (Risco et al., 2012; Criado et al., 2014). These findings strongly suggest that p38γ and p38δ are implicated in linking inflammation and tumour promotion and/or progression.

3.3.2. p38γ and p38δ in keratinocytes and skin.

p38δ has been also suggested to play an important role in inducing keratinocyte differentiation by regulating the expression of involucrin, which is a protein expressed during keratinocyte differentiation (Eckert et al., 2003). It has been shown that activation of exogenously expressed p38δ by differentiation-inducing agents correlates with increased involucrin promoter activity in keratinocytes (Efimova et al., 2003). This occurs in a p38α/β-independent manner, and what is more, p38γ is poorly expressed in keratinocytes (Dashti et al., 2001). More data supporting the idea that p38δ may play a role in keratinocyte differentiation come from a study carried out in lesional psoriasis skin. Psoriasis is a chronic inflammatory skin disorder characterised by keratinocytes hyperproliferation and differentiation. It has been shown that the activity of p38α, p38β, and p38δ is augmented in lesional psoriasis skin compared with nonlesional psoriasis skin (Johansen et al., 2005). Additionally, p38δ may have a dual role in keratinocytes contributing not only to the differentiation process, but also to their apoptosis in a PKCδ-dependent manner, though the exact mechanisms by which p38δ may regulate keratinocyte differentiation or apoptosis are still unknown (Kraft et al., 2007; Adhikary et al., 2010). It is important to notice that most of the pieces of evidence involving p38δ in regulating keratinocyte differentiation or apoptosis are based in overexpression experiments and require verification using other tools to both inhibit the activity or the expression of different p38 MAPKs.

It had been claimed that p38δ deletion in mice brings about a higher resistance to skin carcinogenesis induced chemically by a two-stage DMBA/TPA protocol (Schindler et al., 2009). However, so far there have been no published data on the importance of the other alternative p38 isoform, p38γ, in skin tumour development.

OBJECTIVES

The principal objective of this thesis has been to gain an insight into an involvement of p38γ and p38δ MAPKs in the inflammation-associated skin tumorigenesis using wild type, p38γ$^{-/-}$, p38δ$^{-/-}$ and p38γ/δ$^{-/-}$ mice.

In order to achieve this goal we had the following partial aims:

1. To examine the *in vivo* contribution of p38γ and p38δ in skin tumour development by performing the chemically induced two-stage DMBA/TPA skin tumorigenesis protocol, describing the expression and activation of oncogenic proteins, measuring the infiltration of immune cells and the proliferation of epithelial cells in the tumours.

2. To analyse the p38γ and p38δ involvement in the DMBA-induced apoptosis in the skin.

3. To investigate the implication of p38γ and p38δ in the skin inflammation by measuring epithelial cell proliferation and analysing immune cells infiltration, cytokines production and cell signalling in the TPA-treated skin.

4. To generate stable p38γ, p38δ and p38γ/δ knock-down clones of the human epidermoid cancer (squamous cell carcinoma) A-431 cells and to examine their role in cell proliferation and tumorigenesis by xenograft assay.

MATERIALS AND METHODS

1. Animal-based experiments.

1.1. Mice.

Mice, lacking p38γ (p38γ$^{-/-}$), p38δ (p38δ$^{-/-}$) and p38γ/δ (p38γ/δ$^{-/-}$), used in most of the experiments, have been described (Risco et al., 2012). All strains were backcrossed onto C57BL/6 background for at least nine generations. For xenograft experiments we used Crl:NU(Ico)-Foxn1nu nude mice purchased from Charles River. They had been developed from the transfer of the nude gene to a CD-1 mouse through a series of crosses and back-crosses. The animals do not have a thymus and are therefore unable to produce T-cells and are consequently immunodeficient. Mice used in experiments were housed in specific pathogen-free conditions in accordance with the European Union regulations and the work was approved by a local CNB-CSIC ethical review.

1.2. Two-stage skin tumorigenesis protocol.

Chemically induced two-stage skin tumorigenesis is a widely used protocol, which enables an induction of benign skin papillomas (skin tumours) and malignant squamous cell carcinomas (SCC) in murine dorsal skin. It consists of topical treatment with an inducing agent, carcinogen, called 7,12-dimethylbenz[α]anthracene (DMBA) followed by repeated treatments with an inflammatory and mitogenic, promoting agent – 12-O-tetradecanoylphorbol-13-acetate (TPA). This protocol relies on clonal expansion of initiated epidermal cells (keratinocytes) in response to continuous TPA treatments leading to tumorigenic changes in skin (Fig. M-1).

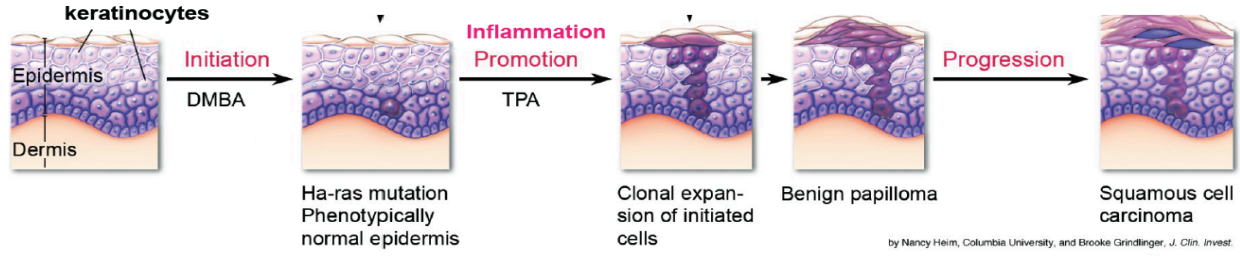

Figure M-1. Schematic representation of chemically induced two-stage skin tumorigenesis protocol. Only some benign papillomas progress to an advanced stage of squamous cell carcinoma in this protocol.

WT, p38γ$^{-/-}$, p38δ$^{-/-}$ and p38γ/δ$^{-/-}$ mice at the age of 6 – 8 weeks were subject to a two-stage induced skin tumorigenesis protocol. Dorsal skin was shaved with a clipper 24 hours prior to initiation. On day 1 the mice were topically treated with DMBA dissolved in acetone. On day 2 topical treatments with TPA, dissolved in acetone were carried out continually every 3 – 4 days (two treatments weekly) for 19 weeks. Mice were regularly examined for tumours appearance

and, from week 15, the growth of tumours was measured with a calliper every fortnight. At the end of the experiment (week 29) mice were sacrificed and samples derived from the tumours and healthy skin were processed for further analysis. Control mice were treated with acetone alone. Details of the compounds used are summarised in Table M-1.

Agent	Full Name	Amount	Utility
DMBA	7,12-dimethylbenz[α]anthracene	100 μg [390 nmol]	Inducer
TPA	12-O-tetradecanoylphorbol-13-acetate	10 μg [16 nmol]	Promoter

Table M-1. Chemical compounds used in the two-stage skin carcinogenesis protocol.

1.3. Acute skin inflammation model.

Acute skin inflammation experiments were carried out using single topical applications of either TPA (10 μg in 200 μl acetone, 16 nmol) or acetone (control) onto shaved dorsal skin. Following mice sacrifice, at different times post-treatment (30 min, 1, 2, 4, 8, 12, 24 and 48 hours), samples were excised and analysed.

1.4. Xenograft model.

Xenograft tumour growth experiment were carried out using athymic nude mice (described in paragraph 1.1) and genetically modified clones of human epidermoid cancer cells, A-431 (described in paragraphs 2.3 and 2.4). The clones were stable knock-down for p38γ and/or p38δ and their establishment has been described in more detail in section 4.1 of Results.

Mice, at the age of 6 – 8 weeks, received subcutaneous injections of 10^6 A-431 cells diluted in sterile DMEM and the growth of tumours was monitored every 2 – 4 days for about 3 weeks. Tumour volume was calculated by the formula: V = (Dxd2)/2, where D and d are the longest and shortest diameter in mm, respectively.

1.5. Assessment of cell proliferation.

We used the 5-bromo-2´-deoxyuridine (BrdU)-based immunofluorescence staining protocol in order to establish the proliferation rates in skin and tumour samples. Mice were given intra-peritoneal injections of BrdU (100 mg/kg body weight), dissolved in sterile PBS, 2 hours prior to sacrifice. Excised skin and tumour samples were fixed in 70% ethanol or in 10% neutral buffered formalin solution (NBF) for up to 48 hours at room temperature (RT) and then processed for

dehydration and paraffin embedded blocks preparation. Tissue sections (of 5 μm of thickness) were immunostained with anti-BrdU antibody (Table M-2), according to a protocol described in section 3.6, and the numbers of BrdU-positive epithelial cells, found in skin interfollicular areas (acute skin inflammation experiments) or in tumours (DMBA/TPA protocol), were counted in at least 8 fields per sample.

Antibody	Company and Reference No.	Dilution	Type
BrdU [BU1/75 (ICR1)] (Rat)	Abcam, ab6326	1:100	Primary
Alexa Fluor 647 Goat Anti-Rat	Molecular Probes, A-21247	1:200	Secondary

Table M-2. Antibodies used in cell proliferation protocol.

2. Cell culture methods.

2.1. General cell culturing.

Human Embryonic Kidney (HEK) 293T and epidermoid carcinoma (A-431) cells were cultured in Dulbecco´s Modified Eagle´s Medium (DMEM) (Lonza, Belgium) routinely supplemented with 10% foetal bovine serum (FBS), 4 mM L-glutamine and 1% antibiotics (penicillin and streptomycin) in 10 cm (P10) cell culture plates at 37°C, 5% CO_2 and 90% relative humidity in an incubator. Cells were split 1:8 every 3-4 days (after reaching 80-90% confluence). Cells were washed once with PBS and disaggregated by incubation with 0.05% trypsin/0.02% EDTA/PBS (1.5 ml per plate) at 37°C for 5-10 min until cells detached. Trypsin was then inactivated by adding 3.5 ml medium with 10% FBS and cells were diluted in fresh medium.

2.2. Cell freezing and thawing.

For long-term storage of cells they were frozen in freezing medium and stored in cryovials in liquid nitrogen. Briefly, the cells were cultured on P10 plates to 70-80% confluency. Following removal of the medium and washing with PBS, the cells were harvested using trypsin/EDTA solution (750 μl) to detach them. Cells suspended in trypsin were then mixed with 750 μl of freezing medium composed of 80% of FBS and 20% DMSO (to get a final DMSO concentration – 10%) and transferred into a 2 ml cryovial. To allow gradual freezing, the cryovials were covered abundantly with paper towel and placed at -80°C for three days. Subsequently, the cryovials transferred to liquid nitrogen (-180°C).

To start a new cell culture from frozen cells, the cryovials were rapidly thawed using a bath (37°C) and diluted in fresh medium in P10 plates. To facilitate the recovery, medium was changed on next day.

2.3. Lentivirus short hairpin RNA production in HEK293T cells.

Short hairpin RNA (shRNA) constructs in the pLKO.1 lentiviral expressing vectors were purchased from Open Biosystems Thermo Scientific (Table M-3) to knock-down endogenous p38γ and p38δ in A-431 cells. HEK293T packaging cell line was used for lentivirus production in so-called 3rd generation packaging system.

Gene Silenced	Clone ID	Catalog No.	Antisense Sequence (5' → 3')	shRNA Name *
p38γ	TRCN0000006145	RHS3979-9575012	AAAGTCCGTGAAGTCATCCAG	145
p38γ	TRCN0000006147	RHS3979-9575014	ATCAGGAGTGAATACGTCCAG	147
p38γ	TRCN0000006148	RHS3979-9575015	TCATCATACTTCTGGACCTGG	148
p38γ	TRCN0000006149	RHS3979-9575016	AACAGCTCGGACTGGAAGGGC	149
p38δ	TRCN0000055428	RHS3979-9569233	TAGAAGTCATAGAAGTTGCGC	428
p38δ	TRCN0000000827	RHS3979-9569234	TTCTAAGGAATCATCAAACGG	827
p38δ	TRCN0000000828	RHS3979-9569235	ATTTGGCCGCTTTGTCGTTCA	828
p38δ	TRCN0000009973	RHS3979-9631088	TTTGGCCGCTTTGTCGTTCAG	973
p38δ	TRCN0000009978	RHS3979-9631084	GAAGATCTCGGACTGAAAGGG	978
p38δ	TRCN0000009979	RHS3979-9631085	TAGAAGTCATAGAAGTTGCGC	979

Table M-3. shRNAs used for lentiviral particles production. (*) shRNA names used in Results.

Briefly, 2.5 x 10^6 cells were seeded on a six-well culture plate (P6) and incubated overnight (day 1). On day 2 the medium was removed and fresh medium was added. Four hours later a mixture of plasmids encoding shRNA and viral components, diluted in 150 mM NaCl solution and containing 5% JetPei, was added drop-wisely onto the medium for transient transfection. Each shRNA lentivirus-containing medium was produced in two wells. The transfection was performed, introducing simultaneously four different plasmids into the cells. The plasmids were suspended in 1 ml of medium per well (Table M-4): shRNA-pLKO.1 (plasmid with puromycin resistance and encoding either p38γ shRNA or p38δ shRNA) and three plasmids belonging to a packaging system, i.e. pRSV-Rev (plasmid encoding Rev, responsible for the RNA transport), pMDLg/pRRE (plasmid containing [1] Gag, coding for the virion main structural proteins; [2] Pol, responsible for the lentivirus-specific enzymes; and [3] Rev-responsive element RRE, a binding site for the Rev

protein) and pMD2.G (plasmid encoding VSV-G, a lentivirus envelope protein). An empty pLKO.1 vector (without any shRNA gene) was used to produce viral particles as well. After 6 hours of the transfection the medium was removed and fresh medium was added. On day 4 the virus-containing medium was collected from each well, filtered with 0.45 μm-pore syringe filters and stored at -80°C. In order to produce more lentivirus with the same cells, fresh medium was added and viral particles were produced for another 24 hours. Collection and filtration of the viral-containing supernatants was repeated on day 5 and the plates were discarded in the end.

Vector	Utility	Amount
pLKO.1	HIV-1-derived transfer plasmid, expressing puromycin resistance proteins (and shRNA)	3.00 μg
pMD2.G	Envelope plasmid, encoding VSV-G-derived heterologous envelope protein for pseudotyping	0.70 μg
pRSV-Rev	Packaging plasmid, producing viral particles, includes Rev (export of RNA from the nucleus)	0.35 μg
pMDLg/pRRE	Packaging plasmid, producing viral particles, includes RRE, Gag and Pol	1.80 μg

Table M-4. Vectors used to produce lentivirus particles in HEK293T. Amounts are given per 2 ml.

2.4. Infection of A-431 cells with lentivirus.

For A-431 infection with shRNA-containing lentivirus, the cells were grown on P6 plates in standard conditions. Once 80-90% of cell confluency was achieved the medium was removed and 1 ml of defrost lentivirus-containing medium (supplemented with 10 mM Hepes and 8 μg/ml hexadimethrine bromide – Polybrene®) was added to each well (two wells in a P6 per one shRNA, in duplicates) and incubated overnight. On next day, 0.4 ml of the same lentivirus-containing medium (with 10 mM Hepes and 8 μg/ml Polybrene®) was added into the wells in order to increase the efficiency of the infection. 48 hours after the initiation of the infection the medium was removed and fresh medium was added. Six hours later selection of antibiotic resistance-bearing cells was started by adding 0.5 μg/ml of puromycin into the medium. The cells were carefully observed and the infection was considered successful when non-infected cells were dead (after 4 - 5 days of selection). To assure that the resistance is not lost and to grow stable clones, the cells were diluted 1:8 and they continued their growth in puromycin-containing medium for at least one week more (two weeks of selection in total). The efficiency of shRNA-mediated down-regulation was addressed by immunoblotting and bands density quantification.

3. General methods.

3.1. Protein and RNA samples preparation.

In order to extract protein and RNA from murine tissue, mice were sacrificed and skin and tumour samples were collected and mechanically disrupted in liquid nitrogen. Tissue powder was processed for protein and RNA extractions. Proteins were extracted using a lysis buffer containing 1% Triton X-100, 50 mM Tris-HCl pH 7.5, 1 mM EDTA, 1 mM EGTA, 50 mM NaF, 10 mM sodium glicerophosphate, 5 mM sodium pyrophosphate, 1 mM sodium orthovanadate, 270 mM sucrose and 0.1% β-mercaptoethanol, supplemented with a mixture of proteinase inhibitors: 1 mM benzamidine and 0.2 mM phenylmethylsulfonyl fluoride (PMSF). Protein concentration in the lysates was measured with the Coomassie Plus (Bradford) reagent. For RNA preparation tissue powder was homogenised in TRI Reagent (Sigma Aldrich) and RNA-containing fraction was mixed with isopropanol for RNA precipitation. After double precipitate washing (with 70% ethanol) and dissolving in RNase-free water, the RNA concentration was measured with Nanodrop spectrophotometer.

For cell-derived protein/RNA extractions the same buffers and procedures were applied. Detached cells were spinned down, supernatants removed and pellets washed once with sterile PBS. Then lysis buffer (for protein extraction) or in TRI Reagent (for RNA extraction) was added to the pellet and the same procedure was followed, as described above. In some cases, the protein extraction from adherent cells was done by adding cold lysis buffer onto the cells just after medium removal and detaching them off the plate with a cell scraper.

Loading buffer 5X		
Compound	**Amount**	**Concentration**
Tris-HCl pH 6.8 [2M]	12.5 ml	250 mM
Glicerol [87%]	34.4 ml	30%
SDS	10 g	10%
β-mercaptoethanol	5 ml	5%
Bromophenol blue	A spatule	0.02%
Distilled water (up to)	100 ml	--

Table M-5. Loading buffer (1X) components.

Running buffer 1X		
Name	**Amount**	**Concentration**
Glycin	14.4 g	192 mM
Tris base	3 g	25 mM
SDS	1 g	0.1%
Distilled water (up to)	1000 ml	--

Table M-6. Running buffer (1X) components.

3.2. Immunoblotting.

Proteins were denatured using standard loading buffer, containing 5% of β-mercaptoethanol (Table M-5), for 10 minutes at 99°C. Polyacrylamide gel electrophoresis (PAGE) was performed according to a common procedure. Denatured protein samples, at volumes corresponding to equal

protein amounts, were loaded into 12.5% polyacrylamide gel wells and proteins were separated in a running buffer (Table M-6) connected to a source of electrical field (120 V, for 2 hours, at RT). Separated proteins were electro-blotted onto a nitrocellulose membrane using a transfer buffer (Table M-7). The membrane was later incubated with a blocking solution, containing 5% skimmed milk dissolved in a TBS buffer (Table M-8) with 0.1% of Tween 20, at RT.

Transfer buffer 1X		
Name	**Amount**	**Concentration**
Glycin	2.9 g	39 mM
Tris base	5.8 g	48 mM
SDS	0.37 g	0.04%
Methanol	200 ml	20%
Distilled water (up to)	1000 ml	--

Table M-7. Transfer buffer (1X) components.

TBS buffer 10X		
Name	**Amount**	**Concentration**
Tris base	60.5 g	100 mM
NaCl	438 g	1.5 M
pH 8.0		
Distilled water (up to)	5000 ml	--

Table M-8. TBS buffer (10X) components.

Antibody	Company and Reference No.	Dilution *	Specificity **
Akt	Cell Signaling, #9272	1:1000 (WB)	Rb
BrdU [BU1/75 (ICR1)]	Abcam, ab6326	1:100 (IF)	Rt
CD3	Dako, A 0452	1:50 (IF)	Rb
Myeloperoxidase (MPO)	Abcam, ab9535	1:500 (WB), 1:25 (IHC)	Rb
P38α (C-20)	Santa Cruz Biotechnology, sc-535	1:1000 (WB)	Rb
P38γ (GST-SAPK3) 0.25 mg/ml	DSTT***, S524A 1st Bleed	0.5 μg/ml (1:500) (WB)	Sh
P38γ (GST-SAPK3) 0.86 mg/ml	DSTT***	1.5 μg/IP	Sh
P38δ 0.30 mg/ml	DSTT***, S526A 3rd Bleed	0.2 μg/ml (1:1500) (WB)	Sh
P38δ 0.28 mg/ml	DSTT***	1.0 μg/IP	Sh
Phospho-Akt (Ser473)	Cell Signaling, #9271	1:1000 (WB)	Rb
Phospho-Akt (Ser473)	Cell Signaling, #9277	1:200 (IHC)	Rb
Phospho-ERK1 (Tyr204)	Santa Cruz Biotechnology, sc-7383	1:200 (IHC)	Rb
Phospho-p38 MAP Kinase (Thr180/Tyr182)	Cell Signaling, #9211	1:500 (WB)	Rb
Phospho-p44/42 (Erk1/2) (Thr202/Tyr204)	Cell Signaling, #9101	1:1000 (WB)	Rb
Phospho-STAT3 (D3A7) (Tyr705)	Cell Signaling, #9145	1:1000 (WB), 1:200 (IHC)	Rb
STAT3	Santa Cruz Biotechnology, sc-482	1:1000 (WB)	Rb
α-Tubulin	Invitrogen, 32-2500	1:1000 (WB)	Ms
β-Catenin	Millipore, MAB2081	1:20000 (WB), 1:100 (IHC)	Ms

Table M-9. Primary antibodies used in the experiments. (*) WB - western blot (immunoblotting); IHC - immunohistochemistry; IF - immunofluorescence; IP -immunoprecipitation. (**) Rb - rabbit; Sh - sheep; Ms - mouse; Rt - rat. (***) Division of Signal Transduction Therapy, Dundee, UK.

The blocked membrane was incubated overnight with a primary antibody (Table M-9) diluted in a blocking solution at 4°C. Protein expression was addressed using fluorescent secondary antibodies (Table M-10) and LI-COR Odyssey infrared scanning.

If not stated otherwise, in the experiments with the mouse skin, total protein lysates from three mice were grouped (pooled) and run in gels in the same well at the amount of 45 μg, which corresponds to the sum of three equal amounts from each animal (15 μg).

Antibody and Specificity	Company and Reference No.	Dilution *
Alexa Fluor 647 Goat Anti-Rat	Molecular Probes, A-21247	1:200 (IF)
Alexa Fluor 680 Donkey Anti-Sheep	Molecular Probes, A-21102	1:5000 (WB)
Alexa Fluor 680 Goat Anti-Rabbit	Molecular Probes, A-21109	1:5000 (WB)
Alexa Fluor 700 Goat Anti-Mouse	Molecular Probes, A-21036	1:5000 (WB)
Alexa Fluor 790 Donkey Anti-Rabbit	Molecular Probes, A-11374	1:20000 (WB)
Biotin Goat Anti-Mouse	Jackson Immunoresearch, 115-066-071	1:500 (IHC)
Biotin Goat Anti-Rabbit	Jackson Immunoresearch, 111-066-008	1:500 (IHC)
CY3 Goat Anti-Rabbit	Jackson Immunoresearch, 111-166-046	1:400 (IF)
CY5 Goat Anti-Mouse	Jackson Immunoresearch, 115-176-071	1:400 (IF)

Table M-10. Secondary antibodies used in the experiments. (*) WB - western blot (immunoblotting); IHC - immunohistochemistry; IF - immunofluorescence.

3.3. Real-time quantitative PCR.

cDNA for real-time quantitative PCR (qPCR) was generated from 0.5 μg of total RNA using the High Capacity cDNA Reverse Transcription Kit (Applied Biosystems) in a 10 μl of final reaction volume. The qPCR reactions were performed in triplicate using 5 μl of each cDNA 1/40 dilutions, 10 μM of each oligonucleotide and HOT FIREPol qPCR mix (Solis Biodyne) in a total volume of 8 μl in MicroAmp Optical 384-well plates (Applied Biosystems). PCR reactions were carried out in an ABI PRISM 7900HT (Applied Biosystems). The amount of amplified DNA was measured through the emission of light by the SYBR green dye, intercalating in synthesised double stranded DNA. All samples were measured in triplicates. SDS v2.2 software was used to analyse results. Specific amplification was controlled by melting-curve analysis. The data were exported, processed to Microsoft Excel and analysed by the Comparative Ct Method (DDCt). X-fold change in mRNA expression was quantified relative to unstimulated WT samples from the same experiment. GAPDH mRNA was used as a housekeeping gene. The sequences of the oligonucleotides used in this thesis can be found in Table M-11.

Gene	Forward Sequence (5' → 3')	Reverse Sequence (5' → 3')
KC (CXCL1)	CCTTGACCCTGAAGCTCCCT	CGGTGCCATCAGAGCAGTCT
MIP-2 (CXCL2)	CCTGGTTCAGAAAATCATCCA	CTTCCGTTGAGGGACAGC
GAPDH	CCCATCACCATCTTCCAGGA	CGACATACTCAGCACCGGC
IL-1β	TGGTGTGTGACGTTCCCATT	CAGCACGAGGCTTTTTTGTTG
IL-6	GAGGATACCACTCCCAACAGACC	AAGTGCATCATCGTTGTTCATACA
p38α	AACCAGACAGTGGATATTTGGTC	TGAGCTTCAACTGATCAATATGGT
p38γ	ACCTGATGAGTCTCTGGACGA	CCAGATCAGTGCCCATGAAT
p38δ	GGACCCTGAGGAGGAGACA	GTTTGAGATCTCTTTGTAGATGTGTTG
TNF-α	CTGTAGCCCACGTCGTAGC	TTGAGATCCATGCCGTTG
TGF-β	GGAACTCTACCAGAAATATAGCAACAATTC	TGTAATCCGTCTCCTTGGTTCAG
β-catenin	GCAGCAGCAGTTTGTGGAG	TGTGGAGAGCTCCAGTACACC

Table M-11. Sequences of the oligonucleotides used in the experiments.

3.4. Immunoprecipitation.

Specific anti-p38γ (1.5 μg) and anti-p38δ (1 μg) primary antibodies were first coupled to 10 μl of Protein G Sepharose beads (GE Healthcare) per one immunoprecipitation by incubating at 4°C for 30 min in a mechanic shaker. In order to remove the excess of the uncoupled antibody PBS was added, the beads spinned down and supernatant removed. Then, skin protein lysates (1.6 mg) were incubated with the beads (containing appropriate coupled antibody) for 2 hours at 4°C. After the incubation the captured proteins on the beads were centrifuged (13.000 x g), supernatants discarded and the beads washed twice in a lysis buffer containing 0.5 M NaCl, and then twice in lysis buffer alone. To visualise the immunoprecipitated proteins pellets were subjected to immunoblotting.

3.5. Immunohistochemistry.

Formalin-fixed, paraffin-embedded skin and tumour sections were deparaffinised using xylene for 20 min and rehydrated with 3-min incubations in ethanol at decreasing concentrations (2x 100%, 1x 90% and 1x 70%). The antigen retrieval was performed by heating up the sections in 0.01 M

citrate buffer (pH 6.0) for 15 min. The samples in hot citrate buffer were placed on ice for 20 min to cool down gradually. The activity of endogenous peroxidase was blocked by incubating for 20-min in 3.3% of hydrogen peroxide (H_2O_2) in methanol at RT. To block unspecific proteins the sections were incubated, for 1 hour at 37°C, in 20% of goat serum in 3% of bovine serum albumin (BSA) in distilled water. After the blocking step, incubations in different primary antibodies were performed in accordance with manufacturer's recommendations. The antibodies were diluted in blocking solution and then added onto the tissue sections that were placed in a humid chamber for an overnight incubation at 4°C. On next day, the sections were washed with PBS-Tween 0.1% (Table M-12) three times for 5 min. Biotinylated secondary antibodies were used to bind to the primary antibodies in accordance with their specificity during 1-hour incubation at RT.

PBS buffer 10X		
Name	**Amount**	**Concentration**
NaH_2PO_4	2.56 g	21 mM
Na_2HPO_4	11.92 g	84 mM
NaCl	87.66 g	1.5 M
pH 6.8		
Distilled water (up to)	1000 ml	--

Table M-12. PBS buffer (10X) components.

Signal amplification was achieved incubating for 40 min at RT in a solution containing avidin–biotin-peroxidase complexes from ABC kit (Vectastain). The oxidation of 3,3'-diaminobenzidine (DAB, Vector Laboratories), catalysed by the peroxidase attached to biotin in avidin-biotin complex enabled visualisation of the protein of interest thanks to (1) the high affinity of avidin to the biotin attached to the secondary antibody and (2) to the brown coloured product of the reaction. The signal was observed by light microscopy. Final processing of the samples consisted in haematoxylin counterstaining and ethanol-based dehydration followed by slides mounting, using VectaMount medium (Vector Laboratories).

3.6. Immunofluorescence of BrdU-positive cells.

Sections were deparaffinised and rehydrated as described in 3.5. Following the last ethanol incubation the sections were rinsed with MiliQ water and PBS and then treated with 1 N ice-cold hydrochloric acid (HCl) for 10 min followed by incubation in 2 N HCl at RT to cause DNA breakage. PBS washings and borate buffer (0.1 M) incubation for 12 min at RT served to neutralise the acidity. Incubation with 5% goat serum in PBS, containing 0.25% Triton X-100, for 1.5 hours at RT was used to block unspecific bindings. The incubation with an anti-BrdU primary antibody (Table

M-2) was performed in a humid chamber overnight at RT. After this the sections were washed three times with PBS. Finally, a secondary antibody (Table M-10), labelled with a fluorescent marker, was added. Nuclei were stained with Hoechst33342 and BrdU-positive cells were observed using Leica MicroFluor microscope.

3.7. TUNEL.

Apoptotic cells in skin epithelium were stained using terminal deoxynucleotidyltransferase (TdT)-mediated dUTP nick-end label (TUNEL) staining. Briefly, paraffin-embedded skin sections were deparaffinised and rehydrated as described above. The cells were washed with PBS and permeabilized in PBS containing 0.5% Triton X-100. Next, the sections were pre-incubated for 15 min at RT in freshly prepared TdT 1X buffer (Table M-13) containing 1mM cobalt (II) chloride. The TdT-based reaction was carried out in a humid chamber at 37°C for 1 hour in the same buffer, containing besides 3% TdT (v/v) (Roche, ref. 03333574001) and 2% biotin-16-dUTP (v/v) (Roche, 11093070910). After this the sections were washed twice with PBS containing 0.01% Tween 20. Sections were then incubated with streptavidin conjugated with a cyanine fluorochrome (Cy5). Nuclei were stained with Hoechst33342. The slides were observed by fluorescent microscopy.

TdT buffer 5X		
Name	**Amount**	**Concentration**
Distilled water	15 ml	--
BSA	0.038 g	0.125%
Tris buffer pH 8.8 [1 M]	3.75 ml	125 mM
Sodium cacodylate trihydrate	6.42 g	1 M
pH 6.6		
Distilled water (up to)	30 ml	--

Table M-13. TdT buffer (5X) components.

4. Statistical analysis.

For statistical analyses GraphPad Prism 5 was used. Differences were considered statistically significant for $P<0.05$ (*). If not stated otherwise, not significant differences between the corresponding groups from different genotypes have not been shown on the graphs.

RESULTS

1. p38γ and p38δ are essential for skin tumorigenesis.

Using a well established procedure, the two-stage DMBA/TPA skin tumour induction, in C57BL/6 mice deficient in p38γ (p38γ$^{-/-}$), p38δ (p38δ$^{-/-}$) and both (p38γ/δ$^{-/-}$), we have addressed p38γ and p38δ role in skin tumour development.

1.1 p38γ and p38δ are expressed in mouse skin.

We first checked that both p38γ and p38δ were expressed in the skin of wild type (WT) mice. We also confirmed the lack of p38γ expression in skin from p38γ$^{-/-}$ mice, the lack of p38δ expression in p38δ$^{-/-}$ skin samples and the lack of both p38s in p38γ/δ$^{-/-}$ by immunoblotting, using anti-p38γ and anti-p38δ specific antibodies (Fig. R-1A).

1.2. p38γ and p38δ deletion impairs chemically induced skin tumorigenesis.

WT, p38γ$^{-/-}$, p38δ$^{-/-}$ and p38γ/δ$^{-/-}$ mice were subjected to the complete DMBA/TPA protocol for 19 weeks and monitored for papillomas formation for another 10 weeks (Fig. R-1B). 29 weeks after DMBA administration WT, p38γ$^{-/-}$ and p38δ$^{-/-}$ but not p38γ/δ$^{-/-}$ mice developed skin papillomas (Fig. R-1C). First skin papillomas were developed in WT and p38γ$^{-/-}$ mice at week 10. Some of the tumours in WT mice disappeared between weeks 12 and 13. In the case of p38δ$^{-/-}$ mice, the development of the earliest papillomas was observed at week 15 (Fig. R-1D, E). The maximum average tumour number in these three genotypes was observed between weeks 19 and 21 (Fig. R-1E). Tumour incidence in that period reached 90% in WT, 80% in p38γ$^{-/-}$and about 60% in p38δ$^{-/-}$ mice and slightly decreased during the remaining time of the experiment, mostly due to the regression of the smallest papillomas (Fig. R-1D, E, F), which is a phenomenon commonly observed in this protocol (Kopp-Schneider and Portier, 1992). Mice deficient in p38γ/δ, on the other hand, developed first small papillomas at week 19 and all of them disappeared after week 20. Therefore, there were no p38γ/δ$^{-/-}$ tumours observed from week 21 until the end of the experiment (Fig. R-1C, D, E).

In addition, tumour size displayed different patterns in WT, p38γ$^{-/-}$ and p38δ$^{-/-}$ mice. Only WT and p38γ$^{-/-}$ mice developed large (above 100 mm^3) and/or medium (21 – 100 mm^3) papillomas during the TPA promotion stage, i.e. until week 19 (Fig. R-1F), while the p38δ deficiency seems to have slowed down the tumour growth. This observation might be due to a markedly delayed appearance of the papillomas in p38δ$^{-/-}$ mice.

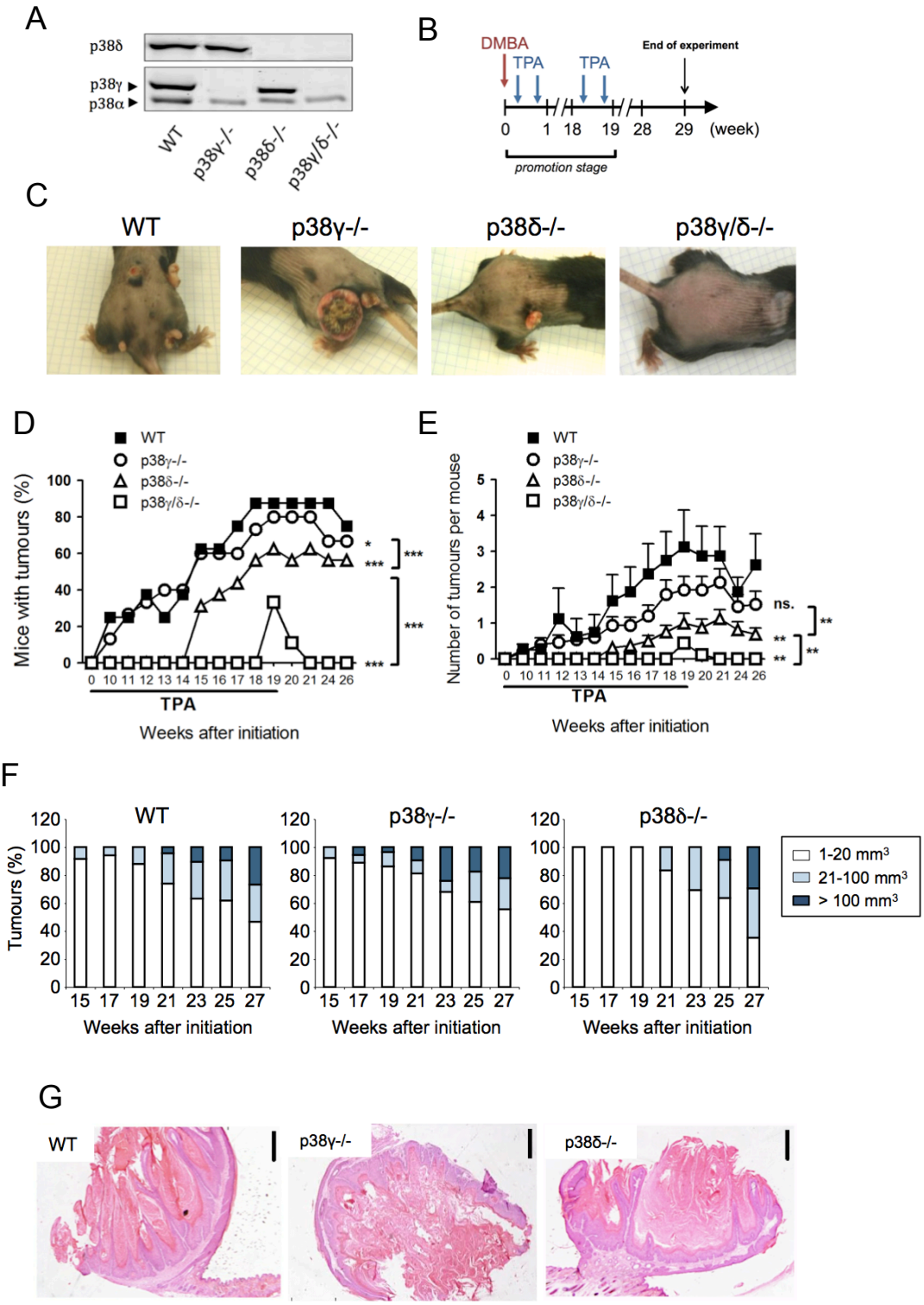

Figure R-1. (A) Immunoblot of p38γ and p38δ in the skin of WT, p38γ$^{-/-}$, p38δ$^{-/-}$ and p38γ/δ$^{-/-}$ mice. (B) Schematic representation of the DMBA/TPA protocol. (C) Representative pictures of the mouse skin at week 29. (D) Tumour incidence (percentage of tumour-bearing mice) in WT (n=8), p38γ$^{-/-}$ (n=15), p38δ$^{-/-}$ (n=16) and p38γ/δ$^{-/-}$ mice (n=9), *P<0.05, ***P<0.001 (two-way ANOVA). (E) Tumour number per mouse. Results are means +/- SEM, ns. - not significant, **P<0.01 (two-way ANOVA). (F) Percentage of tumour size in WT, p38γ$^{-/-}$ and p38δ$^{-/-}$ mice between weeks 15 and 27 of the procedure. (G) Representative images of haematoxylin-eosin (HE) staining of skin papillomas from WT, p38γ$^{-/-}$ and p38δ$^{-/-}$ mice. Scale bars: 500 μm.

In conclusion, our results showed that the absence of the p38δ isoform led to a delayed skin tumour induction and to a more reduced tumour multiplicity. Notably, the deletion of both p38γ and p38δ resulted in a marked resistance to skin tumorigenesis, leading to no mice bearing skin papillomas at the end of the experiment. Besides, the p38γ deficiency reduced tumour incidence comparing with WT (Fig. R-1D), although the differences in tumour numbers between WT and p38γ$^{-/-}$ mice were not signifficant (Fig. R-1E).

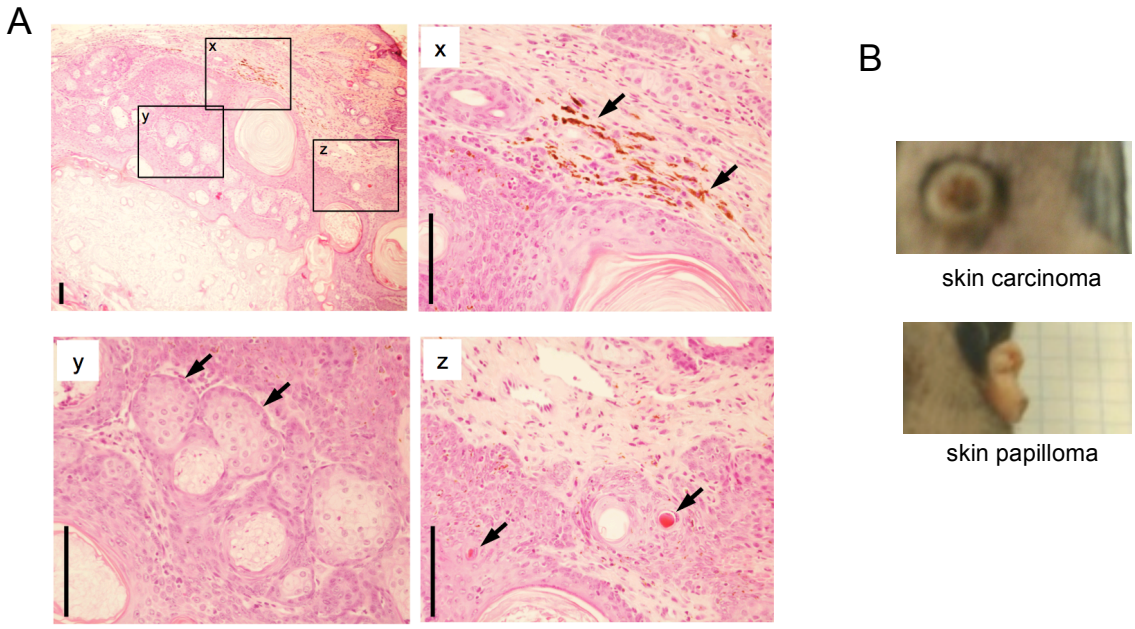

Figure R-2. (A) HE staining of a skin papilloma progressed to carcinoma and three magnifications highlighting its characteristic features marked with black arrows: (x) pigment depositions, (y) squamous cell nests and (z) keratin pearls. Scale bars: 100 μm. (B) A progressed carcinoma and a benign papilloma.

As for the phenotype of the developed skin papillomas we did not find differences between the genotypes. They were benign, non-invasive, keratin-producing skin growths which were formed within overgrown epidermis and contained a conserved, intact basal membrane that surrounded the tumour stroma (Fig. R-1G). In most of the cases the progresssion to malignant state did not take place. We only found one p38γ$^{-/-}$ tumour that displayed features of malignancy typical for squamous cell carcinomas, such as: numerous keratin pearls, squamous cell nests, pigment depositions and, importantly, stromal invasion evidenced by decomposition of basal membrane continuity (lack of clear border between tumour epithelium and tumour stroma) (Fig. R-2A). Besides this tumour was less keratinized at first glance and less exposed outside the skin when compared with the remaining skin tumours (Fig. R-2B).

1.3. Analysis of the expression and activation of different proteins in papillomas.

Mutational activation of a signal transducer H-Ras is very common in DMBA-induced skin papillomas. It provokes changes in a number of signalling pathways - effectors of Ras oncoprotein, which are involved in cell cycle and apoptosis regulations (Schwarz et al., 2013). Among direct and indirect targets of Ras there are MAPKs such as p38 MAPK and Akt, β-catenin and STAT3.

To gain an insight into a possible mechanism, by which p38γ and p38δ affect skin tumour development and tumour growth, we analysed the expression and phosphorylation of the p38 isoforms, as well as expression of STAT3, Akt and β-catenin in the papillomas. The proteins were analysed by immunoblotting from tissue lysates and by immunohistochemistry in paraffin-embedded tissue sections from DMBA/TPA treated WT, p38γ$^{-/-}$ and p38δ$^{-/-}$ mice at the end of the protocol at week 29.

1.3.1. p38.

Immunoblotting analysis of p38s showed that both p38γ and p38δ are expressed in skin papillomas (Fig. R-3A). However, in comparison with the healthy skin, p38δ in papillomas displayed very augmented levels, whereas p38γ was much less expressed. The difference was then confirmed by qPCR of the p38γ/δ genes in healthy skin and papilloma samples (Fig. R-3B).

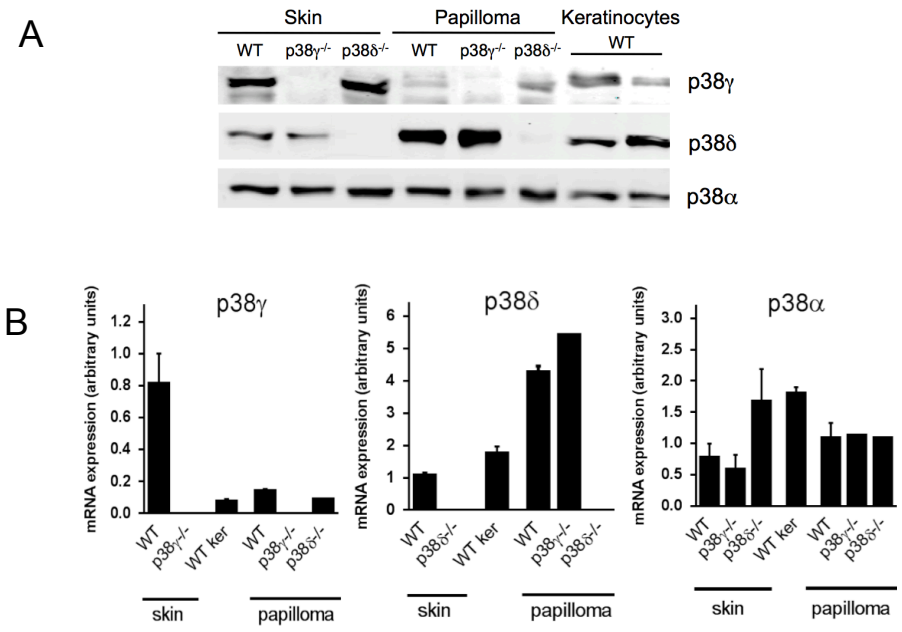

Figure R-3. Expression of p38α, p38γ and p38δ in healthy skin and skin papillomas from WT, p38γ$^{-/-}$ and p38δ$^{-/-}$ mice and in WT keratinocytes by (A) immunoblotting and (B) qPCR. (A) Each well in the blot was loaded with protein from one animal. (B) GAPDH mRNA was used as housekeeping gene. Results were normalised to a WT skin and represented as means +/- SEM (n=3).

Interestingly, primary keratinocytes from WT mice, used as control, were characterised by p38γ/δ expression. p38γ/δ mRNA and proteins levels were more similar to those in papilloma samples than to the healthy skin. This finding correlates with the predominant presence of (transformed) keratinocytes in skin tumours. p38γ was also expressed in p38δ$^{-/-}$ papillomas and p38δ was expressed in p38γ$^{-/-}$ (Fig. R-3A, B). Contrary to p38γ and p38δ expression in the skin and papillomas, the levels of p38α expression did not vary between the three genotypes and were similar in tumours and healthy skin samples (Fig. R-3A, B).

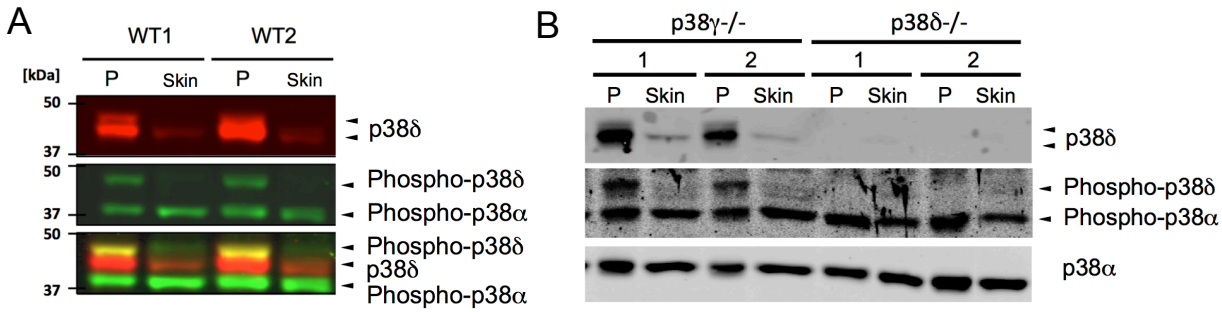

Figure R-4. Immunoblot of p38δ and phospho-p38 in skin papillomas (P) and healthy skin from two WT (A), two p38γ- and two p38δ-deficient mice (B): The upper band in the p38δ blot (red colour in panel A) is phosphorylated p38δ, as confirmed by its colocalisation with the upper band in the phospho-p38 blot (green in panel A) and merging the colours (yellow in panel A). The band shift of phospho-p38δ was also observed in papillomas from p38γ$^{-/-}$ mice. p38α was used as control.

Immunoblot analysis of p38δ in WT papillomas revealed that this is not only highly expressed in but also highly phosphorylated, which indicates a possible contribution of p38δ in the tumour growth and development (Fig. R-4A). Phosphorylated p38δ suffered a band shift in its electrophoresis mobility and it could be also detected with the phospho-p38 antibody, which recognises all four phosphorylated p38 isoforms. Importantly, the deficiency of p38γ did not influence the expression and phosphorylation of p38δ in skin papillomas (Fig. R-4B).

These results indicate that the activation of p38δ is important in skin tumour formation, which is consistent with our previous data showing that p38δ-deficient mice (p38δ$^{-/-}$ and p38γ/δ$^{-/-}$) were more resistant to DMBA/TPA protocol than p38δ-expressing mice (WT and p38γ$^{-/-}$). On the other hand, despite the low abundance of p38γ in skin papillomas, at this stage we could not rule out its role in skin tumorigenesis.

1.3.2. β-catenin, STAT3, Akt.

Wnt/β-catenin signalling has been shown to play an important role in a variety of human tumours. It has been described that nuclear localisation of β-catenin, a hallmark of activated Wnt signalling, is also associated with the malignant transformation of squamous cell carcinoma of the oesophagus, adenocarcinoma of the stomach and adenocarcinoma of the colon (Ogasawara et al., 2006, Takayama et al., 1996).

We have analysed β-catenin localisation in skin papillomas by immunohistochemistry with anti-β-catenin antibody. Similarly to what had been demonstrated by Malanchi et al. (2008), some stainings, regardless of the genotype, displayed an increased accumulation of nuclear β-catenin in the basal layer epithelium (Fig. R-5), whereas the remaining epithelial cells were characterised mostly by membranous staining, which is typical for normal epithelium (Lee at al., 2012).

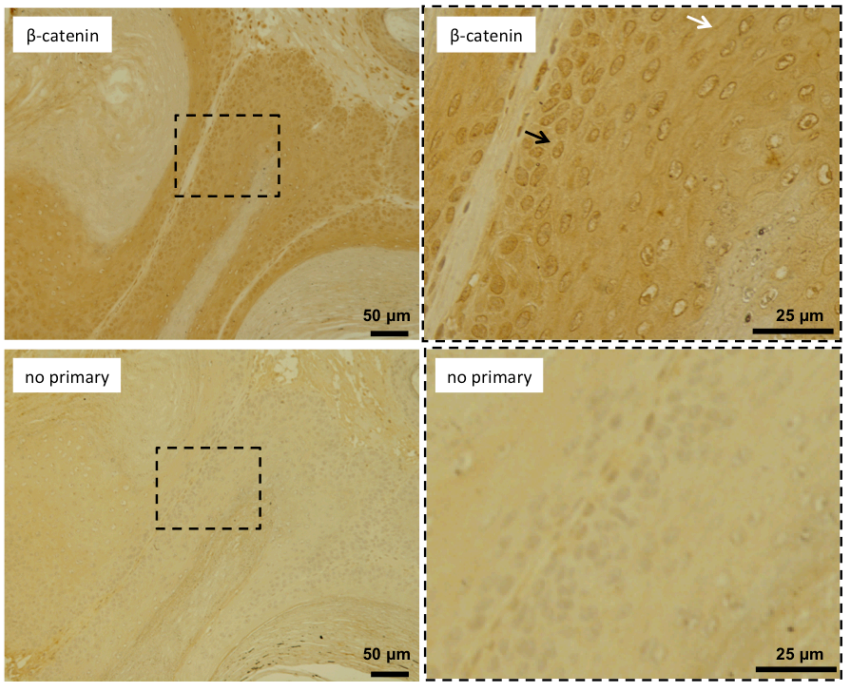

Figure R-5. Immunohistochemistry staining of β-catenin in a WT skin papilloma. The magnified image on the right is highlighted in the left picture. Black arrow: nuclear localisation of β-catenin in the proximity to basal cells. White arrow: membranous localisation of β-catenin in a non-basal cell. No staining was detected in the absence of primary β-catenin antibody.

The analysis of β-catenin in the papilloma samples from WT, p38γ- and p38δ-deficient mice revealed that there were no clear differences between the genotypes in either β-catenin expression or its localisation (Fig. R-6A). Additionally, we could not find clear pattern of β-catenin expression within genotypes, some animals had higher β-catenin expression in the tumours than in healthy skin and *vice versa* (Fig. R-6B).

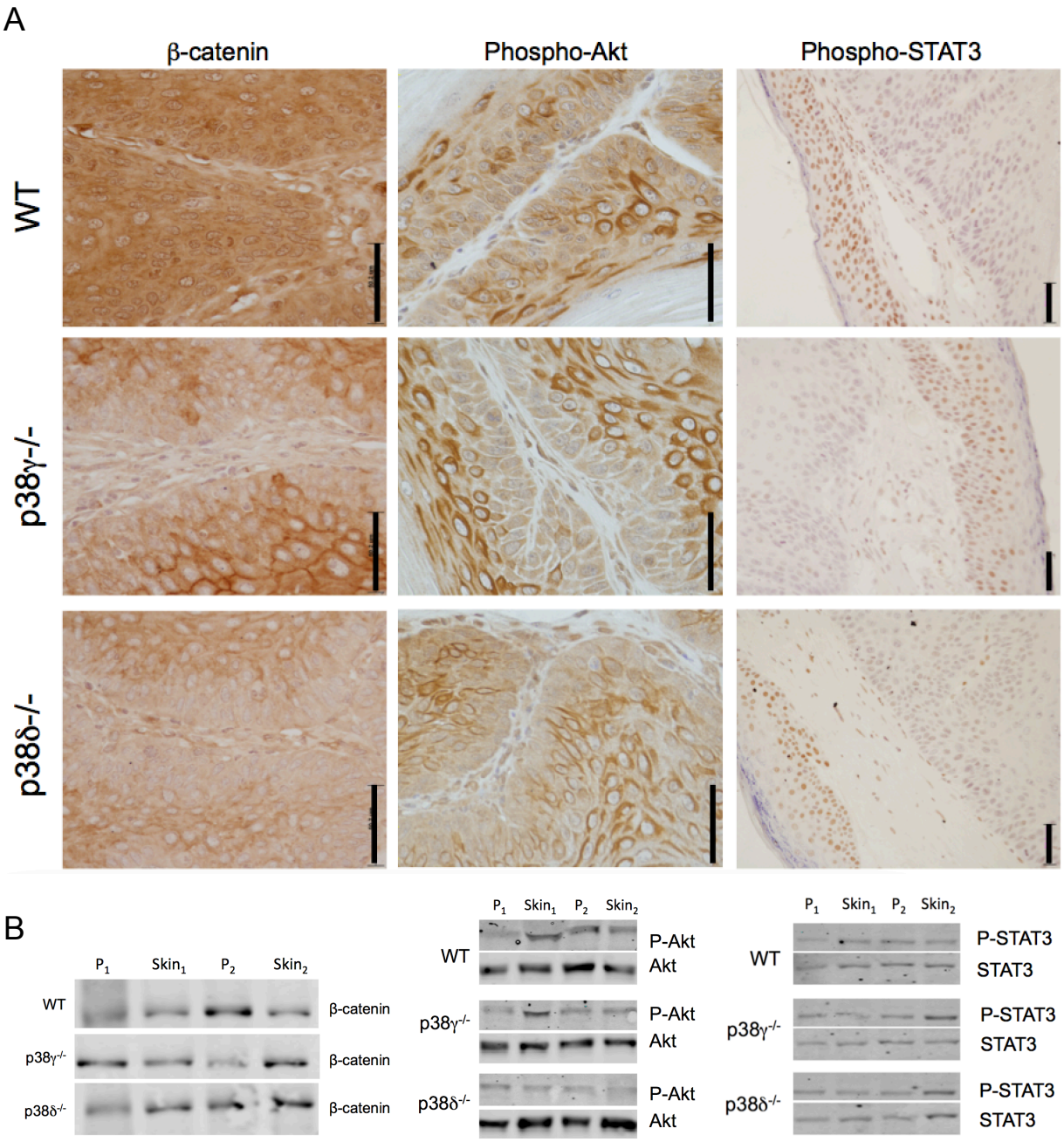

Figure R-6. (A) Representative pictures of immunohistochemistry staining of β-catenin, phospho-Akt and phospho-STAT3 in WT, p38γ$^{-/-}$ and p38δ$^{-/-}$ skin papillomas. Scale bars: 50 μm. (B) Immunoblots of β-catenin, Akt (phosphorylated and total) and STAT3 (phosphorylated and total) in papillomas (P) and healthy skin from WT, p38γ$^{-/-}$ and p38δ$^{-/-}$ mice. Each well in the blot was loaded with protein from one animal.

We also checked STAT3 and Akt expression and activation in skin papillomas. STAT3 is a transcription factor with an important role in cell proliferation control, survival and angiogenesis, all of which are hallmarks of malignancy (Ihle, 2001). Its constitutive activation has been observed in several malignant cell types. STAT3 is required for initiation, promotion and progression to a more malignant phenotype in squamous cell carcinomas (Chan et al., 2004).

Activation of the other protein, Akt, is also frequent in human cancers, including epithelial cancers. Genetically engineered squamous cell carcinoma lines, constitutively expressing Akt, have been shown to lose epithelial cell morphology and to acquire fibroblast-like properties, undergoing epithelial-to-mesenchymal transition (Grille et al., 2003).

We found that phosphorylated STAT3 was detected mainly in nuclei of the cells forming the epithelium surrounding the tumour mass, whereas it was less abundantly expressed in more profoundly located cells. In contrast, phospho-Akt was highly expressed in the cytoplasm of most of the epithelial cells of the papillomas. We observed similar levels of phosphorylated STAT3 and phosphorylated Akt in all papilloma sections regardless of the genotype (Fig. R-6A, B). Their total levels were similar too (Fig. R-6B).

The only exception concerning phosphorylated STAT3 was found in the p38$\gamma^{-/-}$ tumour that was previously recognised as a progressed tumour (Fig. R-7). Contrary to the benign papillomas, STAT3 expression was increased in the majority of its cells, which supports the published data on its implication in squamous cell carcinoma progression (Chan et al., 2004).

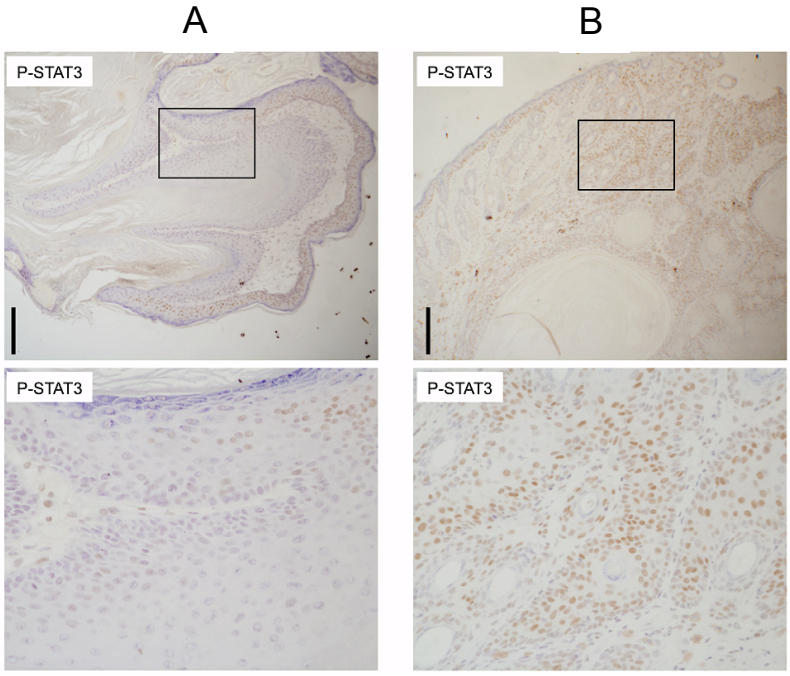

Figure R-7. Comparison of the localisation of phosphorylated STAT3 between a benign skin papilloma (A) and a papilloma progressed to a carcinoma (B). The bottom images are enlarged sections highlighted in the upper images. Scale bars: 200 μm.

1.4. Infiltration of inflammatory cells.

It has been shown that there is an increase in neutrophils infiltrating the skin and the tumours during DMBA/TPA tumorigenesis.

We confirmed the presence of neutrophils in the tumour epithelium and sub-basal tumour stroma in skin papilloma samples by immunohistochemistry staining with anti-myeloperoxidase (MPO) antibody and analysing MPO expression by immunoblotting (Fig. R-8A, C). MPO might serve as a marker for tissue neutrophil content (Bradley et al., 1982). We observed that MPO-positive neutrophils not only infiltrated the stroma, but also penetrated the basal membrane of the tumour in all genotypes (Fig. R-8A).

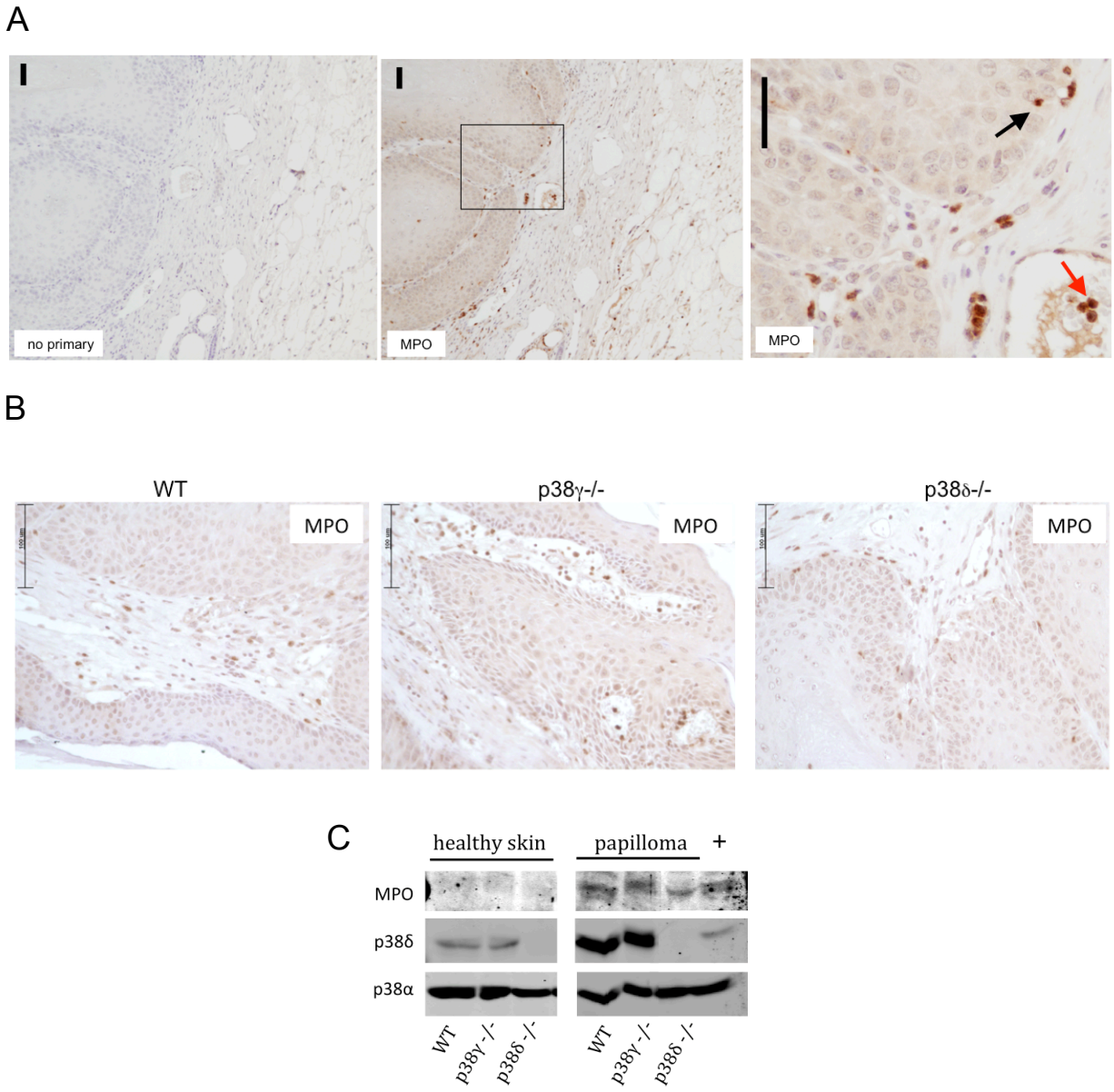

Figure R-8. (A) MPO-positive cells in WT skin papilloma. The last image is magnification of the highlighted field in the middle picture. Black arrow: neutrophil crossing the basal membrane. Red arrow: neutrophils in a blood vessel. No staining was detected in the absence of primary antibody. Scale bars: 40 μm. (B) Immunohistochemistry staining of MPO in WT, p38$\gamma^{-/-}$ and p38$\delta^{-/-}$ skin papillomas. Scale bars: 100 μm. (C) Immunoblot of MPO, p38δ and p38α in total protein lysates from healthy skin samples and papillomas from WT, p38$\gamma^{-/-}$ and p38$\delta^{-/-}$ mice induced with the DMBA/TPA. Positive control (+) is protein from inflamed, TPA-treated skin from a WT mouse. Each well in the blot was loaded with protein from one animal.

We did not observe differences in the levels of tumour-infiltrating neutrophils between the genotypes (Fig. R-8B). Contrary to the tumours, healthy skin from the same mouse was characterised by the absence of MPO expression detected by immunoblotting (Fig. R-8C).

1.5. Epithelial cell proliferation.

Since epithelial cell proliferation is affected during tumorigenesis and uncontrolled growth of mutated cells leads to tumours formation, we analysed the proliferation in skin papillomas. Following the completion of the two-stage skin tumorigenesis protocol, the proliferation was addressed in WT, p38$\gamma^{-/-}$ and p38$\delta^{-/-}$ skin papilloma samples by BrdU staining and counting proliferating cells (Fig. R-9A). No difference was observed between the genotypes (Fig. R-9B). The average percentage of epithelial tumour cells undergoing proliferation (BrdU-positive cells) was just above 15% of total epithelial cells in each group.

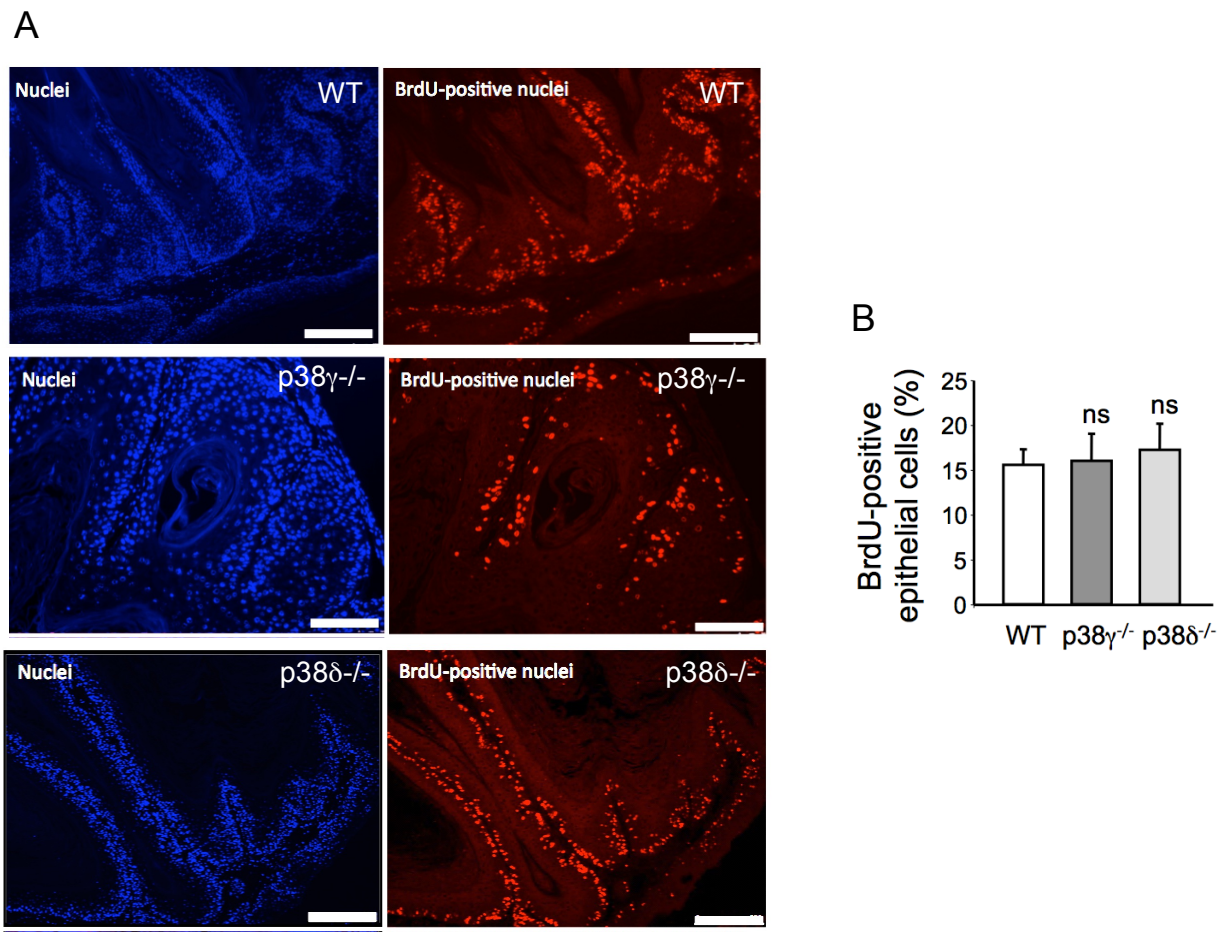

Figure R-9. (A) Representative pictures of total and BrdU-positive nuclei in skin papillomas from three genotypes. Total nuclei were stained with Hoechst. Scale bars: 250 μm. (B) Quantification of BrdU-positive epithelial cells in skin tumours from WT (n=3), p38$\gamma^{-/-}$ (n=3) and p38$\delta^{-/-}$ (n=6) mice. ns: not significant. Results are means +/- SEM.

2. p38γ and p38δ are involved in early phases of skin tumorigenesis.

In order to see if p38γ and p38δ regulate skin tumour formation in the early stages of the skin tumorigenesis we investigated, in WT, p38γ$^{-/-}$, p38δ$^{-/-}$ and p38γ/δ$^{-/-}$ mice, epithelial cell proliferation, treating the skin with a single dose of TPA, and apoptosis after DMBA treatment.

2.1. Epithelial cell proliferation.

In a two-stage tumorigenesis application of the promoter TPA, during the promotion stage, produces hyperplasia, which is an increased cells proliferation.

WT, p38γ$^{-/-}$, p38δ$^{-/-}$ and p38γ/δ$^{-/-}$ mice were treated once with TPA and sacrificed 32 hours later. The skin was excised and the samples were processed for HE and BrdU staining (Fig. R-10). We have measured the increase in epithelial layer thickness caused by hyperplasia in HE-stained sections. After TPA treatment the increase in epidermal thickness was significantly reduced in p38γ$^{-/-}$, p38δ$^{-/-}$ and p38γ/δ$^{-/-}$ mice compared to WT mice (Fig. R-10A). This reduction was similar in all p38-deficient mice. We also found that the skin of p38γ$^{-/-}$, p38δ$^{-/-}$ and p38γ/δ$^{-/-}$ mice contained fewer cells undergoing proliferation when compared with WT (Fig. R-10B). These results correlated with the epidermal thickness measured in these samples and suggested that the affected proliferation can be, at least partially, a mechanism underlying the reduced sensitivity of p38δ$^{-/-}$ and p38γ/δ$^{-/-}$ mice to a two-stage protocol. The results on p38γ$^{-/-}$, however, indicate the existance of an additional factor(s), because the p38γ$^{-/-}$ response to the DMBA/TPA tumour induction resembled wild type phenotype.

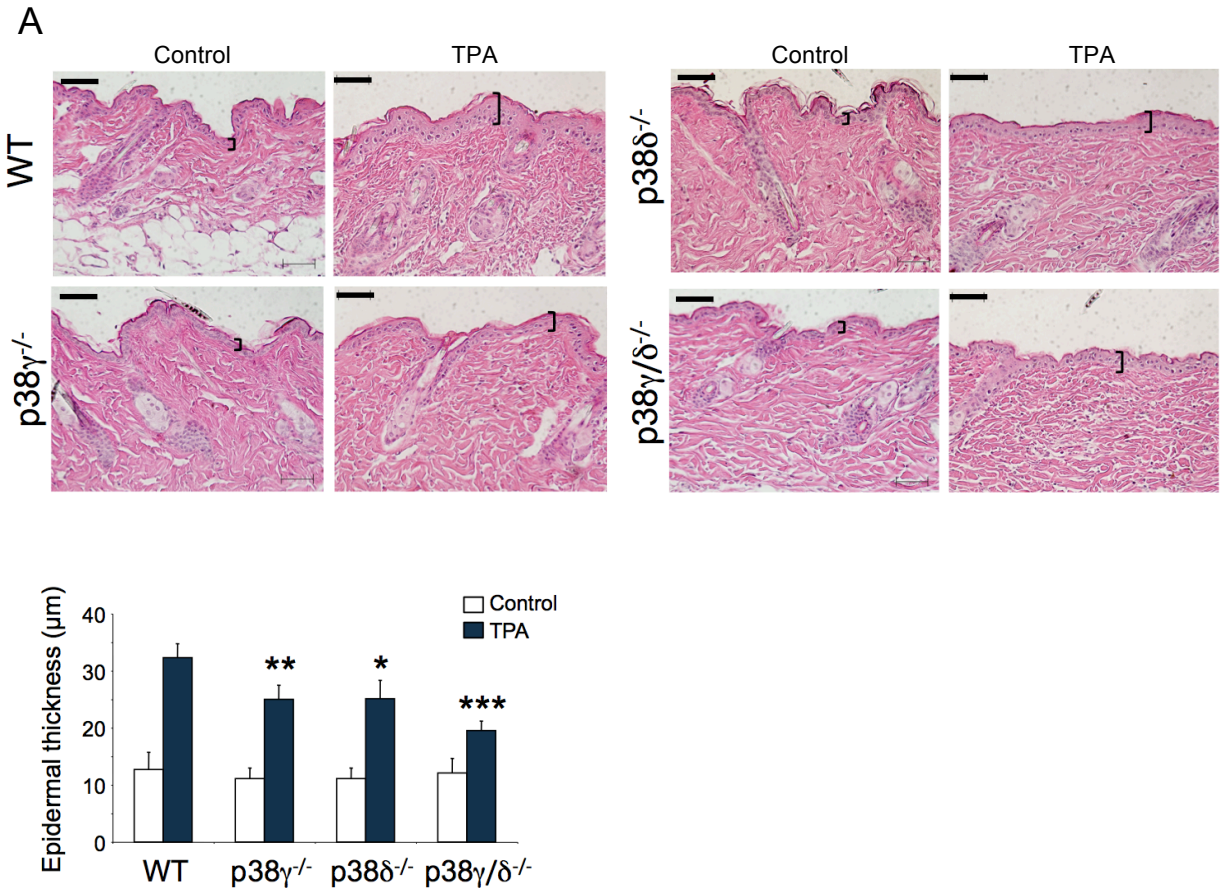
A
Control
TPA
Control
TPA
WT
p38δ-/-
p38γ-/-
p38γ/δ-/-
Epidermal thickness (μm)
Control
TPA
40
30
20
10
0
**
*
***
WT
p38γ-/-
p38δ-/-
p38γ/δ-/-

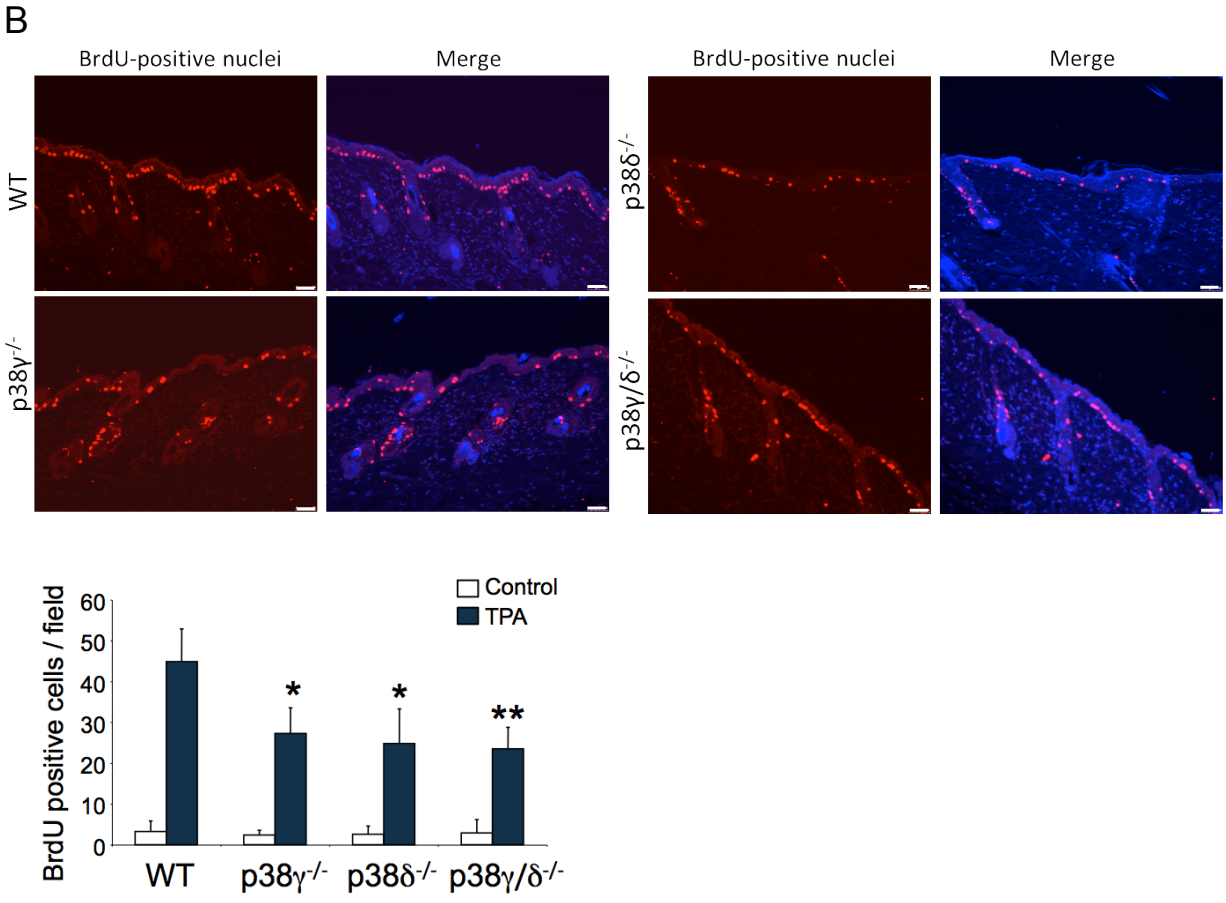
B
BrdU-positive nuclei
Merge
BrdU-positive nuclei
Merge
WT
p38δ-/-
p38γ-/-
p38γ/δ-/-
BrdU positive cells / field
Control
TPA
60
50
40
30
20
10
0
*
*
**
WT
p38γ-/-
p38δ-/-
p38γ/δ-/-

Figure R-10. The previous page. (A) Upper panel: HE staining of epidermis and dermis in skin of WT, p38γ$^{-/-}$, p38δ$^{-/-}$ and p38γ/δ$^{-/-}$ mice treated or not with TPA. Scale bars: 100 μm. Bottom panel: measurement of epidermal thickness (n=4). (B) Upper panel: Immunofluorescent staining of BrdU in WT, p38γ$^{-/-}$, p38δ$^{-/-}$ and p38γ/δ$^{-/-}$ skin treated with TPA. Merge images represent total nuclei, including BrdU-positive. Scale bars: 50 μm. Bottom panel: quantification of BrdU-positive nuclei in 12 fields per mouse (n=4). (A, B) Results are means +/- SEM. *P<0.05, **P<0.01, ***P<0.001 compared with TPA-treated WT (two-tailed Student's t-test).

2.2. Apoptosis.

The carcinogen DMBA used in the initiation stage of the chemically-induced skin carcinogenesis, apart from exerting a mutagenic effect on epidermal cells, also provokes apoptosis, which may contribute to an overall outcome of skin tumours in DMBA/TPA-treated mice.

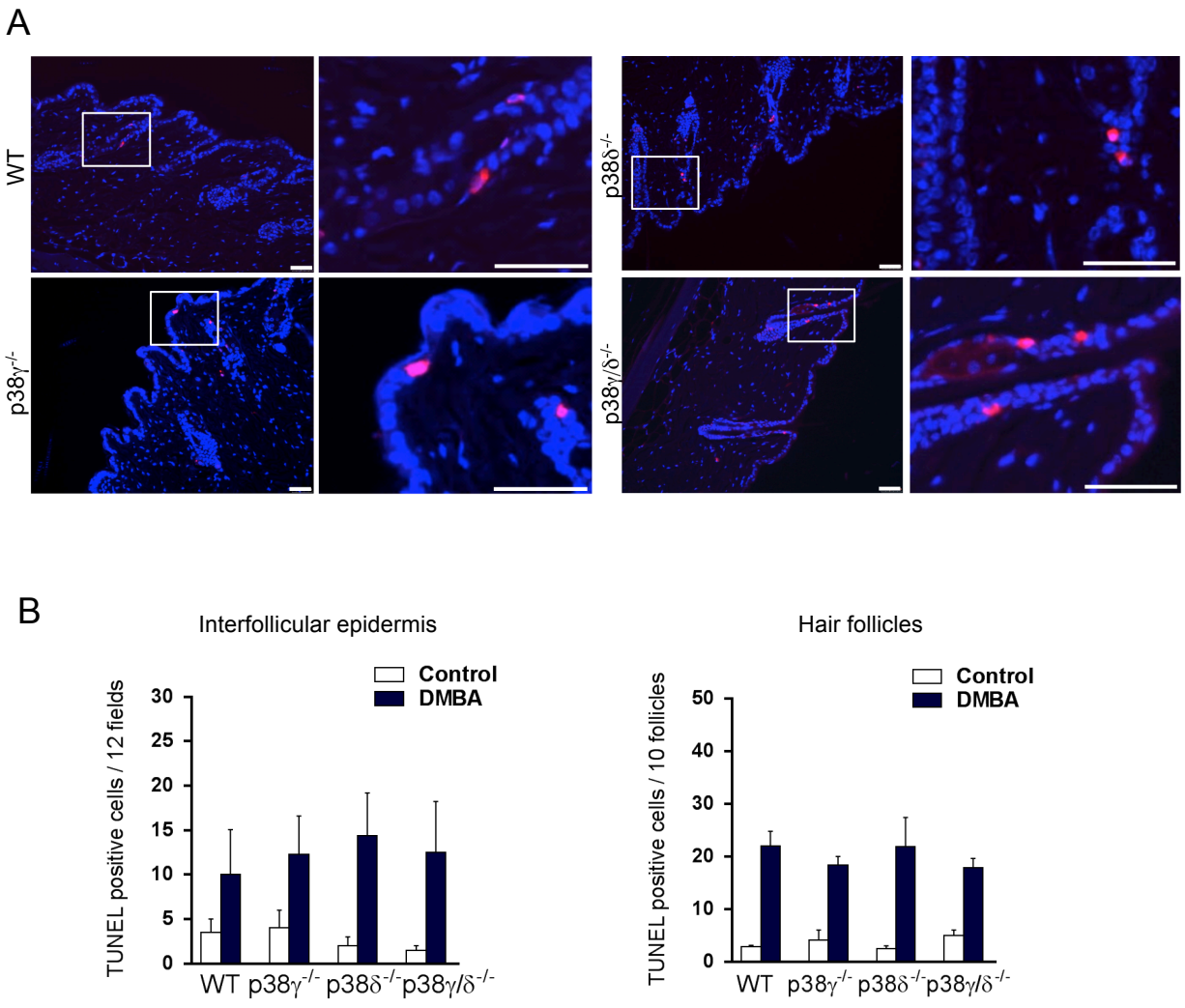

Figure R-11. DMBA-induced apoptosis in epidermis of WT, p38γ$^{-/-}$, p38δ$^{-/-}$ and p38γ/δ$^{-/-}$ mice measured by TUNEL. (A) Representative pictures of fluorescent staining of TUNEL-positive cells (red) in DMBA-treated mice. Nuclei were stained with Hooechst. Scale bars: 50 μm. The images on the right in each genotype are magnifications of the highlighted fields. (B) Quantification of TUNEL positive cells in interfollicular and follicular epidermis of control and treated mice (n=4). Results are means +/- SEM.

By TUNEL staining we observed that DMBA induced cell apoptosis in the epidermis of all mice to a similar extent comparing with control WT mice (Fig. R-11). This was observed both in the interfollicular epidermis and in epidermal cells forming hair follicles. Of note, the apoptosis predominantly took place in follicular epidermis and was less frequent in the proper skin epithelium.

3. p38γ and p38δ are implicated in TPA-induced skin inflammation.

Acting as promoting agents, phorbol esters also drive inflammatory events in a two-stage skin tumorigenesis. For this reason responses associated with TPA-induced inflammation are routinely considered as markers of tumour promotion and include acute inflammatory events such as oedema, neutrophils infiltration and the production of inflammatory molecules. Since we have shown that lack of both p38γ and p38δ impaired the inflammatory response in different animal models such as septic shock (Risco et al., 2012), arthritis (Criado et al., 2014) or colitis (del Reino et al., 2014), we then analysed whether p38γ/δ deletion affected the skin inflammatory response to TPA and was a potential mechanism contributing to decreased tumorigenesis.

3.1. Oedema.

The most visible marker after skin exposure to a phorbol is intercellular oedema, an accumulation of fluid in the dermal and hypodermal part of the skin in response to the chemical induction, which is easily observed in a standard HE staining.

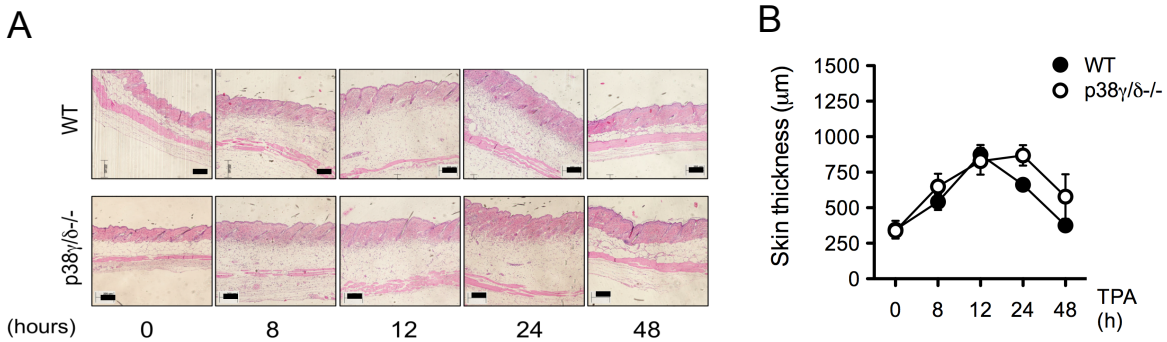

Figure R-12. (A) Representative pictures of HE staining of skin after TPA treatment. Scale bars: 200 μm. (B) Skin thickness measurement at different times after a single dose of TPA in WT and p38γ/δ$^{-/-}$ mice (n=3). Results are means +/- SEM.

We treated p38γ/δ$^{-/-}$ and WT mice with a single application of 10 μg of TPA onto shaved dorsal skin that led to an increase in skin thickness that was maintained for 24 hours (Fig. R-12A).

Histological analysis showed no significant differences in skin thickness between WT and p38γ/δ-deficient mice (Fig. R-12B).

3.2. Early production of inflammation mediators.

The production of cytokines and chemokines in the skin is a common indicator of inflammatory processes in the tissue. Keratinocytes, fibroblasts and skin immune cells are the main sources of inflammation mediators during the first hours after exposure to TPA, because they are either in direct contact or in the closest proximity to the site of treatment. Immune cells, such as macrophages, neutrophils and lymphocytes infiltrating subcutis, dermis and finally dermis from skin blood vessels in response to skin-derived chemokines, produce their own immune factors, contributing to the overall inflammation severity during the acute phase of skin inflammation (Tay et al., 2013).

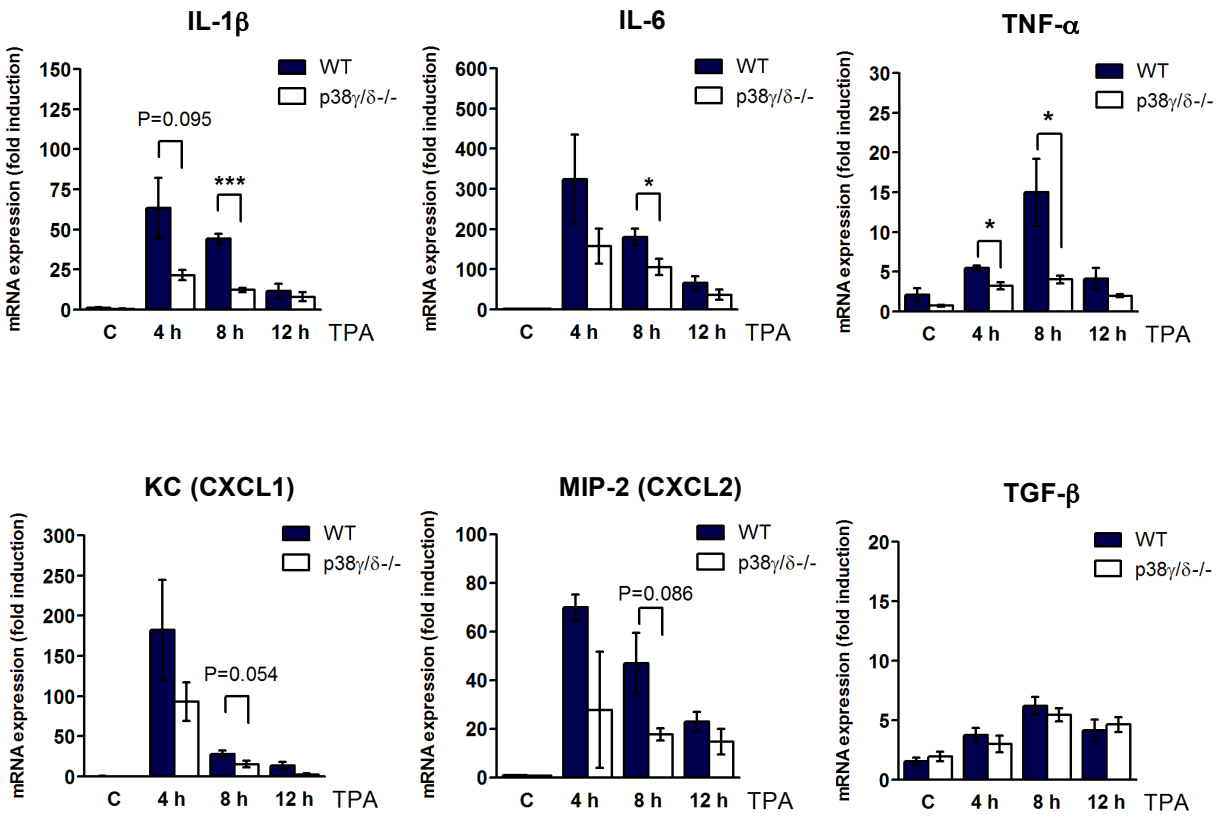

Figure R-13. Expression of IL-1β, IL-6, TNF-α, KC (CXCL1), MIP-2 (CXCL2) and TGF-β in the skin from WT and p38γ/δ$^{-/-}$ mice treated or not with TPA and sacrificed at different times following the treatment. Results were normalised to GAPDH mRNA and represented in arbitrary units as means +/- SEM, where one corresponds to a WT control (n=3). *P<0.05, ***P<0.001. Non-significant P values <0.1 are shown as numbers (two-tailed Student's t-test).

We then checked mRNA levels of cytokines and chemokines produced in inflamed skin after the treatment with TPA in WT and p38γ/δ$^{-/-}$ mice. We measured cytokines, such as: IL-1β, IL-6, TNF-α and TGF-β and two chemokines: keratinocyte-derived chemokine (KC, known as CXCL1 in human) and macrophage-inflammatory protein-2 (MIP-2 or CXCL2). Mouse skin was treated once with 10 μg of TPA and processed for total RNA extraction, cDNA production and RT-qPCR analysis, after either 4, 8 or 12 hours, according to the protocol described in paragraph 3.3 of Materials and Methods. The results are shown in Figure R-13.

We observed time-dependent induction in mRNA levels of all genes in both WT and p38γ/δ-deficient mice, which means that all the proteins take part in TPA-induced inflammatory processes in mouse skin. In particular, the production of IL-1β, IL-6, KC and MIP-2 reached the highest level at 4 hours after TPA, in both WT and p38γ/δ$^{-/-}$ skin, and decreased afterwards. In contrast, the levels of TNF-α and TGF-β were moderately increased at 4 hours comparing with controls and reached the highest level at 8 hours, decreasing 12 hours after TPA.

Interestingly, the expression of all genes in the skin of p38γ/δ-deficient mice was smaller, except for TGF-β, than in WT. In particular, the skin from p38γ/δ$^{-/-}$ mice had significantly (or almost significantly, $P<0.1$) less IL-1β, IL-6, KC, MIP-2 and TNF-α than WT, mainly at 8 hours after the treatment. These observations indicate the implication of p38γ and/or p38δ in the regulation of the cytokine/chemokine-based inflammatory status in TPA-treated skin.

To examine which p38 isoform was the main regulator in skin cytokine production we measured the above mentioned genes in mice deficient in p38γ or deficient in p38δ alone. Having observed the most significant differences between WT and p38γ/δ$^{-/-}$ mice at 8 hours after TPA challenge, we decided to measure the mRNA levels in single knock-out mice 8 hours after TPA (Fig. R-14).

As expected, there was no difference between the three genotypes in the case of TGF-β. The deletion of p38δ alone in mice treated with TPA led to relatively smaller induction of IL-1β, IL-6, TNF-α, KC and MIP-2 mRNA levels comparing with WT. However, only in the case of MIP-2 the difference was statistically significant ($P<0.05$). In the case of the p38γ deletion, it led to a smaller induction of TNF-α and MIP-2 comparing with WT, although none of the differences was statistically significant. These data suggest an implication of both p38s in the regulation of some inflammatory mediators in the skin on the one hand, and a possible synergistic effect of the deletion of both p38s in these processes, on the other.

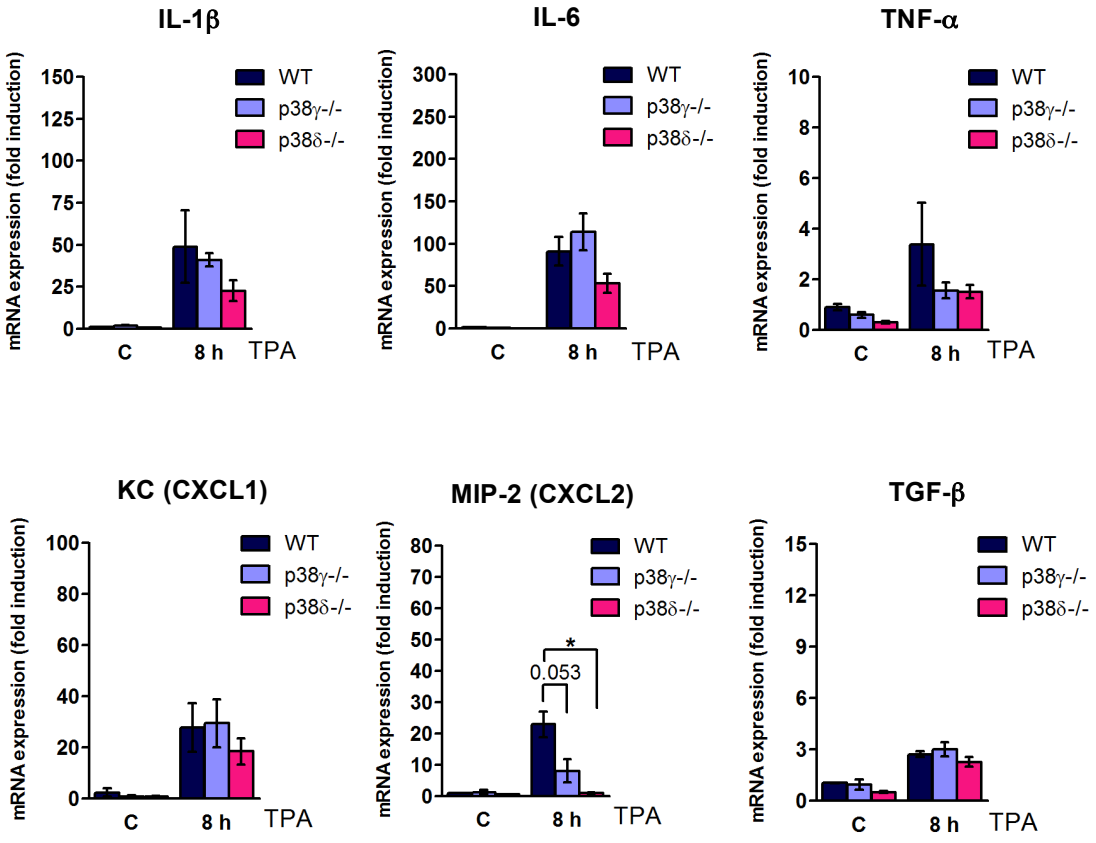

Figure R-14. Expression of IL-1β, IL-6, TNF-α, KC (CXCL1), MIP-2 (CXCL2) and TGF-β in the skin from WT, p38γ$^{-/-}$ and p38δ$^{-/-}$ mice treated or not with TPA and sacrificed 8 hours after the treatment. Results were normalised to GAPDH mRNA and represented in arbitrary units as means +/- SEM, where one corresponds to a WT control (n=3). *P<0.05. Non-significant P values <0.1 is indicated numerically (two-tailed Student's t-test).

3.3. Inflammatory cells infiltration.

TPA treatment in its acute phase, just after the exposure, is also characterised by inflammatory cells infiltration into the skin, including lymphocytes and polymorphonuclear leukocytes, neutrophils.

In order to examine lymphocytes recruitment we stained skin sections from WT and p38γ/δ$^{-/-}$ control mice and mice treated with TPA, 12 or 24 hours prior to sacrifice, with CD3-specific antibodies and analysed by fluorescent microscopy (Fig. R-15A). Anti-CD3 antibody recognises T cell lymphocytes. There was a time-dependent increase in the lymphocyte population infiltrating inflamed skin after TPA treatment; however, we did not observe any differences in numbers of CD3-positive cells between WT and p38γ/δ-deficient mice (Fig. R-15B).

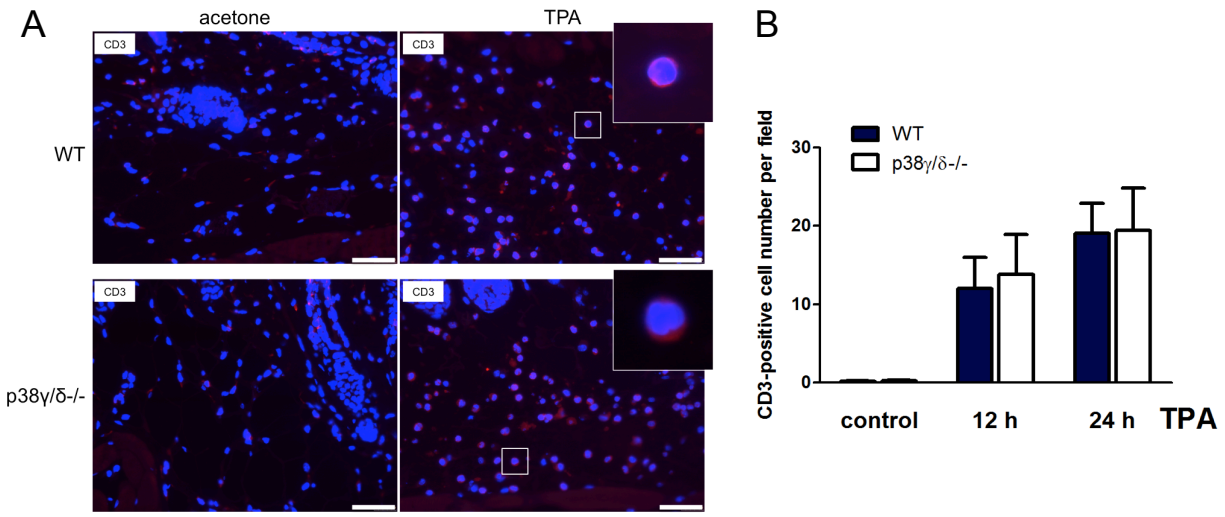

Figure R-15. CD3-positive cells in TPA-treated skin. (A) Representative images of immunofluorescence staining of CD3-positive cells (red) in WT and p38γ/δ$^{-/-}$ skin treated or not with TPA 24 hours after the treatment. Nuclei were stained with Hoechst33342 (blue). The inserts are magnifications of two T lymphocytes. Scale bars: 50 μm. (B) Quantitation of T lymphocytes in WT and p38γ/δ$^{-/-}$ skin at 12 and 24 hours after TPA. Cells were counted in 8 fields per mouse. Results are means +/- SEM (n=3).

Physiologically healthy skin possesses low levels of MPO-positive cells (neutrophils), whereas skin inflamed by an infection, wounding or by the application of tumour promoters enhances the number of MPO-positive cells.

Neutrophils infiltration could be observed in a standard HE staining of WT skin treated with TPA (Fig. R-16A). We also measured MPO levels in total protein lysates from untreated and TPA-treated mouse skin from WT mice using immunoblotting with a specific anti-MPO antibody. We showed a time-dependent change in the expression of MPO in the skin, which was detected as early as at 4 hours after the treatment and increased with the time up to 24 hours and it almost disappeared at 48 hours (Fig. R-16B).

Next, we confirmed the presence of neutrophils in TPA-challenged skin by specific immunohistochemistry staining of MPO positive cells in WT and p38γ/δ-deficient mice (Fig. R-17A). We observed a rise in number of neutrophils migrating towards the site of inflammation during the first 24 hours after the treatment in both genotypes (R-17B). The neutrophil infiltration was observed at 12 hours after TPA and was even higher at 24 hours. We observed a significantly lower number of MPO-positive cells in the double knock-out mice 24 hours after the TPA when compared with WT (Fig. R-17B). This was also confirmed by immunoblotting (Fig. R-17C), suggesting that neutrophil infiltration is partially impaired in p38γ/δ$^{-/-}$ mice.

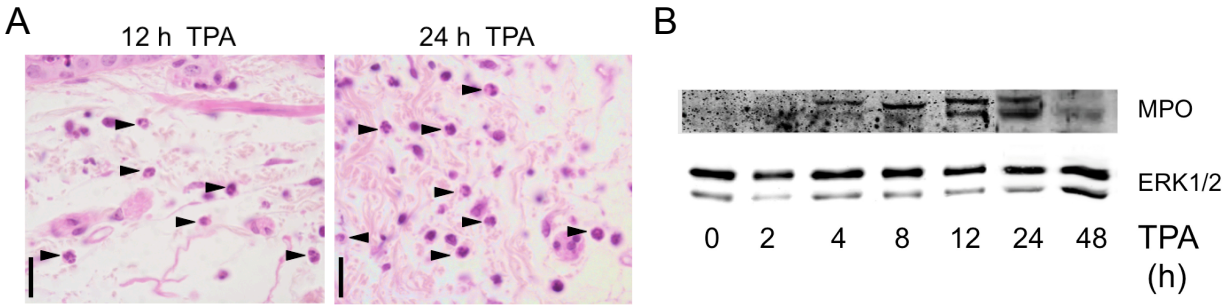

Figure R-16. Neutrophils recruitment in TPA-treated skin in WT mice. (A) HE staining of the skin at 12 and 24 hours after TPA treatment showing neutrophils infiltrating dermal and hypodermal regions of skin (black arrows). Scale bars: 20 μm. (B) Immunoblot of MPO in total protein lysates from WT skin at different times after TPA challenge. ERK1/2 was used as loading control.

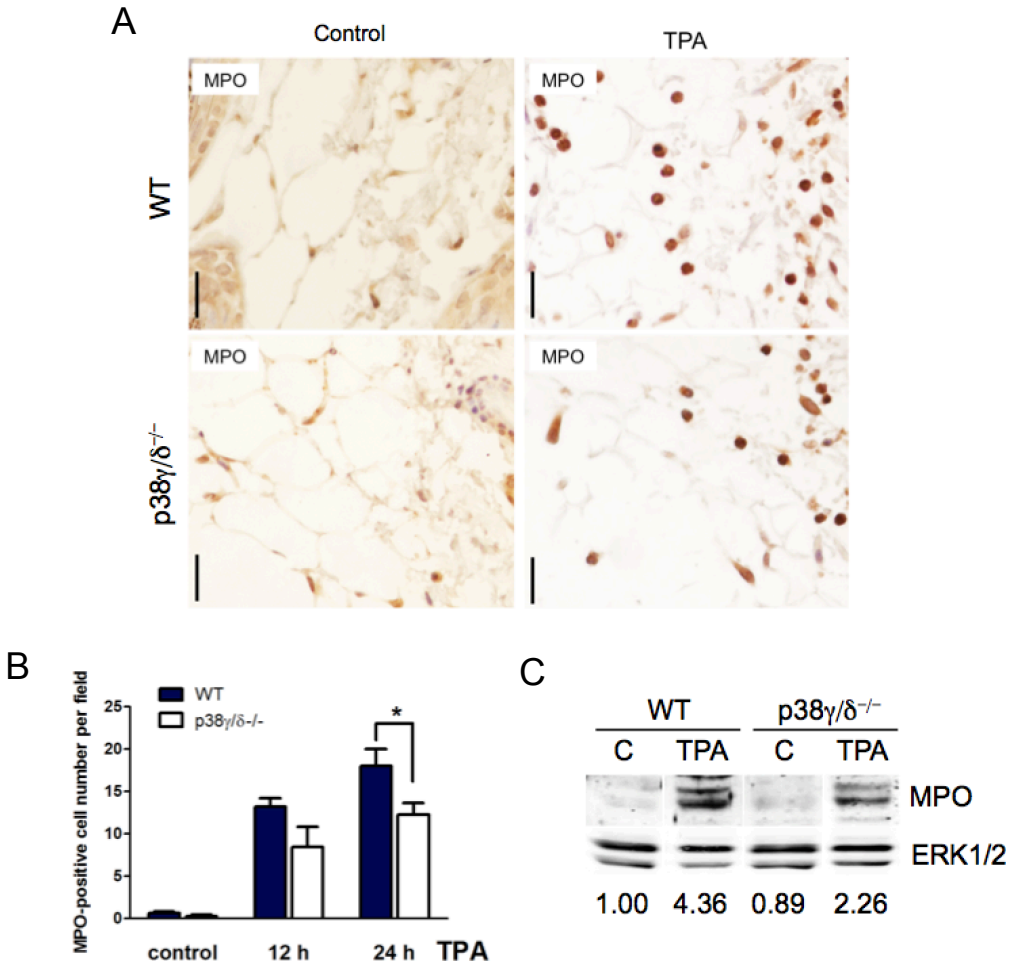

Figure R-17. Neutrophil recruitment in WT and p38γ/δ$^{-/-}$ mice after TPA treatment. (A) Representative images of immunohistochemistry staining of MPO-positive cells in skin from WT and p38γ/δ$^{-/-}$ mice treated or not with TPA and sacrificed 24 hours later Scale bars: 20 μm. (B) Quantitation of neutrophils. Cells were counted in at least 8 randomly selected fields per mouse. Results are means +/- SEM (n=3). *P<0.05 (one-tailed Student's t-test). (C) Immunoblot of MPO in total protein lysates from skin of WT and p38γ/δ$^{-/-}$ control mice and 24 hours after TPA treatment. ERK1/2 was used as loading control. The numbers under the blot indicate relative MPO band intensity normalised to WT control.

3.4. Late production of inflammation mediators.

It has been demonstrated that the production of cytokines and chemokines in TPA-treated skin might be restored in the presence of immune cells, accumulating in the inflamed skin (Gebhardt et al., 2008). Bearing this in mind, we supposed that the decrease in the production of inflammatory mediators observed at 12 hours following TPA treatment (Fig. R-13) might only be transient. As expected, when we checked the mRNA production of the previously measured genes, we confirmed that at 24 hours there was a dramatic increase in the mRNA expression of three out of four measured genes: IL-1β, IL-6, MIP-2 (CXCL2) and TNF-α. While MIP-2 was efficiently recovered, the level of IL-6 mRNA was lower at 24 hours than at 12 hours, indicating that the restoration did not take place (Fig. R-18). The remaining two genes, *Il-1β* and *Tnf-α* were partially brought back to a higher level.

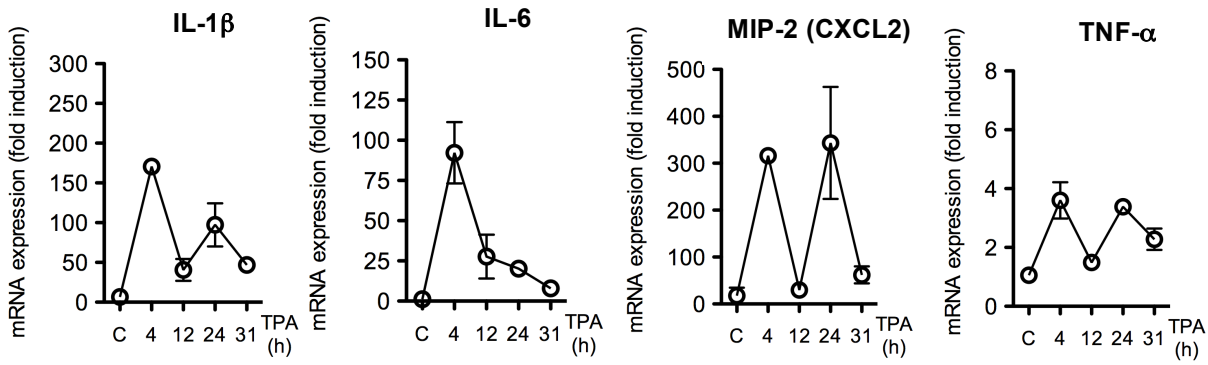

Figure R-18. Production of IL-1β, IL-6, MIP-2 and TNF-α in the WT skin at 4, 12, 24 and 31 hours after TPA treatment. Results were normalised to GAPDH mRNA and represented in arbitrary units as means +/- SEM, where one corresponds to control (n=3).

In order to establish a possible contribution of the p38γ/δ deficiency to the production of inflammatory factors in the skin at longer times after TPA treatment, WT and p38γ/δ knock-out mice were treated once with TPA and sacrificed at 12, 24 and 31 hours later. The mRNA levels of IL-1β, IL-6, MIP-2 (CXCL2) and TNF-α were measured by qPCR in total RNA extracted from skin necropsies and shown in Figure R-19. Expectedly, WT mice were characterised by a growing expression of IL-1β, MIP-2 and TNF-α at 12 and 24 hours and a subsequent decrease, whereas IL-6 was at the similar levels at 12 and 24 hours and close to control level at 31 hours. At 24 hours after TPA, mice deficient in both p38γ and p38δ had an impaired production of IL-1β (*P<0.05) and MIP-2 (**P<0.01), and a slightly lower increase of TNF-α (P<0.1), as compared with WT. Interestingly, the level of IL-6, which did not grow at 24 hours in WT, was found to be significantly

lower in p38γ/δ$^{-/-}$ mice, indicating a sooner decrease of this cytokine in the mutants under the same conditions.

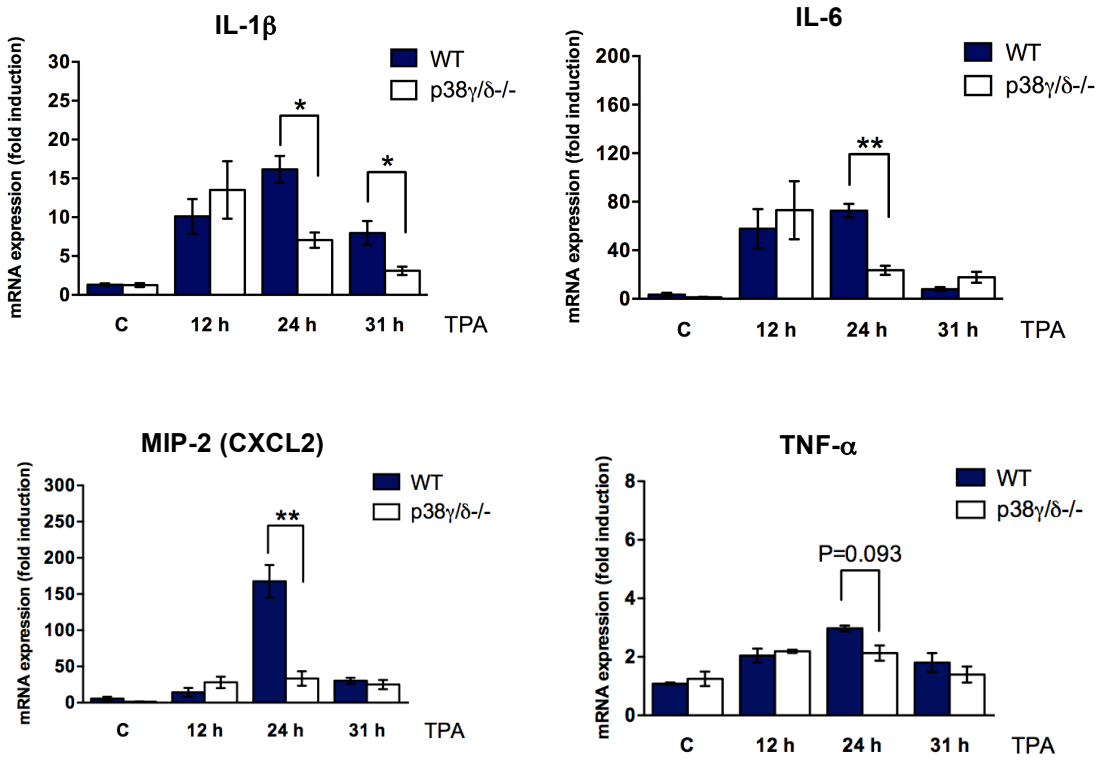

Figure R-19. Expression of IL-1β, IL-6, TNF-α and MIP-2 (CXCL2) in the skin from WT and p38γ/δ$^{-/-}$ mice treated or not with TPA and sacrificed at different times following the treatment. Results were normalised to GAPDH mRNA and represented in arbitrary units as means +/- SEM, where one corresponds to a WT control (n=3). *P<0.05, **P<0.01. Non-significant P value <0.1 is represented numerically (two-tailed Student's t-test).

Overall, the time of the second wave of inflammation mediators' production in the skin of WT mice exposed to TPA coincides with the peak of lymphocytes and neutrophils infiltration as shown in section 3.3 of Results. The smaller numbers of neutrophils in the TPA-treated skin of p38γ/δ-deficient mice coincides, besides, with a decreased production of IL-1β, IL-6 and MIP-2, all evidenced to be products of neutrophils (Fridlender and Albelda, 2012).

3.5. Signalling pathways activation in TPA-treated skin.

TPA is known to activate different signalling pathways implicated in skin inflammation. In order to check TPA-dependent signalling activation in skin of WT, p38γ$^{-/-}$, p38δ$^{-/-}$ and p38γ/δ$^{-/-}$ mice, we prepared total protein lysates from skin at different times after TPA treatment and

immunoblotted them with specific antibodies for activated (phosphorylated) p38, JNK1/2, NFκB-p105, STAT3 and ERK1/2. Moreover, we checked total levels (phosphorylated and un-phosphorylated) of these proteins, as well as the expression of p38γ and p38δ under the same conditions.

3.5.1. p38 MAPKs.

First we checked the activation of p38 MAPKs in TPA-treated skin of WT and p38γ/δ$^{-/-}$ mice using anti-phospho p38 antibody (Fig. R-20). The p38α isoform was activated as early as at 30 min after the treatment in both genotypes (Fig. R-20A). Phospho-p38γ could also be detected by immunoblot from total lysates (Fig. R-20A). The phosphorylation of p38γ and p38δ was checked by immunoprecipitation of these proteins from total protein lysates two hours after TPA treatment and immunoblotting with anti-phospho p38 antibody (Fig. R-20B and R-20C, respectively).

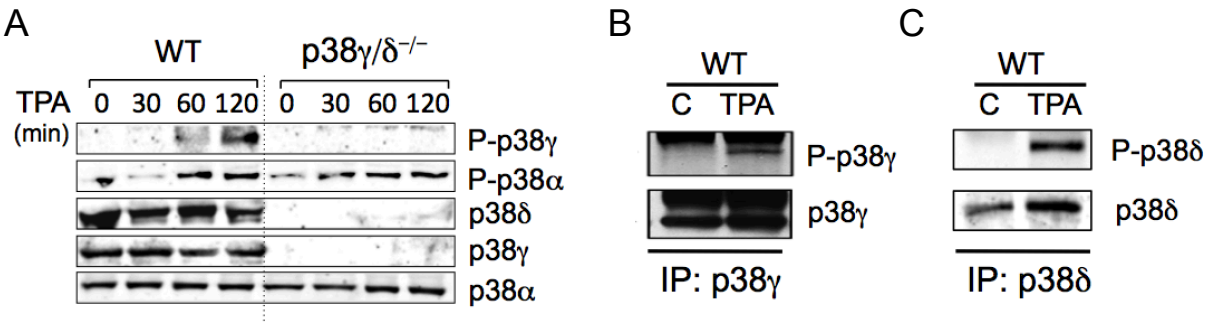

Figure R-20. Activation of p38α, p38γ and p38δ in the skin from WT and p38γ/δ$^{-/-}$ mice in response to TPA. (A) Immunoblot of p38α, p38γ, p38δ and phospho-p38 at different times after the treatment. (B, C) Immunoblots of immunoprecipitation with, respectively, p38γ and p38δ antibodies in skin lysates from WT mice treated or not with TPA (2 hours). The upper blots were incubated with anti-phospho p38 antibody and the bottom ones – with a specific anti-p38γ (B) or p38δ (C) antibody.

We then wanted to check if p38γ is also phosphorylated in p38δ$^{-/-}$ mice and p38δ in p38γ$^{-/-}$ mice under the same conditions (Fig. R-21A). Since the phospho-p38δ band was detected in a very close proximity to the phospho-p38α band, the phosphorylation of p38δ in p38γ$^{-/-}$ mice was confirmed by immunoprecipitation (Fig. R-21B). The results showed that TPA led to the phosphorylation of p38δ in these mice. Interestingly, we observed that TPA-induced p38γ phosphorylation in mice lacking p38δ was severely impaired (Fig. R-21A). Taking into consideration that the observed disruption in p38γ phosphorylation could be due to a delay in p38γ activation, we also checked the phospho-p38γ at longer times following the TPA treatment in

WT and p38δ$^{-/-}$ mice (Fig. R-21C, D). This time, we observed a weak band not only at 4 hours but also at 2 hours in p38δ$^{-/-}$ mice. Nonetheless, we confirmed that p38γ phosphorylation was affected in these mice comparing with WT (Fig. R-21C, D).

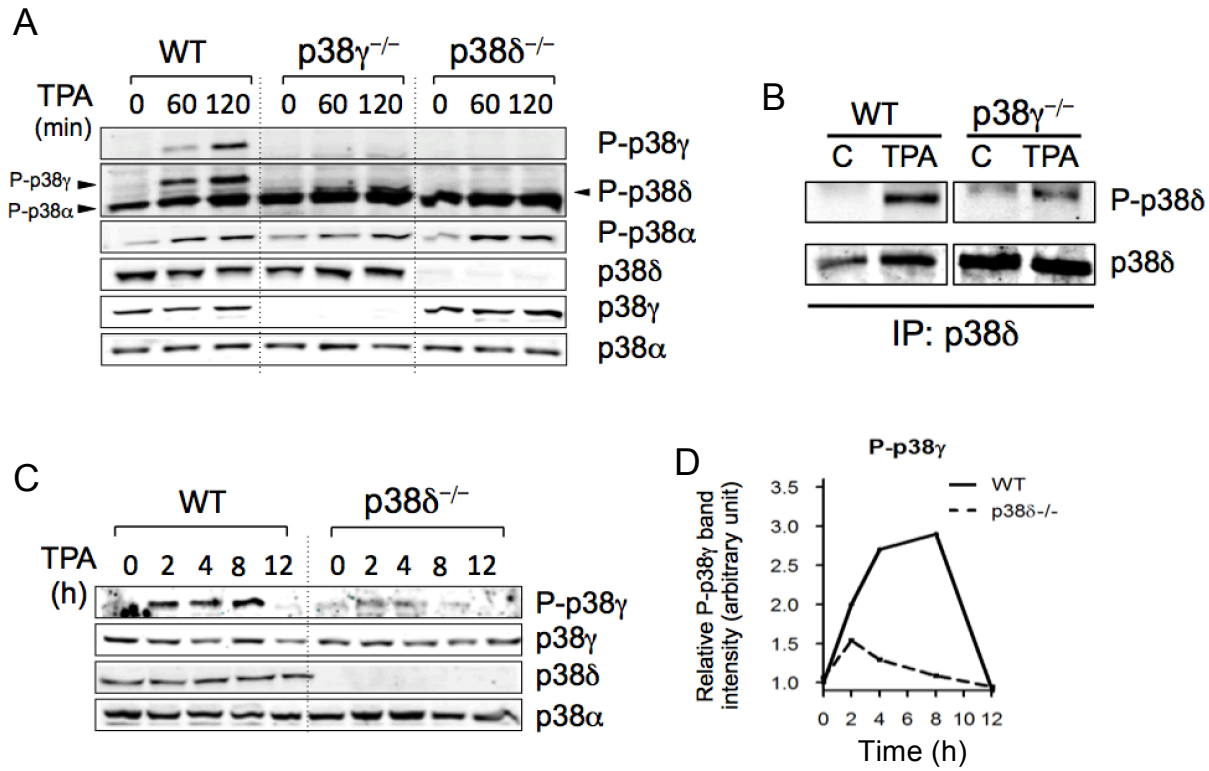

Figure R-21. Activation of p38γ and p38δ in the skin from WT, p38γ$^{-/-}$ and p38δ$^{-/-}$ mice in response to TPA treatment. (A) Immunoblot of p38α, p38γ, p38δ and phospho-p38 at 0, 1 and 2 hours after TPA. (B) Immunoblots of p38δ immunoprecipitation in skin lysates from WT and p38γ$^{-/-}$ mice treated or not with TPA (2 hours). The upper blots were incubated with anti-phospho p38 antibody and the bottom ones – with specific anti-p38δ antibody. (C) Immunoblot of p38α, p38γ, p38δ and phospho-p38γ in WT and p38δ$^{-/-}$ mice. (D) Phospho-p38γ bands intensity in WT and p38δ$^{-/-}$ mice normalised to total p38γ protein and represented in arbitrary units.

We concluded that p38δ deficiency leads to a blockade in the phosphorylation of p38γ in skin in response to TPA, suggesting that p38δ regulates p38γ phosphorylation under these conditions.

3.5.2. ERK1/2, JNK1/2, STAT3 and NFκB.

We also found that the phosphorylation of JNK1/2, STAT3, ERK1/2 and NFκB-p105 occurs in TPA-treated skin of WT and p38γ/δ$^{-/-}$ mice. Except for STAT3 and ERK1/2, we did not observe consistent differences in the phosphorylation levels between the genotypes (Fig. R-22). Therefore, we also measured the phosphorylation of STAT3 and ERK1/2 at longer times after the treatment with TPA (Fig. R-22B) and also quantified the intensity of the bands (Fig. R-22C). The quantification revealed that, while phospho-ERK1/2 differences between WT and p38γ/δ$^{-/-}$ could

be due to the loading variability, phospho-STAT3 was diminished in p38γ/δ-deficient mice compared with WT (Fig. R-22C).

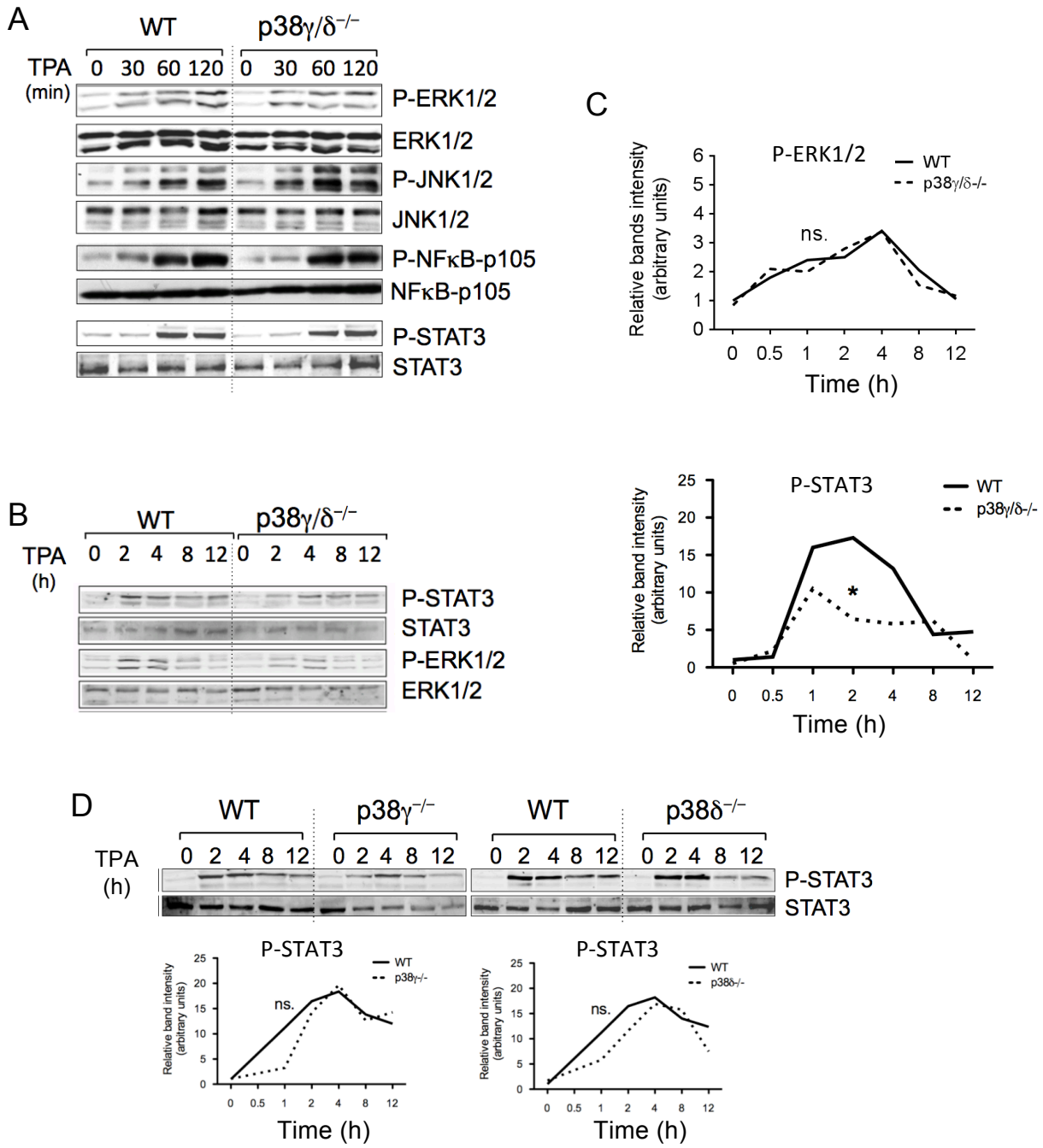

Figure R-22. Activation of ERK1/2, STAT3, NFκB and JNK1/2 in the skin after TPA treatment. (A) Immunoblot of the mentioned proteins in WT and p38γ/δ$^{-/-}$ mice at shorter times after TPA. (B) Immunoblot of ERK1/2 and STAT3 in WT and p38γ/δ$^{-/-}$ mice at longer times after TPA. (C) Bands intensity of phospho-ERK1/2 and phospho-STAT3 in WT and p38γ/δ$^{-/-}$ mice. *P<0.05; ns: not significant (two-way ANOVA). (D) Phospho-STAT3 in WT and single p38γ- and p38δ-knock-out mice and the quantification of bands intensity.

In order to check whether the lack of either p38γ or p38δ alone affected STAT3 signalling we measured phospho-STAT3 in p38γ$^{-/-}$ and p38δ$^{-/-}$ mice under the same conditions and compared them with WT (Fig. R-22D). In both cases STAT3 phosphorylation was affected only during the fist hour and resembled WT afterwards, reaching the maximum at 4 hours.

3.5.3. β-catenin.

Epithelial-to-mesenchymal transition (EMT) often occurs during the progression of many epithelial tumours and may be regulated by β-catenin. There are published data on TPA-induced EMT, in which β-catenin plays important roles (Zucchini-Pascal et al., 2013). There is also growing evidence that it is required for development of non-melanoma skin cancers (Beronja et al., 2013).

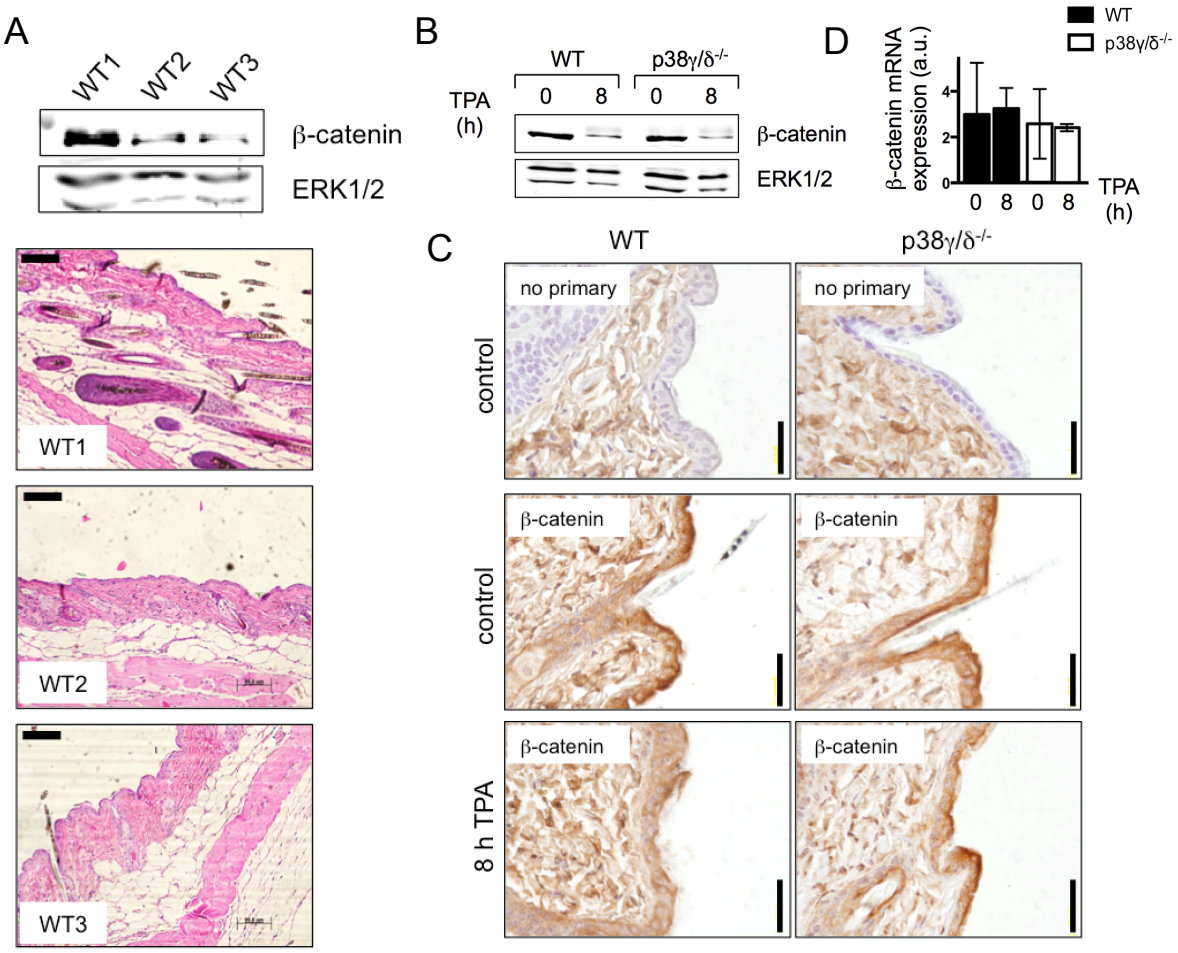

Figure R-23. β-catenin expression in non-treated and TPA-treated skin. (A) Immunoblot of β-catenin and HE staining of the skin of three WT mice: one in anagen (WT1) and two in telogen (WT2, WT3). Scale bars: 100 μm. (B) Immunoblot of β-catenin in the skin of WT and p38γ/δ$^{-/-}$ mice in telogen treated or not with TPA (8 h). ERK1/2 was used as loading control. (C) Representative pictures of immunohistochemistry staining of β-catenin in skin sections from WT and p38γ/δ$^{-/-}$ mice treated or not with TPA (8 h). No staining was detected in the absence of primary antibody. Scale bars: 40 μm. (D) β-catenin mRNA expression in WT and p38γ/δ$^{-/-}$ mice in response to TPA. GAPDH mRNA was used as reference gene. Results are mean +/- SEM (n=3).

We observed that β-catenin in the skin is abundantly expressed in keratinocytes found both in interfollicular epidermis (Fig. R-23C) and hair follicles. To produce new hairs, existing hair follicles undergo cycles of growth (anagen), regression (catagen) and rest (telogen) (Alonso and Fuchs, 2006). Unsurprisingly, therefore, the skin at growth phase of the hair cycle, which is characterised by the penetration of the follicular epidermis into deeper layers of the skin, contains much more β-catenin than the skin in a resting phase as observed by immunoblotting (Fig. R-23A).

We investigated whether the expression of β-catenin in murine skin changes in response to a single topical TPA treatment at the concentration used in the DMBA/TPA protocol. We observed a decrease in β-catenin expression between untreated and TPA-treated skin in both WT and p38γ/δ$^{-/-}$ mice (Fig. R-23B). This downregulation was detected at 8 hours after the treatment and the β-catenin levels were even lower at 12 hours and started to recover afterwards. At 48 hours β-catenin was expressed at the basal level (data not shown). The immunohistochemistry staining of β-catenin confirmed the decrease in β-catenin expression in epidermal keratinocytes in both genotypes (Fig. R-23B).

The downregulation of β-catenin was observed only at the protein level because its mRNA did not change after TPA treatment (Fig. R-23D). This suggests an existence of β-catenin post-transcriptional regulation in TPA-treated mouse skin, which is, however, independent on the p38γ/δ proteins.

4. Xenograft A-431 tumour growth is dependent on p38γ and p38δ.

We had observed that the mice deficient in both p38γ and p38δ were highly resistant to an induced skin carcinogenesis in the DMBA/TPA protocol. We hypothesised, that the aggressiveness of cell growth in epithelial tumours might depend on the p38γ/δ expression. To address this question we performed xenotransplantation of human epidermoid (squamous) cancer cells (A-431) (Giard et al., 1973) with depleted p38γ, p38δ and both p38γ and p38δ, into athymic (Swiss nu/nu Nu(Ico)-Fox n1nu) mice.

4.1. Establishment of p38γ- and p38δ-knock-down A-431 cells.

In order to obtain stable clones of A-431 cells deficient in p38γ and/or p38δ we used lentiviral transduction as described in sections 2.3 and 2.4 of Materials and Methods. We chose pLKO.1 vectors with different short-hairpin RNAs (shRNA), designed to downregulate the expression of

either p38γ or p38δ (four with p38γ shRNA and six with p38δ shRNA). We screened these shRNAs for silencing efficiency (Fig. R-24). Three p38γ shRNAs and three p38δ shRNAs highly silenced the expression of the corresponding genes, as observed by immunoblotting with specific anti-p38γ and anti-p38δ antibodies.

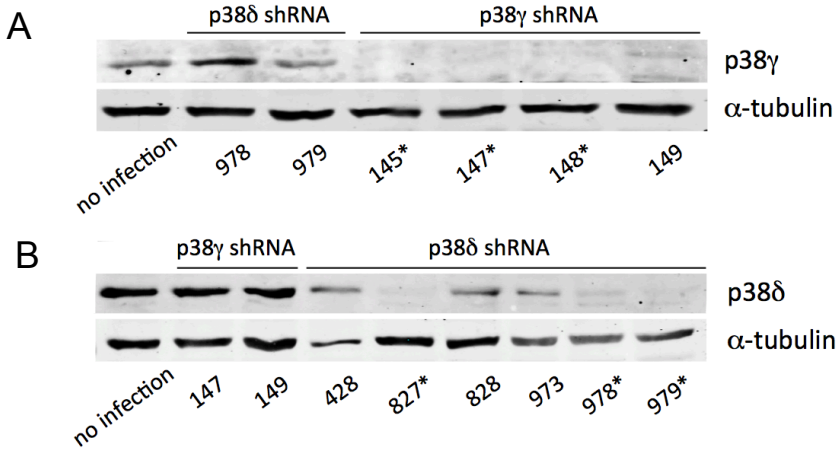

Figure R-24. Immunoblot of p38γ (A) and p38δ (B) in 30 μg of total protein lysate from non-transduced A-431 cells (no infection) and cells transduced with p38γ shRNAs (clones 145, 147, 148, 149) and p38δ shRNAs (clones 428, 827, 828, 973, 978, 979). The clones were selected in puromycin for 10 days. Asterisks indicate the most successful downregulations. α-tubulin was used as loading control.

Next, the highly efficient plasmids "145" (p38γ shRNA) and "827" (p38δ shRNA) (with over 90% of expression decrease) were selected for double gene silencing by performing two consequent transductions as described in Materials and Methods. The A-431 clone "145" with knocked-down p38γ gene was re-transduced with a shRNA against p38δ called "827" (145/827). The second transduction in this p38γ-knocked-down clone led to a level of just above 30% of the initial p38δ expression. The remaining clones were re-transduced with an empty vector pLKO.1 alone: pLKO/pLKO (2x pLKO), 145/pLKO and 827/pLKO (Fig. R-25).

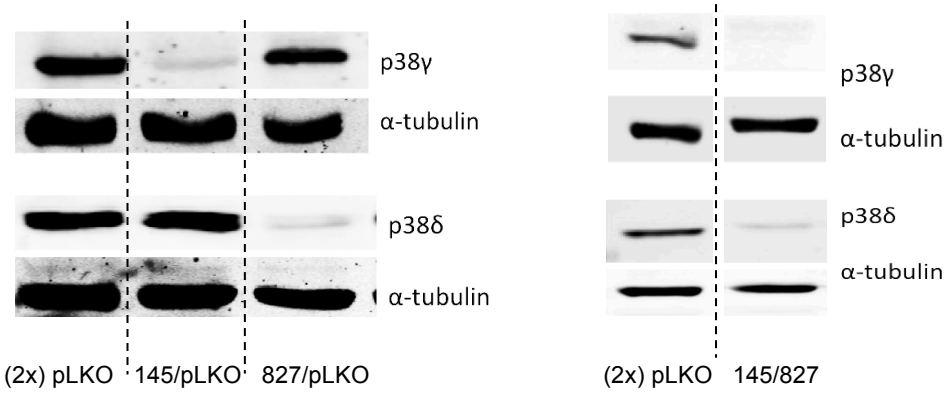

Figure R-25. Immunoblot of p38γ and p38δ in 30 μg of total protein lysate from A-431 cells transduced with the indicated combinations of three different pLKO.1 vectors: an empty vector (pLKO), vector with p38γ shRNA (145) and with p38δ shRNA (827). α -tubulin was used as loading control.

4.2. Growth of A-431 xenotransplants and cell proliferation *in vitro*.

We wanted to see whether or not the depletion of p38γ and/or p38δ in A-431 cells would change the growth of xenograft tumours in athymic nude mice. For this we used the established knock-down cells: sh-control (pLKO/pLKO), sh-p38γ (145/pLKO), sh-p38δ (827/pLKO) and sh-p38γ/δ (145/827) (Fig. R-26A). On day 0 mice received subcutaneous injections of 10^6 cells per flank (n = 6 flanks per group), as shown in Figure R-26B. The tumour growth was measured every 2 – 4 days from day 7 until day 19 after the injection (Fig. R-26C).

WT (control), p38γ$^{-/-}$ and p38δ$^{-/-}$ xenograft tumours were characterised by similar growth during the whole experiment, reaching on average 700 – 900 mm^3 of volume at day 19. Strikingly, the A-431 with downregulated expression of both p38γ and p38δ grew very slowly reaching about 100 mm^3 of volume at day 19. We concluded that the absence of both p38γ/δ proteins in these epidermoid cancer cells diminished the tumour growth.

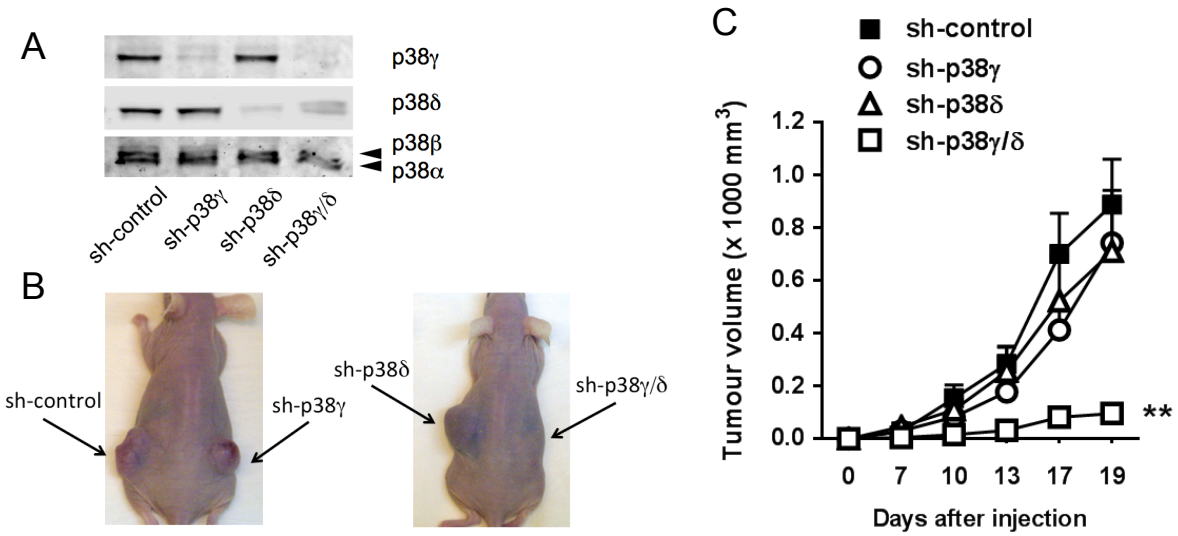

Figure R-26. Growth of A-431 xenograft tumours in athymic mice. (A) Immunoblot of p38s in total protein lysates from the A-431 clones used for the experiment. (B) Representative pictures of mice at the end of experiment (day 19). Arrows indicate sites of the injections. (C) Tumour volumes of sh-control, sh-p38γ, sh-p38δ and sh-p38γ/δ tumours at different times after the injection. Results are means +/- SEM (n=6). **P<0.01 (two-way ANOVA).

The diminished proliferation of sh-p38γ/δ A-431 cells in the tumours was later confirmed by quantifying cells growth in culture medium (Fig. R-27). We plated the same numbers of sh-control and sh-p38γ/δ A-431 cells on plates and grew them for up to three days, counting cell numbers every 24 hours. Similarly to what we had observed *in vivo*, the lack of both kinases p38γ and p38δ significantly impaired the A-431 proliferation comparing with WT.

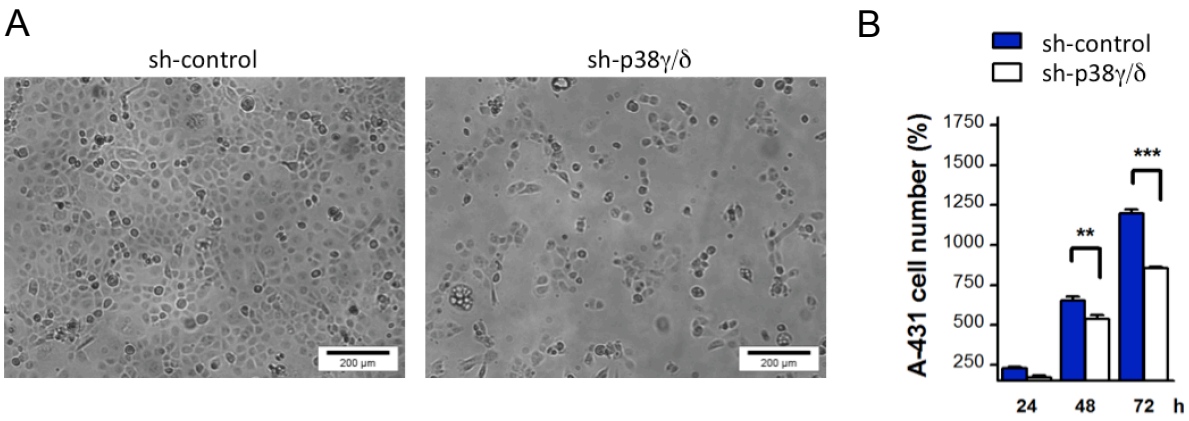

Figure R-27. Proliferation of sh-control and sh-p38γ/δ A-431 cells *in vitro*. 0.8 x 10^5 cells were seeded on tissue culture plates on day 0 and the cell number was quantified on day 1, 2 and 3. (A) Representative images of the cell culture on day 24 hours after the seeding. (B) Cell numbers at different times after the culture initiation. Data are percentage versus number of cells seeded. Results are expressed as means +/- SEM (n=3). **P<0.01, ***P<0.001 (two-way ANOVA).

DISCUSSION

1. Introduction.

Published data highlight the importance of p38γ and p38δ MAPKs in malignant transformation. Cell-based assays showed their functions in tumorigenesis, controlling processes such as cell proliferation, cell migration and cell contact inhibition (Faraone et al., 2009; Cerezo-Guisado et al., 2011; Risco and Cuenda, 2012; Yang et al., 2013). p38γ and p38δ are also implicated in linking inflammation and tumour promotion and/or progression, since impaired cytokine production was demonstrated in p38γ/δ-deficient mice in different disease models such as septic shock, arthritis and colitis-associated colon cancer (Risco et al., 2012; Criado et al., 2014, del Reino et al., 2014). In addition, in the two-stage DMBA/TPA protocol, which depends on pro-inflammatory processes in the skin (Swann et al., 2008), p38δ has a pro-tumorigenic role. Mice that lack p38δ have reduced susceptibility to development of skin papillomas after DMBA/TPA treatment (Schindler et al., 2009). The authors claim that skin carcinogenesis in p38δ-deficient mice involves a defect in proliferative responses associated with abnormal signalling through two major transformation-promoting pathways, ERK1/2 and STAT3. In this thesis, we have defined the importance of p38γ and of p38δ in mouse skin inflammation and tumorigenesis.

2. Expression and activation of p38γ and p38δ in the skin and skin papillomas.

p38α and p38δ are the predominant p38 isoforms in normal human and mouse keratinocytes, and it is commonly claimed that p38γ is virtually undetectable in normal epidermis (Junttila et al., 2007). Another study reported expression of p38α, p38β and p38δ in healthy and psoriatic keratinocytes (Johansen et al., 2005). Psoriasis is a chronic inflammatory skin disorder characterised by keratinocyte hyperproliferation and differentiation. The activity of the three isoforms is augmented in lesional compared with nonlesional psoriatic skin. The same study claimed that p38γ is undetectable in skin (Johansen et al., 2005). Whereas p38α and p38δ have been studied preferentially in skin and in skin-derived cell, the role of p38γ has been neglected so far, and little is known about its functions in the skin. One study showed that activated p38γ could be involved in human melanoma cell death in response to genotoxic stresses such as UV radiation or cisplatin (Pillaire et al., 2000); another revealed increased p38γ expression in melanoma cells that overexpressed the platelet-derived growth factor receptor (Faraone et al., 2009). Here we demonstrate that p38γ is expressed (although to a lesser extent than p38δ) in keratinocytes and skin. p38γ can be detected both at the mRNA level by qPCR and as a protein by immunoblotting. We cannot explain with certainty the differences between the results obtained by other groups and our own, although different antibodies/oligonucleotides, their specificity and/or exposure intensities when developing immunoblots could be, at least in part, the answer. Moreover, in

contrast to our model, the cited studies used only human cells. Results of a recent work by Sano and Park (2014) on p38γ and p38δ expression in mouse skin coincide with our data; they show that both p38γ and p38δ are expressed in the epidermis and in isolated keratinocytes. p38γ, but not p38δ, is also expressed in the dermis (including dermal fibroblasts).

3. p38γ and p38δ in human SCC and in mouse skin papillomas.

There are few published clinical data on p38γ and/or p38δ in skin cancer, including squamous cell cancer. The Oncomine/Compendia Bioscience (Life Technologies) database shows no consistent p38γ or p38δ expression patterns in the relatively few squamous cancer cases available (Fig. D-1). For instance, p38δ expression, which is quite highly expressed in the oral cavity, is significantly downregulated in transformed OSCC tissue, whereas p38γ, normally less abundant than p38δ, is upregulated in this type of carcinoma (Peng et al., 2011). In contrast, p38γ and p38δ expression in tongue SCC cases is characterised by the opposite effect; p38γ expression is decreased in cancer tissue compared with healthy tissue, while p38δ is upregulated (Estilo et al., 2009).

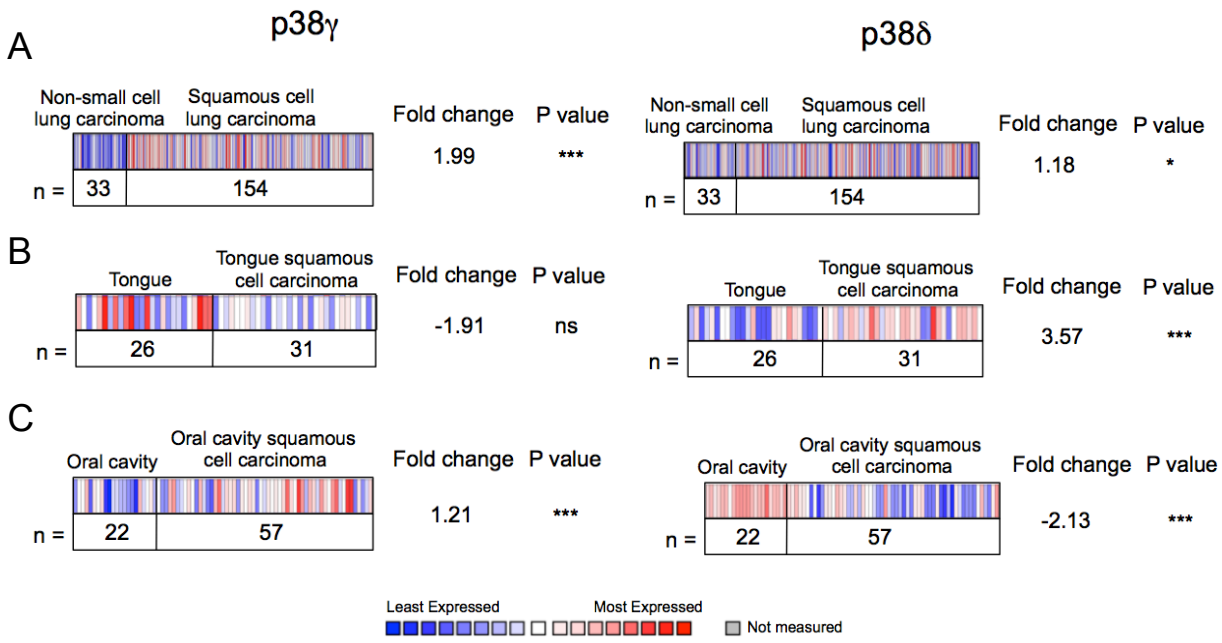

Figure D-1. Relative levels of p38γ (left) and p38δ (right) in biopsies from patients with non-small cell lung carcinoma and lung SCC (A), tongue SCC (B) and oral cavity SCC (C). ns: not significant. *P <0.05, ***P <0.001. n: number of samples. Analysis was performed using the Oncomine database and data come from Hammerman et al., 2012 (A); Estilo et al., 2009 (B); Peng et al., 2011 (C).

Interestingly, in our experiments, p38γ and p38δ protein and mRNA levels showed marked differences between papillomas developed in the DMBA/TPA protocol and healthy skin as well.

An epithelial fraction of skin papillomas is constituted by mutated hyperproliferating keratinocytes (Cataisson et al., 2012), which originate when the mouse epidermis undergoes a DMBA-provoked mutational initiation, followed by TPA-dependent promotion. p38δ is relatively abundant in this type of skin tumour, as observed in WT and p38γ$^{-/-}$ mice and compared with healthy skin; in contrast, p38γ expression is lower in tumours from WT and p38δ$^{-/-}$ mice than in healthy skin. These differences in p38γ and p38δ expression are comparable to those observed between WT keratinocytes and healthy skin. p38δ is expressed slightly more in keratinocytes than in whole skin, whereas p38γ is expressed more abundantly in skin than in keratinocytes alone. These findings indicate that p38γ is also expressed by cells other than keratinocytes (e.g. dermal fibroblasts), whereas p38δ is expressed predominantly in keratinocytes. These data are supported by the fact that tumour tissue where p38δ is highly expressed is formed largely by keratinocytes.

In the WT and p38γ$^{-/-}$ tumours that develop in the DMBA/TPA protocol, p38δ is not only expressed strongly but is also highly phosphorylated, compared with healthy skin in the same mouse. In contrast, we detected no differences in p38α phosphorylation between papillomas and healthy skin. Moreover, phosphorylated p38α levels are comparable among all genotypes. These data highlight the possible importance of p38δ-mediated processes in murine epidermal cells during tumorigenesis.

4. p38γ and p38δ isoform redundancy and synergism of the p38γ/δ deficiency.

Our results from the DMBA/TPA experiment are in agreement with observations of the tumorigenic role of p38δ in skin carcinogenesis (Schindler et al., 2009; Efimova, 2010), which we also confirmed. We demonstrated that compared to all other genotypes, WT mice that underwent DMBA/TPA treatment showed the greatest susceptibility to skin tumour development. In contrast, mice deficient in both p38γ and p38δ were the most resistant to skin tumorigenesis, whereas p38γ$^{-/-}$ and p38δ$^{-/-}$ mice had an intermediate phenotype; the p38γ knock-outs were more susceptible (partially resembling WT) and p38δ knock-outs were slightly more resistant.

This intermediate phenotype of p38γ$^{-/-}$ and p38δ$^{-/-}$ compared to WT and p38γ/δ$^{-/-}$ mice could be due to partial isoform redundancy, with predominance of neither isoform. Functional overlap of the two isoforms has been reported (Criado et al., 2014; Risco et al., 2012) and might account for the partial effects observed in p38γ$^{-/-}$ and p38δ$^{-/-}$ mice. *In vitro* experiments in MEF also demonstrated this redundancy. SAP97/hDlg (synapse-associated protein 97/human discs large

homolog 1) is a physiological p38γ substrate that in WT cells is normally phosphorylated at Ser^{158}, Thr^{209} and Ser^{442}. In $p38\gamma^{-/-}$ cells, this substrate is also phosphorylated by the remaining isoforms, p38δ (at Thr^{209}), p38α and p38β (both at Ser^{442}) (Sabio et al., 2005).

Our results emphasise the existence of p38γ and p38δ functions associated with tumour development and indicate the synergistic impact of p38γ and p38δ deficiency on skin during chemically induced tumorigenesis. Reduced incidence of tumours, with no apparent change in size or growth, in $p38\gamma^{-/-}$ and $p38\delta^{-/-}$ compared with WT mice further suggests a role for these isoforms in skin tumour initiation rather than its progression.

5. Crosstalk between p38γ and p38δ in skin and in transformed keratinocytes.

In light of our *in vivo* findings on p38γ, we could not rule out possible functions in healthy or transformed epithelium, or in conditions such as TPA-induced skin tumour promotion in the DMBA/TPA protocol. This idea is also supported by *in vitro* and *in vivo* data from our experiments on human A-431 epidermoid cancer cells. We showed that wild type A-431 cells not only express p38γ and p38δ, but are also characterised by phosphorylation of both p38 isoforms in response to TPA treatment; p38α is also phosphorylated in these cells after TPA treatment (Fig. D-2).

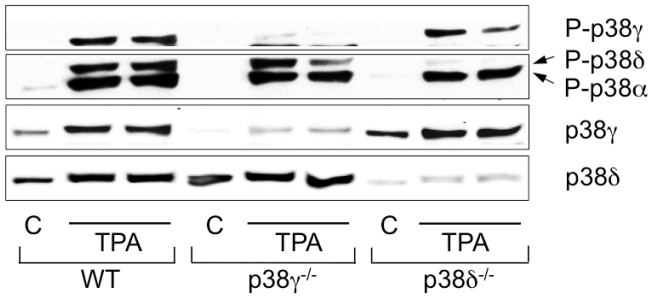

Figure D-2. Phosphorylation of p38α, p38γ and p38δ in wild type A-431 cells and in p38γ- and p38δ-deficient clones in response to TPA treatment (300 ng/ml; 20 min).

Given that p38γ expression is higher in healthy skin than in keratinocytes or skin papillomas, we hypothesised that p38γ functions in skin might not be restricted to keratinocytes. This idea was supported by our observations of the effect of TPA treatment on skin in mice and on A-431 cells, in the absence of either p38γ or p38δ. We show that a single TPA treatment had a different effect on p38γ and on p38δ phosphorylation in mouse skin, depending on the presence/absence of the other isoform. Specifically, TPA treatment induced p38γ and p38δ phosphorylation in WT mice, whereas p38δ-deficient mice did not phosphorylate p38γ to the extent observed in WT mice. In contrast, p38γ deficiency did not impede p38δ phosphorylation (Fig. D-3). This effect was not

observed in A-431 cells in which p38δ expression was silenced. p38γ was phosphorylated in the p38δ$^{-/-}$ clone after TPA treatment and *vice versa* (Fig. D-2). These results suggest the existence of a crosstalk between p38γ and p38δ in the skin that does not necessarily take place in isolated A-431 cells. Our *in vivo* results thus indicate that p38γ and p38δ can each modulate phosphorylation of the other, probably in different skin compartments by a mechanism that needs further clarification.

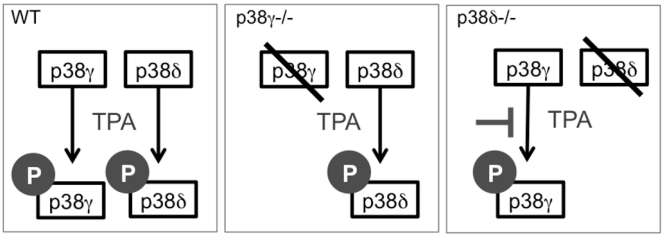

Figure D-3. Hypothetical crosstalk between p38γ and p38δ in the skin of WT, p38γ$^{-/-}$ and p38δ$^{-/-}$ mice in the context of TPA-induced p38γ/δ phosphorylation.

A-431 cells express an extremely large number of EGF receptors on their surface (3 x 10^6/cell); this is due, at least in part, to *EGFR* gene amplification (Janmaat et al., 2003). For comparison, normal human fibroblasts have a much lower EGFR density, approximately 10^5/cell. The physiology of the transformed A-431 cells thus does not exactly reflect the processes in normal keratinocytes, especially after TPA treatment, which is known to activate EGFR. TPA-induced receptor activation was demonstrated by chemical inhibition of EGFR, which resulted in effective, dose-dependent reduction of EGFR tyrosine phosphorylation (Lu et al., 2007). Since we cannot exclude possible reciprocal regulation of p38γ and p38δ in healthy keratinocytes, it is difficult to determine precisely whether conserved p38γ phosphorylation in the p38δ$^{-/-}$ A-431 clone is due to high EGFR or is a consequence of other keratinocyte transformation events. Another possible explanation is that p38δ downregulation is incomplete and the remaining p38δ protein (~10% of the control clone) is sufficient to facilitate TPA-induced p38γ phosphorylation.

Regulation of p38γ and p38δ expression and activity in mouse skin cells might thus be context-dependent, and probably differs between cell types and between steady state and inflammatory/tumorigenic conditions. Resistance of p38δ$^{-/-}$ mice to skin tumorigenesis could result from reduced p38γ activity during tumour promotion rather than from lack of p38δ alone; this is supported by the observation of increased tumour suppression in p38γ/δ$^{-/-}$ compared to p38δ$^{-/-}$ mice.

6. p38γ and p38δ in epidermis proliferation.

As disruption of cell cycle control contributes to malignant transformation, increased proliferation is a common indicator of tumorigenesis. Tumour promoters used in skin carcinogenesis models, such as TPA, have several activities including generation of epidermal hyperplasia through induction of skin keratinocyte division (Aldaz et al., 1985). We showed that after a single TPA treatment, the skin of mice deficient in p38γ or p38δ or both showed fewer proliferating epidermal cells compared with WT mice. This was also reflected in epidermis thickening, most noticeable in WT mice, whereas this layer was thinner in the remaining genotypes (p38$\gamma^{-/-}$, p38$\delta^{-/-}$, p38$\gamma/\delta^{-/-}$). These results are in accordance with observations from the Efimova group, who studied p38δ functions in TPA-treated skin and obtained similar data showing that p38δ-null skin is proliferation-deficient (Schindler et al., 2009).

At difference from epidermis treated with TPA alone, the epithelium of papillomas that developed in the DMBA/TPA protocol showed similar numbers of proliferating cells in WT, p38$\gamma^{-/-}$ and p38$\delta^{-/-}$ mice. The Efimova group found that in p38$\delta^{-/-}$ mice, besides its reduction in skin, epithelial cell proliferation was also diminished in skin papillomas (Schindler et al., 2009); this contradicts our observations. We hypothesise that this difference is due to the distinct protocols used in the two studies. We analysed proliferation in papillomas 10 weeks after the last TPA treatment (at week 29), whereas Schindler et al. examined the papilloma samples immediately after the final TPA treatment (at week 19). This would suggest that the implication of p38δ (and p38γ) in control of proliferation depends on the accompanying TPA induction in the skin and tumour epithelium.

The proliferative effect of TPA treatment manifested by epidermal hyperplasia is also associated with important molecular changes. Signalling pathways induced in TPA-treated skin are defined by the activation of factors such as MAPK (p38α, p38γ, p38δ, ERK1/2, JNK1/2) and STAT3, all transiently phosphorylated in skin cells. STAT3 is a common oncogenic transcription factor in many tumours and its activation mediates malignant cell proliferation and their escape from apoptosis (Yu et al., 2007). Its role in promoting DMBA/TPA-induced epithelial hyperproliferation was highlighted by a report of suppressed skin cell division by a STAT3 antagonist (Chan et al., 2004). Multistage skin carcinogenesis assays in skin-specific gain and loss of STAT3 function transgenic mice showed that STAT3 is necessary for tumour initiation and tumour promotion through regulation of survival and proliferation, respectively. This regulation leads to survival of DNA-damaged stem cells and the maintenance of proliferation necessary for clonal expansion of initiated cells. STAT3 also plays a role in malignant progression of skin tumours, by regulating

genes involved in angiogenesis and invasion (Kim et al., 2007). We show that the vast majority of epithelial cells in a progressed skin tumour, which are found in both peripheral and interior tumour masses, are marked by nuclei with phosphorylated STAT3, whereas benign papillomas were phospho-STAT3-positive mainly in the outermost tumour stroma-surrounding epithelium. Nonetheless, we found no differences in STAT3 phosphorylation among WT, p38$\gamma^{-/-}$ and p38$\delta^{-/-}$ mice. Total STAT3 expression in skin papillomas was also similar among the genotypes. In contrast, in the acute skin inflammation experiment with TPA alone, we observed a significantly less STAT3 phosphorylation in the skin of p38γ/δ knock-out mice compared with WT mice during the first four hours after skin exposure to TPA. We therefore hypothesised that the reduced proliferation of epidermal keratinocytes in these mice might be due, at least in part, to disrupted STAT3 signalling. STAT3 activation in p38$\gamma^{-/-}$ and p38$\delta^{-/-}$ mice in the same conditions was only affected at shorter times post-TPA treatment. At longer times, STAT3 phosphorylation was comparable with WT mice, which suggests a synergistic role of p38γ/δ deficiency in STAT3 signalling regulation, as well as involvement of additional mechanism(s) that underlie the cell proliferation reduction in single p38γ and p38δ knock-out mice.

7. Inflammation as a pro-tumorigenic factor.

A broad range of experimental and clinical evidence highlights the central role of chronic inflammation in promoting tumour development (Hanahan and Weinberg, 2000). The molecular mechanisms that convert transient inflammatory reactions in tissues, including the skin, into a tumour-promoting microenvironment nonetheless remain largely unknown. Keratinocytes undergo transformation in the course of the DMBA/TPA protocol, leading to skin papilloma growth, which is dependent on clonal expansion of mutated, initiated cells. Since not all skin papillomas culminate as differentiated skin outgrowths, but rather disappear (Kopp-Schneider and Portier, 1992), the molecular events that lead to epithelial cell transformation during early stages of skin tumour promotion must be very complex and highly contextual. DMBA/TPA-treated epidermal cells are subject to molecular changes that are reflected in the constitutive phosphorylation of proteins such as p38δ, Akt and STAT3 in the skin tumours, as shown by immunoblot and/or immunohistochemistry staining in our papilloma biopsies. As predicted, these proteins were also activated in inflamed skin.

Skin inflammation underlies development and progression of a number of disorders including psoriasis, atopic dermatitis and skin cancer. The infiltration of immune cells such as neutrophils, T lymphocytes and macrophages, as well as local production of inflammatory cytokines and other mediators are essential during skin carcinogenesis. Resistance to DMBA/TPA-induced skin

tumorigenesis is linked to a defect in sustaining inflammation during the promotion phase (Gebhardt et al., 2008). Another study suggested that p38 MAPK-dependent responses might include inflammatory reactions, whose onset can be determined by interleukin production (Lilleholt et al., 2011). In that study, WT and p38β/p38δ double knock-out mice were examined for their response to TPA. The authors observed lower IL-1β protein production in p38β/$\delta^{-/-}$ than in WT mice, while mRNA production was unaffected. They claimed that p38β and/or p38δ might be involved in the post-transcriptional regulation of this cytokine, although the exact contribution of either isoform was not specified (Lilleholt et al., 2011). Recent publications have shown the synergistic anti-inflammatory effect of p38γ/δ deficiency in several mouse models such as LPS-induced septic shock, rheumatoid arthritis and colitis-associated colon cancer (Risco et al., 2012; Criado et al., 2014; del Reino et al., 2014). We hypothesised that induced epithelial proliferation and altered cell signalling in skin chronically exposed to TPA during tumour promotion and after single TPA administration could be a result, at least in part, of inflammatory conditions.

8. p38γ and p38δ in cytokine production in inflamed skin.

Neutrophil-derived products have critical roles at different stages of tumour progression, from initial genotoxic insult to metastasis to distant sites. Although early studies indicated that neutrophils might be cytotoxic to tumour cells (particularly in their regulation of cytotoxic T cells), recent work has shown overwhelmingly that neutrophils promote tumour progression via angiogenesis, matrix degradation, immune surveillance, as well as secretion of chemokines (including KC and MIP-2) and cytokines (IL-1β, IL-6, IL-12, TNF-α), and production of reactive oxygen species, all of which contribute to the pro-tumorigenic environment and metastasis (Gregory and Houghton, 2011; Fridlender and Albelda, 2012). MIP-2 (or CXCL2 in humans) is a CXC chemokine (with two N-terminal cysteine residues separated by one amino acid) has potent neutrophil chemotactic activity as well as mitogenic activity for epithelial cells in a rat lung model (Driscoll et al., 1995). Several *in vitro* studies also demonstrated that non-immune cells, such as epithelial cells or fibroblasts, also produce MIP-2 (Driscoll, 2000). Chemokine production in the skin is cell type-dependent and their expression patterns at inflammation sites might reflect the temporally ordered contribution of distinct cell types. In the inflammation-associated skin injury model, distinct CXC chemokines show restricted expression in myeloid *versus* non-myeloid cell types (Armstrong et al., 2004). In this model, dermal fibroblasts and endothelial cells are primarily responsible for KC expression in the skin, whereas MIP-2 production, especially at longer times after injury, appears to be restricted to infiltrating inflammatory leukocytes, including neutrophils and monocytes.

Here we report that, in comparison with WT mice, TPA-treated skin of p38γ/δ-deficient mice not only produces less IL-1β, IL-6 and TNF-α, but also shows reduced KC and MIP-2 expression. Since leukocyte recruitment to inflammatory sites is a process largely orchestrated by chemokines (Garin and Proudfoot, 2011), the reduction in KC and MIP-2 levels coincides with lower neutrophil myeloperoxidase expression in skin and fewer neutrophils infiltrating TPA-challenged skin in p38γ/δ$^{-/-}$ than in WT mice.

Cytokine production in the skin is also crucial for epithelial hyperproliferation. IL-6 induces epidermal dysplasia through STAT3 induction (Yu et al., 2007). In our study, although there was no second IL-6 production peak at 24 h post-TPA treatment, p38γ/δ$^{-/-}$ mice expressed significantly lower levels of this cytokine compared with WT mice. The protective effect of the p38γ/δ deficiency in DMBA/TPA-treated skin could be therefore explained, at least in part, by reduced IL-6 expression linked to lower STAT3 phosphorylation and less proliferation in TPA-treated skin. We hypothesise that both p38γ and p38δ are important for the regulation of skin inflammation after TPA treatment, and that their deletion has an anti-inflammatory, anti-tumorigenic role via mechanisms that involve signalling regulation and cell proliferation in the epithelium. Both skin-residing and skin-infiltrating immune cells could drive local inflammation, whose regulation might depend, to a certain extent, on functional p38γ and p38δ proteins.

We also showed that TPA-induced proliferation of epidermal cells is reduced in p38γ$^{-/-}$ and p38δ$^{-/-}$ compared with WT mice. The absence of one isoform alone is thus sufficient to exert an anti-proliferative effect. STAT3 phosphorylation is not affected in these mice to the extent observed in p38γ/δ$^{-/-}$ mice, however, and with one exception, cytokine production in single knock-out mice resembles the WT phenotype. Other tumour-promoting contributors, dependent on p38γ and/or p38δ, should undoubtedly be considered. It remains to be determined whether the decrease observed in TPA-induced cytokine and chemokine production in p38γ/δ$^{-/-}$ mice compared with WT, is due only to a synergistic effect of the lack of both isoforms in the same cell type in skin, or is due to reduced leukocyte (mainly neutrophil) infiltration, both of which would contribute to overall inflammation.

9. Concluding remarks.

It is very likely that cells other than keratinocytes, such as dermal fibroblasts, skin-resident and skin-infiltrating immune cells, as well as biological factors produced in the skin, are all important

during TPA-induced skin inflammation, including the promotion stage of skin tumorigenesis. The exact contribution of p38γ/δ deficiency in each skin compartment remains to be established.

We have shown that whereas the lack of p38γ or p38δ alone does not reduce A-431 tumour growth when these cells are injected subcutaneously into nude mice, deletion of both p38γ and p38δ affects this growth acutely/really a lot. This observation supports the synergism observed in our experiments on skin tumorigenesis and sheds light on possible applications of dual p38γ and p38δ inhibitors in clinical trials for treatment of inflammatory diseases, including human skin SCC.

CONCLUSIONS

CONCLUSIONES

1. p38γ and p38δ have a pro-tumorigenic role in the DMBA/TPA protocol as the lack of both isoforms exerts a highly tumour-suppressive effect in this model.

2. Cell proliferation, neutrophil infiltration and signalling pathways activation in the tumours do not depend on the presence or absence of either p38γ or p38δ in developed skin papillomas, pointing out to TPA-induced promotion stage as crucial for the p38γ/δ roles in the skin tumorigenesis.

3. DMBA responsiveness is unaffected by the lack of p38γ and/or p38δ, since the DMBA-treated skin has the same number of epithelial cells undergoing apoptosis independently of the presence or absence of either p38γ and/or p38δ.

4. Both p38γ and p38δ are involved in the control of epidermal cell proliferation induced by single TPA treatment of the skin, the depletion of either or both p38 isoforms leads to a reduction in the number of BrdU-positive cells in the treated epidermis.

5. The dramatic resistance of p38γ/δ$^{-/-}$ mice to skin tumorigenesis, comparing with WT mice, can be caused by the impairment of TPA-induced cytokine and chemokine expression, coinciding with a decrease in neutrophils recruitment and lower levels of STAT3 phosphorylation.

6. The activation of p38γ in TPA-treated skin is regulated by p38δ as shown by the impairment of p38γ phosphorylation in p38δ-deficient mice.

7. p38γ and p38δ have a pro-tumorigenic role in human transformed keratinocytes A-431, since the depletion of both kinases in these cells leads to impaired proliferation, *in vitro*, and diminished tumour growth of xenotransplants, *in vivo*, in athymic mice.

1. p38γ y p38δ tienen un papel oncogénico en el modelo de cáncer de piel inducido por DMBA/TPA ya que la falta de ambas isoformas produce una reducción en la formación de tumores en este modelo.

2. La proliferación celular, infiltración de neutrófilos y activación de rutas de señalización en los tumores de piel no depende de la presencia o ausencia de p38γ y p38δ en los papilomas, indicando que las isoformas p38γ y p38δ están implicadas en el estadio de promoción dependiente de TPA.

3. La respuesta de la piel al tratamiento con DMBA no depende de p38γ y/o p38δ, ya que el epitelio tratado con este compuesto contiene comparables cantidades de células apoptóticas independientemente de la ausencia o presencia de p38γ y p38δ.

4. Las dos proteínas p38γ y p38δ controlan la proliferación de las células de la epidermis inducida por TPA. Le falta de una de las dos o de ambas isoformas de p38 causa una reducción de las células epiteliales BrdU-positivas.

5. La pronunciada resistencia de los ratones p38γ/δ$^{-/-}$ en el protocolo de la tumorigénesis de piel, comparando con los ratones silvestres, puede deberse a la insuficiente producción de citoquinas y quimioquinas tras el tratamiento con TPA, coincidiendo con un menor reclutamiento de neutrófilos y un descenso en la fosforilación de STAT3.

6. La activación de p38γ en la piel tratada con TPA está regulada por p38δ, ya que la fosforilación de p38γ en los ratones deficientes en p38δ está severamente reducida.

7. p38γ y p38δ desempeñan un papel oncogénico en la línea celular de queratinocitos humanos A-431, puesto que la reducción de expresión de las dos quinasas en estas células afecta la proliferación tanto *in vitro* como *in vivo* en los xenotransplantes en los ratones atímicos.

REFERENCES

1. Aberle H. et al. beta-catenin is a target for the ubiquitin-proteasome pathway. EMBO J. 1997; 16: 3797-3804.
2. Adams C.L. et al. Quantitative analysis of cadherin-catenin-actin reorganisation during development of cell-cell adhesion. J. Cell. Biol. 1996; 135: 1899-1911.
3. Adhikary G. et al. PKC-delta and –eta, MEKK-1, MEK-6, MEK-3, and p38-delta are essential mediators of the response of normal human epidermal keratinocytes to differentiating agents. J. Invest. Dermatol. 2010; 130: 2017-2030.
4. Aguirre-Ghiso J.A. Models, mechanims and clinical evidence for cancer dormancy. Nat. Rev. Cancer. 2007; 7: 834-846.
5. Al Zaid S.K., Turkson J. STAT3 as a target for inducing apoptosis in solid and hematological tumors. Cell Res. 2008; 18: 254-267.
6. Aldaz C.M. et al. Cutaneous changes during prolonged application of 12-O-tetradecanoylphorbol-13-acetate on mouse skin and residual effects after cessation of treatment. Cancer Res. 1985; 45: 2753-2759.
7. Allen M. et al. Deficiency of the stress kinase p38alpha results in embryonic lethality: characterisation of the kinase dependence of stress responses of enzyme-deficient embryonic stem cells. J. Exp. Med. 2000; 191: 859-870.
8. Alonso L., Fuchs E. The hair cycle. J. Cell Science. 2006; 119: 391-393.
9. Ananthaswamy H.N., Pierceall W.E. Molecular alterations in human skin tumors. Prog. Clin. Biol. Res. 1992; 376: 61-84.
10. Apte R.N., Voronov E. Interleukin-1—a major pleiotropic cytokine in tumor-host interactions. Semin. Cancer Biol. 2002; 12: 277-290.
11. Armstrong D.A. et al. Neutrophil chemoattractant genes KC and MIP-2 are expressed in different cell populations at sites of surgical injury. J. Leukoc. Biol. 2004; 75: 641-648.
12. Arnott C.H. et al. Expression of both TNF-α receptors subtypes is essential for optimal skin tumour development. Oncogene. 2004; 23: 1902-1910.
13. Arthur J.S., Ley S.C. Mitogen-activated protein kinases in innate immunity. Nat. Rev. Immunol. 2013; 13: 679-692.
14. Balkwill F. et al. Smoldering and polarized inflammation in the initiation and promotion of malignant disease. Cancer Cell. 2005; 7: 211-217.
15. Balkwill F. TNF-alpha in promotion and progression of cancer. Cancer Metastasis Rev. 2006; 24: 409-416.
16. Balmain A. et al. Activation of the mouse cellular Harvey-ras gene in chemically induced benign skin papillomas. Nature. 1984; 307: 658-660.
17. Balmain A., Brown K. Oncogene activation in chemical carcinogenesis. Adv. Cancer Res. 1988; 51: 147-182.
18. Beardmore V.A. et al. Generation and characterization of p38beta (MAPK11) gene-targeted mice. Mol. Cell Biol. 2005; 25: 10454-10464.
19. Bedoui S. et al. Cross-presentation of viral and self antigens by skin-derived CD103+ dendritic cells. Nat. Immunol. 2009; 10: 488-495.
20. Beronja S. et al. RNAi screens in mice identify physiological regulators of oncogenic growth. Nature. 2013; 501: 185-190.
21. Blees J.S. et al. Erioflorin stabilizes the tumor suppressor Pdcd4 by inhibiting its interaction with the E3-ligase β-TrCP1. PLoS One. 2012; 7: e46567.

22. Border W.A., Noble N.A. Transforming growth factor β in tissue fibrosis. N. Engl. J. Med. 1994; 331: 1286-1292.
23. Bos J.L. *Ras* oncogenes in human cancers: a review. Cancer Res. 1989; 49: 4682-4689.
24. Boutwell R.K. Some biological aspects of skin carcinogenesis. Prog. Exp. Tumor Res. 1964; 19: 207-250.
25. Bradley P.P. et al. Measurement of cutaneous inflammation: estimation of neutrophil content with an enzyme marker. J. Invest. Dermatol. 1982; 78: 206–209.
26. Brancho D. et al. Mechanism of p38 MAP kinase activation in vitro. Genes Dev. 2003; 17: 1969-1978.
27. Brown K. et al. The malignant capacity of skin tumours induced by expression of a mutant H-ras transgene depends on the cell type targeted. Curr. Biol. 1998; 8: 516-524.
28. Cataisson C. et al. IL-1R-MyD88 signaling in keratinocyte transformation and carcinogenesis. J. Exp. Med. 2012; 209: 1689-1702.
29. Cataisson C., Yuspa S.H. Interacting Signaling Pathways in Mouse Skin Tumor Initiation and Progression. Signaling Pathways in Squamous Cancer. Chapter 7. Springer. 2011; 149-164.
30. Cerezo-Guisado M.I. et al. Evidence of p38γ and p38δ involvement in cell transformation processes. Carcinogenesis. 2011; 32: 1093-1099.
31. Chan E.F. et al. A common human skin tumour is caused by activating mutations in beta-catenin. Nat. Genet. 1999; 21: 410-413.
32. Chan K.S. et al. Disruption of Stat3 reveals a critical role in both the initiation and the promotion stages of epithelial carcinogenesis. J. Clin. Invest. 2004; 114: 720-728.
33. Chan K.S. et al. Epidermal growth factor receptor-mediated activation of Stat3 during multistage skin carcinogenesis. Cancer Res. 2004; 64: 2382-2389.
34. Chen J.G. et al. Cost of nonmelanoma skin cancer treatment in the United States. Dermatol. Surg. 2001; 27: 1035-1038.
35. Chen Z. et al. MAP kinases. Chem. Rev. 2001; 101: 2449-2476.
36. Cichocki M. et al. Correlation between EGFR Y1068 tyrosine phosphorylation and AP-1 activation by tumor promoter 12-O-tetradecanoylphorbol-13-acetate in mouse skin. Environ. Toxicol. Pharmacol. 2012; 33: 92-97.
37. Criado G. et al. Alternative p38 mitogen-activated protein kinases are essential for collagen-induced arthritis. Arthritis Rheum. 2014; 66: 1208-1217.
38. Cuadrado A., Nebreda A.R. Mechanisms and functions of p38 MAPK signalling. Biochem. J. 2010; 429: 403-417.
39. Cuenda A. et al. Activation of stress-activated protein kinase-3 (SAPK3) by cytokines and cellular stresses is mediated via SAPKK3 (MKK6); comparison of the specificities of SAPK3 and SAPK2 (RK/p38). EMBO J. 1997; 16: 295-305.
40. Cuenda A., Rousseau S. p38 MAP-kinases pathway regulation, function and role in human diseases. Biochim. Biophys. Acta. 2007; 1773: 1358-1375.
41. Culig Z. Interleukin-6 as a therapy target in oral squamous carcinoma. Expert. Opin. Ther. Targets. 2013; 17: 53-59.
42. Dashti S.R. et al. MEK6 regulates human involucrin gene expression via a p38α- and p38δ-dependent mechanism. J. Biol. Chem. 2001; 276: 27214-27220.

43. del Reino P. et al. Pro-oncogenic role of alternative p38 mitogen-activated protein kinases p38γ and p38δ, linking inflammation and cancer in colitis-associated colon cancer. Cancer Res. 2014; [Epub ahead of print]
44. DiGiovanni J. Multistage carcinogenesis in mouse skin. Pharmacol. Ther. 1992; 54: 63-128.
45. Dlugosz A.A. et al. Autocrine transforming growth factor is dispensable for v-ras^{Ha}-induced epidermal neoplasia: potential involvement of alternate epidermal growth factor receptor ligands. Cancer Res. 1995; 55: 1883-1893.
46. Driscoll K.E. et al. Cloning, expression, and functional characterization of rat MIP-2: a neutrophil chemoattractant and epithelial cell mitogen. J. Leukoc. Biol. 1995; 58: 359-364.
47. Driscoll K.E. TNFalpha and MIP-2: role in particle-induced inflammation and regulation by oxidative stress. Toxicol. Lett. 2000; 112-113: 177-183.
48. Dubas L.E., Ingraffea A. Nonmelanoma Skin Cancer. Facial Plast. Surg. Clin. N. Am. 2013; 21: 43-53.
49. Eckert R.L. et al. p38 mitogen-activated protein kinases on the body surface- a function for p38δ. J. Invest. Dermatol. 2003; 120: 823-828.
50. Efimova T. et al. A regulatory role for p38δ MAPK in keratinocyte differentiation: evidence for p38δ-ERK1/2 complex formation. J. Biol. Chem. 2003; 278: 34277-34285.
51. Efimova T. p38delta mitogen-activated protein kinase regulates skin homeostasis and tumorigenesis. Cell Cycle. 2010; 9: 498-505.
52. Ehrenreiter K. et al. Raf-1 addiction in Ras-induced skin carcinogenesis. Cancer Cell. 2009; 16: 149-160.
53. Estilo C.L. et al. Oral tongue cancer gene expression profiling: Identification of novel potential prognosticators by oligonucleotide microarray analysis. B.M.C. Cancer. 2009; doi: 10.1186/1471-2407-9-11.
54. Evan G.I., Vousden K.H. Proliferation, cell cycle and apoptosis in cancer. Nature. 2001; 411: 342-348.
55. Faraone D. et al. Platelet-derived growth factor-receptor alpha strongly inhibits melanoma growth in vitro and in vivo. Neoplasia. 2009; 11: 732-742.
56. Foster W.H. et al. P38γ activity is required for maintenance of slow skeletal muscle size. Muscle Nerve. 2012; 45: 266-273.
57. Freshney N.W. et al. Interleukin-1 activates a novel protein kinase cascade that results in the phosphorylation of Hsp27. Cell. 1994; 78: 1039-1049.
58. Fridlender Z.G., Albelda S.M. Tumor-associated neutrophils: friend or foe? Carcinogenesis. 2012; 33: 945-955.
59. Garin A., Proudfoot A.E. Chemokines as targets for therapy. Exp. Cell. Res. 2011; 317: 602-612.
60. Gasche J.A. et al. Interleukin-6 promotes tumorigenesis by altering DNA methylation in oral cancer cells. Int. J. Cancer. 2011; 129: 1053-1063.
61. Gebhardt C. et al. RAGE signaling sustains inflammation and promotes tumor development. J. Exp. Med. 2008; 205: 275-285.
62. Giard D.J. et al. In vitro cultivation of human tumors: establishment of cell lines derived from a series of solid tumors. J. Natl. Cancer Inst. 1973; 51: 1417-1423.

63. Giles R.H. et al. Caught up in a Wnt storm: Wnt signaling in cancer. Biochim. Biophys. Acta. 2003; 1653: 1-24.
64. Goedert M. et al. Activation of the novel stress-activated protein kinase SAPK4 by cytokines and cellular stresses is mediated by SKK3 (MKK6); comparison of its substrate specificity with that of other SAP kinases. Embo J. 1997; 16: 3563-3571.
65. Grandis J.R., Tweardy D.J. Elevated levels of transforming growth factor alpha and epidermal growth factor receptor messenger RNA are early markers of carcinogenesis in head and neck cancer. Cancer Res. 1993; 53: 3579-3584.
66. Gregory A.D., Houghton A.M. Tumor-associated neutrophils: new targets for cancer therapy. Cancer Res. 2011; 71: 2411-2416.
67. Grille S.J. et al. The protein kinase Akt induces epithelial mesenchymal transition and promotes enhanced motility and invasiveness of squamous cell carcinoma lines. Cancer Res. 2003; 63: 2172-2178.
68. Halawani D. et al. p38 MAP kinase signaling is necessary for ratchondrosarcoma cell proliferation. Oncogene. 2004; 23: 3726-3731.
69. Hammerman P.S. et al. Comprehensive genomic characterization of squamous cell lung cancers. Nature. 2012; 489: 519-525.
70. Han J. et al. A MAP kinase targeted by endoxin and hyperosmolarity in mammalian cells. Science. 1994; 265: 808-811.
71. Hanahan D., Weinberg R.A. Hallmarks of Cancer: The Next Generation. Cell. 2011; 144: 646-674.
72. Hanahan D., Weinberg R.A. The hallmarks of cancer. Cell. 2000; 100: 57-70.
73. Harari P.M. Epidermal growth factor receptor inhibition strategies in oncology. Endocr. Relat. Cancer. 2004; 11: 689-708.
74. Harris R.C et al. EGF receptor ligands. Exp. Cell. Res. 2003; 284: 2-13.
75. Heath W.R., Carbone F.R. The skin-resident and migratory immune system in steady state and memory: innate lymphocytes, dendritic cells and T cells. Nat. Immunol. 2013; 14: 978-985.
76. Hennings H., Boutwell R.K. Studies on the mechanism of skin tumor. Cancer Res. 1970; 30: 312-330.
77. Hirst G.L., Balmain A. Forty years of cancer modelling in the mouse. Eur. J. Cancer. 2004; 40: 1947-1980.
78. Hou S.W. et al. PTPH1 dephosphorylates and cooperates with p38gamma MAPK to increase ras oncogenesis through PDZ-mediated interaction. Cancer Res. 2010; 70: 2901-2910.
79. Ihle J.N. The Stat family in cytokine signaling. Curr. Opin. Cell Biol. 2001; 13: 211-217.
80. Ittner A. et al. Regulation of PTEN activity by p38δ-PKD1 signaling in neutrophils confers inflammatory responses in the lung. J. Exp. Med. 2012; 209: 2229-2246.
81. Janda E. et al. Ras and TGF[beta] cooperatively regulate epithelial cell plasticity and metastasis: dissection of Ras signalling pathways. J. Cell. Biol. 2002; 156: 299-313.
82. Janmaat M.L. et al. Response to epidermal growth factor receptor inhibitors in non-small cell lung cancer cells: limited antiproliferative effects and absence of apoptosis associated with persistent activity of extracellular signal-regulated kinase or Akt kinase pathways. Clin. Cancer Res. 2003; 9: 2316-2326.

83. Jansen L.A. et al. Inhibition of gap junctional intercellular communication and delocalization of the cell adhesion molecule E-cadherin by tumour promoters. Carcinogenesis. 1996; 17: 1527-1531.
84. Jiang Y. et al. Characterization of the structure and function of a new mitogen-activated protein kinase (p38beta). J. Biol. Chem. 1996; 271: 17920-17926.
85. Jiang Y. et al. Characterization of the structure and function of the fourth member of p38 group mitogen-activated protein kinases, p38delta. J. Biol. Chem. 1997; 272: 30122-30128.
86. Johansen C. et al. The mitogen-activated protein kinases p38 and ERK1/2 are increased in lesional psoriatic skin. Br. J. Dermatol. 2005; 152: 37-42.
87. Junttila M.R. et al. p38alpha and p38delta mitogen-activated protein kinase isoforms regulate invasion and growth of head and neck squamous carcinoma cells. Oncogene. 2007; 26: 5267-5279.
88. Kakimoto T. et al. Expression patterns of the tumour suppressor PDCD4 and correlation with β-catenin expression in gastric cancers. Oncol. Rep. 2011; 26: 1385-1392.
89. Kaplan D.H. et al. Autocrine/paracrine TGFβ1 is required for the development of epidermal Langerhans cells. J. Exp. Med. 2007; 204: 2545-2552.
90. Keshet Y., Seger R. The MAP kinase signaling cascades: a system of hundreds of components regulates a diverse array of physiological functions. Methods Mol. Biol. 2010; 661: 3-38.
91. Kim D.J. et al. Signal transducer and activator of transcription 3 (Stat3) in epithelial carcinogenesis. Mol. Carcinog. 2007; 46: 725-731.
92. Kim R.H., Armstrong A.W. Nonmelanoma Skin Cancer. Dermatol. Clin. 2012; 30: 125-139.
93. King C.C. et al. Secretion and inactivation of myeloperoxidase by isolated neutrophils. J. Leukoc. Biol. 1997; 61: 293-302.
94. Konig H.G. et al. TGF-β1 activates two distinct type I receptors in neurons: implication for neuronal NF-κB signaling. J. Cell. Biol. 2005; 168: 1077-1086.
95. Kopp-Schneider A., Portier C.J. Birth and death/differentiation rates of papillomas in mouse skin. Carcinogenesis. 1992; 13: 973-978.
96. Kraft C.A. et al. Activation of PKCdelta and p38delta MAPK during okadaic acid dependent keratinocytes apoptosis. Arch. Dermatol. Res. 2007; 299: 71-83.
97. Kupper T.S. et al. Interleukin 1 gene expression in cultured human keratinocytes is augmented by ultraviolet radiation. J. Clin. Invest. 1987; 80: 430-436.
98. Kwong J. et al. p38alpha and p38gamma mediate oncogenic ras-induced senescence through differential mechanisms. J. Biol. Chem. 2009; 284: 11237-11246.
99. Kyriakis J.M., Avruch J. Mammalian MAPK signal transduction pathways activated by stress and inflammation: a 10-year update. Physiol. Rev. 2012; 92: 689-737.
100. Latres E. et al. The human F box protein beta-Trcp associates with the Cul1/Skp1 complex and regulates the stability of beta-catenin. Oncogene. 1999; 18: 849-854.
101. Laurent-Puig P. et al. Mutations and response to epidermal growth factor receptor inhibitors. Clin. Cancer Res. 2009; 15: 1133-1139.
102. Lechner C. et al. ERK6, a mitogen-activated protein kinase involved in C2C12 myoblast differentiation. Proc. Natl. Acad. Sci. USA. 1996; 93: 4355-4359.
103. Lee J.C. et al. A protein kinase involved in the regulation of inflammatory cytokine biosynthesis. Nature. 1994; 372: 739-746.

104. Lee J.C. et al. Inhibition of p38 MAP kinase as a therapeutic strategy. Immunopharmacol. 2000; 47: 185-201.
105. Lee S.S. et al. β-catenin expression in areca quid chewing-associated oral squamous cell carcinomas and upregulated by arecoline in human oral epithelial cells. J. Formosan Med. Assoc. 2012; 111: 194-200.
106. Lee T.L. et al. Epigenetic modification of SOCS-1 differentially regulates STAT3 activation in response to interleukin-6 receptor and epidermal growth factor receptor signaling through JAK and/or MEK in head and neck squamous cell carcinomas. Mol. Cancer Ther. 2006; 5(1): 8-19.
107. Levy L., Hill C.S. Alterations in components of the TGF-beta superfamily signaling pathways in human cancer. Cytokine Growth Factor Rev. 2006; 17: 41-58.
108. Li Z. et al. The primary structure of p38 gamma: a new member of p38 group of MAP kinases. Biochem. Biophys. Res. Commun. 1996; 228: 334-340.
109. Lilleholt L.L. et al. Role of p38 mitogen-activated protein kinase isoforms in murine skin inflammation induced by 12-O-tetradecanoylphorbol 13-acetate. Acta Derm. Venerol. 2011; 91: 271-278.
110. Lin H.W., Rocco J.W. Molecular-targeted chemotherapy for head and neck squamous cell carcinoma. Signaling Pathways in Squamous Cancer. Chapter 17. Springer. 2011; 365-382.
111. Liu F., Millar S.E. Wnt/beta-catenin signaling in oral tissue development and disease. J. Dent. Res. 2010; 89: 318-330.
112. Loesch M., Chen G. The p38 MAPK stress pathway as a tumor suppressor or more? Front. Biosci. 2008; 13: 3581-3593.
113. Lopez-Pajares V. et al. Genetic pathways in disorders of epidermal differentiation. Trends Genet. 2013; 29: 31-40.
114. Lu J. et al. Activation of epidermal Akt by diverse mouse skin tumor promoter. Mol. Cancer Res. 2007; 5: 1342-1352.
115. MacLeod A.S. et al. Dendritic epidermal T cells regulate skin antimicrobial barrier function. J. Clin. Invest. 2013; 123: 4364-4374.
116. Malanchi I. et al. Cutaneous cancer stem cell maintenance is dependent on β-catenin signalling. Nature. 2008; 452: 650-653
117. Manoukian A.S., Woodgett J.R. Role of glycogen synthase kinase-3 in cancer: regulation by Wnts and other signaling pathways. 2002; 84: 203-229.
118. Markovic A., Chung C.H. Current role of EGF receptor monoclonal antibodies and tyrosine kinase inhibitors in the management of head and neck squamous cell carcinoma. Exper. Rev. Anticancer Ther. 2012; 12: 1149-1159.
119. Martin B. et al. Interleukin-17-producing gammadelta T cells selectively expand in response to pathogen products and environmental signals. Immunity. 2009; 31: 321-330.
120. Massague J. TGFβ in cancer. Cell. 2008; 134: 215-230.
121. Meng F. et al. p38γ mitogen-activated protein kinase contributes to oncogenic properties maintenance and resistance to poly(ADP-ribose)-polymerase-1 inhibition in breast cancer. Neoplasia. 2011; 13: 472-482.
122. Mertens S. et al. SAP kinase-3, a new member of the family of mammalian stress-activated protein kinases. FEBS Lett. 1996; 383: 273-276.

123. Moore R.J. et al. Mice deficient in tumor necrosis factor-alpha are resistant to skin carcinogenesis. Nat. Med. 1999; 5: 828-831.
124. Motley R. et al. Multiprofessional guidelines for the management of the patient with primary cutaneous squamous cell carcinoma. Br. J. Dermatol. 2002; 146: 18-25.
125. Mueller M.M. Inflammation in epithelial skin tumours: old stories and new ideas. Eur. J. Cancer. 2006; 42: 735-744.
126. Nishizuka Y. The molecular heterogeneity of protein kinase C and its implications for cellular regulation. Nature. 1988; 334: 661-665.
127. Oberyszyn T.M. et al. Interleukin-1 alpha gene expression and localization of interleukin-1 alpha protein during tumor promotion. Mol. Carcinog. 1993; 7: 238-248.
128. Ogasawara N. et al. Mutations and nuclear accumulation of beta-catenin correlate with intestinal phenotypic expression in human gastric cancer. Histopathology. 2006; 49: 612-621.
129. Peng C.H. et al. A novel molecular signature identified by systems genetics approach predicts prognosis in oral squamous cell carcinoma. PLoS One. 2011; 6: doi: 10.1371/journal.pone.0023452.
130. Pillaire M.J. et al. Cisplatin and UV radiation induce activation of the stress-activated protein kinase p38gamma in human melanoma cells. Biochem. Biophys. Res. Commun. 2000; 278: 724-728.
131. Quintanilla M. et al. Carcinogen-specific mutation and amplification of Ha-ras during mouse skin carcinogenesis. Nature. 1986; 322: 78-80.
132. Raychaudhuri S.P. Role of IL-17 in psoriasis and psoriatic arthritis. Clin. Rev. Allergy Immunol. 2013; 44: 183-193.
133. Remy G. et al. Differential activation of p38MAPK isoforms by MKK6 and MKK3. Cell. Signal. 2010; 22: 660-667.
134. Repertinger S.K. et al. The epidermal growth factor receptor in normal and neoplastic epithelia. Signaling Pathways in Squamous Cancer. Chapter 5. Springer. 2011; 113-129.
135. Ridky T.W., Khavari P.A. Pathways sufficient to induce epidermal carcinogenesis. Cell Cycle. 2004; 3: 621-624.
136. Risco A. et al. p38γ and p38δ kinases regulate the Toll-like receptor 4 (TLR4)-induced cytokine production by controlling ERK1/2 protein kinase pathway activation. Proc. Nat. Acad. Sci. USA. 2012; 109: 11200-11205.
137. Risco A., Cuenda A. New Insights into the p38γ and p38δ MAPK Pathways. J. Signal Transduct. 2012;
138. Roberts A.B. et al. Is Smad3 a major player in signal transduction pathways leading to fibrogenesis? Chest. 2001; 120: 43S-47S.
139. Roberts A.B., Sporn M.B. Physiological actions and clinical applications of transforming growth factor-beta (TGF-beta). Growth Factors. 1993; 8: 1-9.
140. Rodriguez-Viciana P. et al. Phosphatidylinositol-3-OH kinase as a direct target of Ras. Nature. 1994; 390: 527-532.
141. Rouse J. et al. A novel kinase cascade triggered by stress and heat shock that stimulates MAPKAP kinase-2 and phosphorylation of the small heat shock proteins. Cell. 1994; 78: 1027-1037.
142. Rousseau S. et al. CXCL12 and C5a trigger cell migration via a PAK1/2-p38α MAPK-MAPKAP-K2-HSP27 pathway. Cell Signal. 2006; 18: 1897-1905.

143. Rundhaug J.E., Fischer S.M. Molecular Mechanisms of Mouse Skin Tumor Promotion. Cancers. 2010; 2: 436-482.
144. Sabio G. et al. p38gamma regulates the localisation of SAP97 in the cytoskeleton by modulating its interaction with GKAP. EMBO J. 2005; 24: 1134-1145.
145. Saitoh A. et al. Characterization of Wnt gene expression in murine skin: possible involvement of epidermis-derived Wnt-4 in cutaneous epithelial-mesenchymal interactions. Exp. Cell. Res. 1998; 243: 150-160.
146. Sano Y., Park J.M. Loss of Epidermal p38α Signaling Prevents UVR-Induced Inflammation via Acute and Chronic Mechanisms. J. Invest. Dermatol. 2014; 134: 2231-2240.
147. Schindler E.M. et al. P38delta mitogen-activated protein kinase is essential for skin tumor development in mice. Cancer Res. 2009; 69: 4648-4655.
148. Schioppa T. et al. B regulatory cells and the tumor-promoting actions of TNF-α during squamous carcinogenesis. Proc. Natl. Acad. Sci. 2011; 108: 10662-10667.
149. Schmid T. et al. Translation inhibitor Pdcd4 is targeted for degradation during tumor promotion. Cancer Res. 2008; 68: 1254-1260.
150. Schwarz M. et al. Non-melanoma skin cancer in mouse and man. Arch. Toxicol. 2013; 87: 783-798.
151. Shin H., Iwasaki A. Tissue-resident memory T cells. Immunol. Rev. 2013; 255: 165-181.
152. Siljamäki E. et al. p38δ mitogen-activated protein kinase regulates the expression of tight junction protein ZO-1 in differentiating human epidermal keratinocytes. Arch. Dermatol. Res. 2014; 306: 131-141.
153. Singh A. et al. Keratinocyte stem cells and the targets for nonmelanoma skin cancer. Photochem. Photobiol. 2012; 88: 1099-1110.
154. Sumara G. et al. Regulation of PKD by the MAPK p38delta in insulin secretion and glucose homeostasis. Cell. 2009; 136: 235-248.
155. Sumaria N. et al. Cutaneous immunosurveillance by self-renewing dermal gammadelta T cells. J. Exp. Med. 2011; 208: 505-518.
156. Swann J.B. et al. Demonstration of inflammation-induced cancer and cancer immunoediting during primary tumorigenesis. Proc. Natl. Acad. Sci. USA. 2008; 105: 652-656.
157. Takayama T. et al. Beta-catenin expression in human cancers. Am. J. Pathol. 1996; 148: 39-46.
158. Tang J. et al. Essential role of p38γ in K-Ras transformation independent of phosphorylation. J. Biol. Chem. 2005; 280: 23910-23917.
159. Tay S.S. et al. The Skin-Resident Immune Network. Curr. Dermatol. Rep. 2013; 3: 13-22.
160. Teichert A, Bikle D.D. Regulation of Keratinocyte Differentiation by Vitamin D and Its Relationship to Squamous Cell Carcinoma. Signaling Pathways in Squamous Cancer. Chapter 14. Springer. 2011; 283-303.
161. Thomas M. et al. 7 P38γ mitogen-Activated Protein Kinase is a Mediator of Pathological Cardiac Hypertrophy. Heart. 2014; 100: Suppl. 1, A3-A4.
162. Thomas-Ahner J.M. et al. Gender differences in UVB-induced skin carcinogenesis, inflammation, and DNA damage. Cancer Res. 2007; 67: 3468-3474.
163. Tuomi S. et al. PKCepsilon regulation of an alpha5 integrin-ZO-1 complex controls lamellae formation in migrating cancer calls. Sci. Signal. 2009; 2: ra32.

164. Ventura J. et al. p38α MAP kinase is essential in lung stem and progenitor cell proliferation and differentiation. Nat. Genet. 2007; 39: 750-758.
165. Wagner E. and Nebreda A.R. Signal integration by JNK and p38 MAPK pathways in cancer development. Nat. Rev. Cancer. 2009; 9: 537-549.
166. Wajant H. et al. Tumor necrosis factor signaling. Cell Death Differ. 2003; 10: 45-65.
167. Wang L. et al. IL-17 enhances tumor development in carcinogen-induced skin cancer. Cancer Res. 2010; 70: 10112-10120.
168. Wang X.J. et al. Epidermal expression of transforming growth factor-alpha in transgenic mice: induction of spontaneous and 12-O-tetradecanoylphorbol-13-acetate-induced papillomas via a mechanism independent of Ha-ras activation or overexpression. Mol. Carcinog. 1994; 10: 15-22.
169. Weber-Matthiesen K., Sterry W. Organization of the monocyte/macrophage system of normal human skin. J. Invest. Dermatol. 1990; 95: 83-89.
170. Woodworth C.D. et al. Strain-dependent differences in malignant conversion of mouse skin tumors is an inherent property of the epidermal keratinocyte. Carcinogenesis. 2004; 25: 1771-1778.
171. Yang K. et al. p38γ overexpression in gliomas and its role in proliferation and apoptosis. Sci. Rep. 2013; 3: 1-5.
172. Yoshimura A. Signal transduction of inflammatory cytokines and tumor development. Cancer Sci. 2006; 97: 439-447.
173. Yu H. et al. Crosstalk between cancer and immune cells: role of STAT3 in the tumour microenvironment. Nat. Rev. Immunol. 2007; 7: 41-51.
174. Zitelli K.B. et al. Squamous cell carcinoma of the lip associated with adalimumab therapy for ankylosing spondylitis: a case report and review of TNF-α inhibitors and cutaneous carcinoma risk. Cutis. 2013; 92: 35-39.
175. Zucchini-Pascal N. et al. Crosstalk between beta-catenin and snail in the induction of epithelial to mesenchymal transition in hepatocarcinoma: role of the ERK1/2 pathway. Int. J. Mol. Sci. 2013; 14: 20768-20792.